Power-law attenuation of acoustic waves in random stratified viscoelastic media

by

EIVIND J. G. STORDAL

THESIS

for the degree of

MASTER OF SCIENCE

(Master i Modellering og dataanlyse)

Faculty of Mathematics and Natural Sciences
University of Oslo

November 2011

Det matematisk- naturvitenskapelige fakultet
Universitetet i Oslo

Acknowledgment

First and foremost I wish to express the most hearty gratitude to my supervisor, Prof. Dr. Sverre Holm, for mentoring me on an interesting and topical subject, and giving me creative freedom, support and guidance throughout. I also owe true gratitude to Dr. Sven Peter Näsholm for eagerly answering questions at all hours of the day. This thesis would not have been possible without you.

Also thanks to Patrick Bannister for helpful proofreading, and to Simen Kvaal for answering many strange questions. This thesis would be worse off without you.

Thanks to Fourier for conceiving the beautiful ideas of Fourier analysis, Hervik for producing the most satisfying fruit juice in the world and Bill Evans and Maurice Ravel for showing us just how profound music expressed by the human soul is capable of being. Writing this thesis would feel indifferent without you.

Lastly, thanks to all my friends and family who make life worthwhile. This thesis would be meaningless without you.

Eivind J. G. Stordal

Contents

List of Figures

Chapter 1

Introduction

The basic premise of this thesis is deceptively simple to describe. As acoustic waves propagate through a variety of naturally occurring materials they undergo a certain attenuation. This common frequency dependent pattern in attenuation is captured by the power-law:

$$|\text{Signal out}| = \exp\{-\mathcal{A}(\omega)L\} \times |\text{Signal in}| \tag{1.0.1}$$

with attenuation relation

$$\mathcal{A}(\omega) = A\omega^{\gamma}, \tag{1.0.2}$$

where ω is the frequency, L is the length of the medium, A is a constant coefficient, and γ is the exponent of the power-law relation. We see that the higher the frequency, the higher the attenuation, which gives it a low-pass filter quality, though with long tails that never quite die out.

Power-law attenuation typically arises in complex media such as biological tissues and the sedimentary layers of the earth's upper crust. Understanding acoustic wave propagation through such media is therefore essential to a range of related imaging applications. It is significant to medical ultrasound [Holm and Näsholm, 2011] and elastography [Sinkus et al., 2007], as well as in the reduction of distortion in photoacoustic imaging and tomography [Treeby and Cox, 2009]. All these imaging techniques may be of great aid in detecting maladies, such as tumors and fibrosis, without the need for invasive surgery. Finally, the study of propagation though complex media is crucial to seismic imaging which provides an indispensable alternative to drilling boreholes in the search for minerals and oil.

1.1 Empirical evidence of power-law attenuation

To support the theory which this thesis will explore, I will begin by shining some light on the empirical evidence for power-law attenuation. First we observe the fundamental fact that taking the logarithm of the power-law attenuation relation $\mathcal{A}(\omega) = A\omega^{\gamma}$ yields

$$\log \mathcal{A}(\omega) = \log A + \gamma \log \omega, \tag{1.1.1}$$

which is simply a straight line in the $\log \mathcal{A} - \log \omega$ plane. Figure 1.1, taken directly from Szabo and Wu [2000], is a striking demonstration of this as measured in three different media: human liver, the single crystalline material called yttrium indium

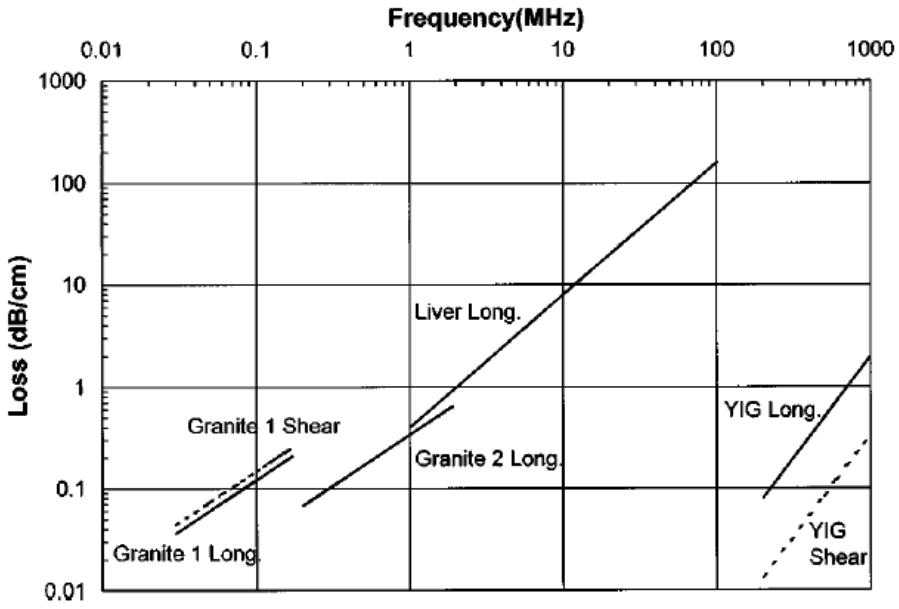

Figure 1.1: Data for shear and longitudinal wave loss which show power-law dependence over four decades of frequency [Szabo and Wu, 2000]

garnet (YIG), and granite. As a testament to the strength of the power-law model, we see that these media exhibit power-law attenuation over several decades of frequency. Note from (1.1.1) that the exponent γ is the slope of the line. From this we may approximate, just by glancing at figure 1.1, that liver and granite has an exponent close to 1, and YIG has a slope which is close to 2.

In a study of freshly excised animal tissue [Kadaba et al., 1980] power-law attenuation is observed in a great variety of tissues: kidney, spleen, muscle and liver from rats and dogs. These are also compared to corresponding measurements of human liver. Here, the animal tissue was submerged in a fluid and acoustic pulses were sent through. The variables A and γ were fitted to the measured material transfer functions and are listed in table 1.1. This study bolsters the impression from figure 1.1 that some biological tissue has an exponent γ close to 1.

Finally, it is a fundamental observation that acoustic waves traveling through air and water follow power-law attenuation with exponent $\gamma = 2$, at least within several distinct bands in the frequency domain, each band corresponding to one chemical component of air. At what frequencies the transitions occur from one band to the other varies with temperature and moisture amongst others. This may be seen, for instance, in the classic text Kinsler et al. [1999].

It seems then, that our overarching aim should be to explain power-law attenuation with an exponent γ in the range of $(0, 2)$. This catch-all interval seems to include all the interesting scenarios. We should also direct special attention to the case γ is near 1 as this seems especially pertinent in medical applications.

As a captivating digression one may interject that there is a tremendously varied collection of phenomena which exhibit power-law spectra unrelated to acoustics.

Animal	**Tissue**	$A(\mathbf{dB/cm/MHz}^\gamma)$	γ
Rat	Liver	0.97	0.97
	Kidney	0.96	1.03
	Gastrocnemium muscle	1.04	1.06
Dog	Liver	0.98	0.987
	Spleen	0.687	1.08
	LV muscle	0.949	1.09
	Kidney	0.97	1.04
Human	Liver	1.16	0.96

Table 1.1: Summary of attenuation coefficients found from observing wave attenuation in freshly excised animal tissue

For example, power-law behavior has been observed in neural recordings both on the microscopic scale of membrane currents [Derksen and Verveen, 1966] and on the macroscopic scale of EEG [Freeman et al., 2003]. Other than that one could mention such diverse phenomena as the water level of the river Nile, economic time series, texture variation in terrain, landscapes and cloud formation, as well as electromagnetic noise in electronics [Wornell, 1996]. We will not study these phenomena here, but it serves as a satisfying backdrop to be aware that our subject of study, in different shapes and forms, has more general implications, and a wide presence throughout nature. With any luck some of the concepts we develop here may be applied to other areas.

1.2 The two theories: scattering and viscoelasticity

The two theories we will explore which explain power-law attenuation are scattering in media with a fractal spatial correlation, and fractional viscoelasticity. Scattering is associated with elastic scattering of waves upon contact with spatial variation in acoustic impedance. The O'Doherty-Anstey theory [O'Doherty and Anstey, 1971] describes this regime for fractal spatial correlations with short-range dependence. Fractional viscoelasticity is associated with thermodynamic absorption of the attenuating wave. The fractional Zener model [Holm and Näsholm, 2011] is an extension of the classic viscoelastic Zener model which allows for power-law attenuation with exponents other than 2, 0.5 and 0. These models are usually separately handled, though it is reasonable to expect, a priori, that complex materials exhibit both phenomena at once.

One question immediately prompts itself: Which source of attenuation is most important? In Campbell and Waag [1984] calf liver is exposed to ultrasonic pulses, and it is estimated that for frequencies between 3 MHz and 7 MHz, only 2% of the observed attenuation is due to scattering. In other words, viscoelastic absorption seems to be dominant in medical applications. However, there is reason to question whether they underestimate the role of scattering as they might mistake some of the scattering for absorption. In the geophysical literature there exists a great variety of opinion. Comparing theoretical expectations of attenuation due to scattering with observations [Schoenberger and Levin, 1974] suggests that between 1/3 and 1/2 of attenuation is due to scattering. This study seems to attribute more of attenuation to scattering than most – some studies estimate scattering to be of several orders

of magnitude smaller [Resnick, 1990]. The review paper Resnick [1990] concludes that "... the available data suggest that absorption is the most important dispersive mechanism in many geologic formations, but that stratigraphic filtering dominates in some." In the context of seismic applications, stratigraphic filtering refers to a specific kind of scattering. Finally, newly developed techniques in elastography suggests it is likely that scattering is the dominant effect in elastography of the human liver [Sinkus et al., 2011]. From this we may derive that they are both present at various degrees in different circumstances. Also it seems broadly reasonable that none of them are small enough to be justifiably ignored. It therefore seems pertinent to study models which accounts for both effects and that explore the interaction between them.

1.3 Thesis outline

First we elucidate the two core theories, namely scattering in media with a fractal spatial correlation structure and fractal viscoelasticity. The opening chapters 2 – 4 introduce these phenomena separately. This inevitably leads to a bifurcation of our exposition into two distinct branches – two branches that do not relate to, nor inform each other. Following, in chapter 5, we rejoin these branches into a combination model which takes them both into account. Then chapter 6 presents a proposed model with spatial variation in the viscoelastic behavior. This chapter also contains some numerical simulations which illustrate the theory. Finally, chapter 7 collects the loose ends and the opportunities for future work, and chapter 8 concludes with a final summary and discussion.

1.4 Process

The original task was to elaborate and expand upon *two* articles. The first article [Burridge et al., 1993] covers a theoretical combination of a thinly layered media with a viscoelastic model called the Zener model. However, the classic Zener model fails to explain power-law attenuation with arbitrary exponents γ. This is the impetus behind introducing *fractional* viscoelastic models which successfully do. The challenge then, was to extend the theory of Burridge et al. [1993] to incorporate the fractional Zener model.

Extending the model in Burridge et al. [1993] called for a thorough understanding of the mathematics behind the fractional Zener model. Admittedly, the long and rigid calculations of chapter 4 are an example of this text being more a legacy of a process of discovery rather than a polished text book. One could argue that the prominence and space awarded to such computations do not necessarily expedite the answering of the fundamental question: How do we explain power-law attenuation? Though such impatience would be unfortunate as the calculations undoubtedly bring relevant insight.

The second article [Le and Burridge, 1998] explores numerically the validity of the theoretical combination models derived in Burridge et al. [1993]. The final task was to see if I could run similar numerical experiments in a fractional viscoelastic setting. My original intent was to do just that, and some progress was made in that direction. The fruits of this may be found in appendix H. However, the proposed model of chapter 6 was deemed more interesting and was prioritized.

As a reader's guide, an effort has been made to relate the content of this work to

specific equations and passages in Burridge et al. [1993] and Le and Burridge [1998]. Yet keeping these article alongside is completely optional as the theory herein is (for the most part) self-contained.

1.5 Summary of contributions

The general theory of the opening chapters 2 – 4 has been collected from many different sources, ranging from text books to topical literature, to provide a coherent introduction to our two core models.

The proof of the ODA theory in section 3.3 is different from the original [O'Doherty and Anstey, 1971]. Though I am sure other people have proven the ODA theory in the same way before, this is my own take at the problem through some simple Taylor expansions. The same goes for the proof of Banik et al.'s result in section 3.4. It is reformulated in my own words and concepts.

The explicit calculations of chapter 4 were made to empower us with the necessary technical equipment to deal with problems often arising in power-law settings.

Section 4.2 proves in detail the behavior of the fractional Zener model close to two very relevant extreme cases. It also presents an original theoretical tool, not only for expressing the approximate power-laws which the attenuation follows at different bands, but also for finding a complete explicit expression. This theory provides some advantage, albeit very modest, over existing theory, in that one could study in detail the transition between the different bands.

In chapter 5 I extend the model from Burridge et al. [1993] to the fractional Zener case.

In chapter 6 I describe an original idea which departs from the conventional scattering ideas described by the ODA theory. The proposed theory describes how acoustic waves propagate through a media with spatial structure not in the elastic properties, but in the viscoelastic state variables. This chapter also contains a proposed algorithm for solving the wave equation in such a medium in the frequency domain.

Since power-laws with exponent $\gamma = 1$ seem especially important in medical ultrasound, I have throughout the thesis attempted to collect and create theory which may provide explanations. This may be seen in section 3.4.1, section 4.2 and chapter 6.

1.6 Technical tools

The thesis is written in LaTeX and all illustrations are written using the `tikz` package. All code is written in the free programming language R and the code may be found in appendix G. All plots are produced in R with the `ggplot2` package with the output produced in tikz code using the `tikzDevice` package. Producing output in tikz code rather than postscript allows for LaTeX fonts inside the plots.

Chapter 2

Derivation of the acoustic wave equation

We seek to describe media that leaves a power-law fingerprint on acoustic waves traveling through them. Empirically, we have seen that this frequently occurs in biological tissue. As a starting point, one might point out the naive observation that such materials share a common mechanical property – they are not quite fluids, yet they are not quite solids either. Such materials fall under the purview of rheology. The wave equation is in turn founded on some fundamental physical principles and a mechanical model of rheology. One could say that **rheology** is the study of "thick" fluids (non-Newtonian fluids) and deformation of soft solids. An analogous term is viscoelasticity, though this usually refers to a specific mathematical formulation expressed by the two mechanical entities stress (σ) and strain (ϵ). And this is exactly where we will begin.

2.1 Rheological models

The purpose of this section is to introduce the fundamental concepts and nomenclature of **linear viscoelasticity**. This introduction is much in the vein of Mainardi and Spada [2011]. According to the viscoelastic theory, the viscoelastic body can be considered a system with the stress as excitation function (input) and strain as the response function (output). Furthermore, within the domain of small amplitude distortions, the mechanism by which the stress excitation is transferred to the strain response is assumed to follow the rules of an LTI (linear time invariant) system. See figure 2.1. This gives the reader familiar with digital signal processing a platform of intuition, the most fundamental of which is that the transfer function is completely described by the response of the unit step or impulse excitation. In fact, we will examine, and name, both the step response and the impulse response as they both occur in the traditions of the different subject areas we are about to encounter.

2.1.1 Step response. Denote by $J(t)$ the strain response to a unit step stress excitation. The unit step stress excitation may be written in mathematical terms as

$$\sigma(t) = H(t) = \begin{cases} 0 & \text{for } x < 0 \\ 1 & \text{if } x \geq 0 \end{cases},$$

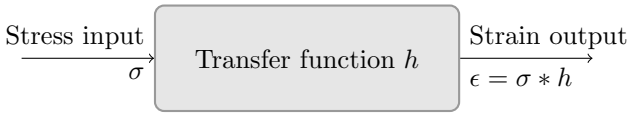

Figure 2.1: Linear viscoelastic stress-strain model

where $H(t)$ is the so-called **Heaviside function**. (Sources in digital signal processing often give this a different name – the unit step function $u(t)$.) Note that this stress excitation is more than just a mathematical entity. It constitutes the physical experiment where a stress loading is suddenly applied and sustained at a constant level. This is called the **creep test**. After applying the stress loading one may observe $J(t)$ by measuring the development of strain. Note also, that mathematically speaking, the impulse response is more standard, but from a physical point of view, applying a sudden stress impulse is impractical. That is why we are interested in studying the step response.

Conversely, one may see stress as the output and strain as the input. Denote by $G(t)$ the stress response to a unit step strain excitation. This is called a **relaxation test**. This is the physical test where a sudden strain program is applied and $G(t)$ is observed by measuring the development in stress.

The functions $J(t)$ and $G(t)$ are respectively referred to as the **creep compliance** and the **relaxation modulus**. Together, $J(t)$ and $G(t)$ are called the **material functions**. From observations, $J(t)$ is non-decreasing and $G(t)$ is non-increasing.

Furthermore we will examine the instantaneous and equilibrium behavior of the material functions. Denote by $J_{\text{in}} := \lim_{t\to 0^+} J(t)$ the **instantaneous compliance**, $J_{\text{eq}} := \lim_{t\to\infty} J(t)$ the **equilibrium compliance**, $G_{\text{in}} := \lim_{t\to 0^+} G(t)$ the **instantaneous modulus**, $G_{\text{eq}} := \lim_{t\to\infty} G(t)$ the **equilibrium modulus**. Throughout literature, these entities have many different names and annotations. Amongst others, J_{in} may be called *glass compliance* (J_g) or *unrelaxed compliance* (J_u), and J_{eq} may be called *relaxed compliance* (J_r) [Mainardi and Spada, 2011; Le and Burridge, 1998]. Many new concepts have been introduced, and they may all be observed in figure 2.2, where viscoelastic responses may be seen on the right hand side, and elastic responses to the left.

To ensure that $J(t)$ is casual we may establish that it can be written as

$$J(t) = \bar{J}(t)H(t) = \begin{cases} 0 & \text{for } t < 0 \\ \bar{J}(t) & \text{for } x \geq 0. \end{cases}$$

We may think of $\bar{J}(t)$ as the mathematical expression describing the curves of figure 2.2 and $J(t)$ as the actual step response. The distinction is mainly introduced to make the following notation more precise.

We may express the stress-strain relationship in term of the creep compliance $J(t)$ as

$$\epsilon(t) = J(t) * D_t\sigma(t), \tag{2.1.1}$$

where D_t is the derivative in the sense of distributions. Let us just take a quick reality check to see if this formulation agrees with the creep test. If $\sigma(t) = H(t)$, the strain output becomes by (2.1.1)

$$\epsilon(t) = J(t) * \delta(t) = J(t),$$

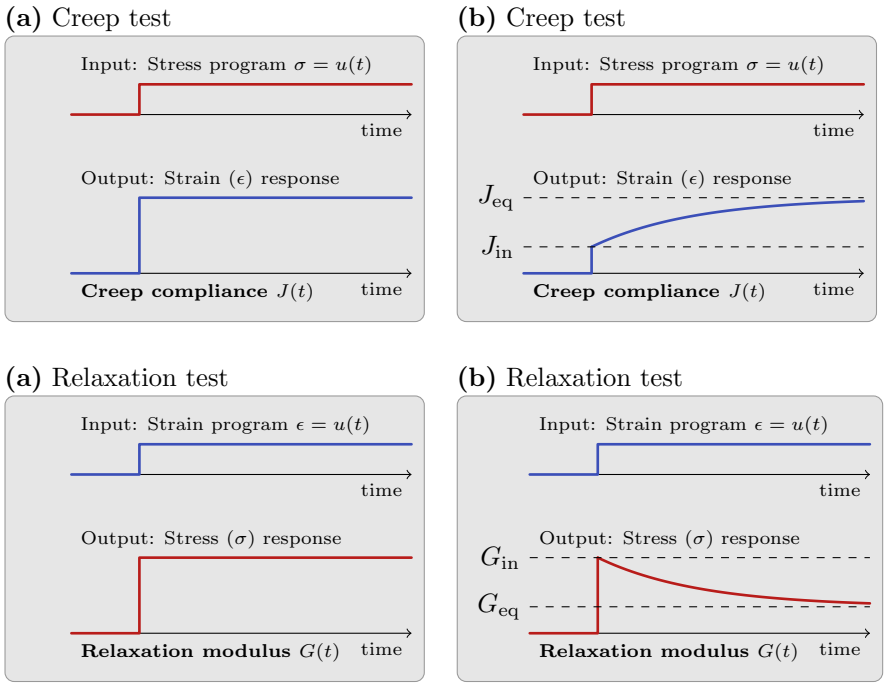

Figure 2.2: (Strain is in blue, stress is in red) (a) Deformation of elastic solid (b) Deformation of a linear viscoelastic solid with immediate elastic response J_{in}

since $D_t H(t) = \delta(t)$. This is exactly in accordance with the creep test. We may also express (2.1.1) as the Riemann–Stieltjes integral

$$\epsilon(t) = \int_{-\infty}^{t} J(t-\tau) d\sigma(\tau) \tag{2.1.2}$$

which is the standard text book definition of creep compliance.

In chapter 5 we examine models where we separate the instantaneous elastic response J_{in} from the slow creep of $J(t)$ thereafter. In view of this we will try to make the instantaneous behavior explicit in our equations. By the well known property of convolution (A.0.1) we may switch the derivatives around in (2.1.1) and get

$$\epsilon(t) = D_t J(t) * \sigma(t). \tag{2.1.3}$$

Let us take a closer look at $D_t J(t)$. Looking at (b) of figure 2.2 we may intuit the derivative to be 0 for $t < 0$, then a sudden jump at 0 followed by the derivative of the creep. This can be formally expressed by differentiating (2.1.1) with the product rule.

$$\underbrace{D_t J(t)}_{\substack{\text{Derivative in the} \\ \text{sense of distributions}}} = \underbrace{J_{\text{in}}\delta(t)}_{\text{Instantaneous leap}} + H(t) \times \underbrace{(\partial_t \bar{J}(t))}_{\text{Derivative in the classic sense}} \tag{2.1.4}$$

For those who wish to delve into the formalism of distributions, Gasquet and Witomski [1998] is an accessible, yet not superficial, introduction which may be heartily recommended.

Putting (2.1.4) into (2.1.3) we get

$$\epsilon(t) = J_{\text{in}}\sigma(t) + (H(t)\partial_t \bar{J}(t)) * \sigma(t) \tag{2.1.5}$$

When we study step responses it is not surprising that we study its Laplace transform. Recall that the Laplace transform of the derivative of a function (see property A.0.4) is given by

$$\mathcal{L}\{f'(x); s\} = s\mathcal{L}\{f(x); s\} - f(0^+)$$

We may write (2.1.5) in the Laplace domain as

$$\begin{aligned}\widehat{\epsilon}(s) &= J_{\text{in}}\widehat{\sigma}(s) + (s\widehat{J}(s) - J_{\text{in}})\widehat{\sigma}(s) \\ &= s\widehat{J}(s)\widehat{\sigma}(s)\end{aligned} \tag{2.1.6}$$

The same exact procedure may be applied to the relaxation modulus, and we may summarize all this in

$$\begin{aligned}&\epsilon(t) = \int_{-\infty}^{t} J(t-\tau)d\sigma(\tau) && \sigma(t) = \int_{-\infty}^{t} G(t-\tau)d\epsilon(\tau) \\ &\epsilon(t) = J_{\text{in}}\sigma(t) + (H(t)\partial_t \bar{J}(t)) * \sigma(t) && \sigma(t) = G_{\text{in}}\epsilon(t) + (H(t)\partial_t \bar{G}(t)) * \epsilon(t).\end{aligned}$$

And in the Laplace domain we have

$$s\widehat{J}(s) = \frac{\widehat{\epsilon}(t)}{\widehat{\sigma}(t)}, \quad \text{and} \quad s\widehat{G}(s) = \frac{\widehat{\sigma}(t)}{\widehat{\epsilon}(t)}.$$

It is then evident that

$$s\widehat{J}(s) = \frac{1}{s\widehat{G}(s)},$$

from which we may surmise by applying the initial and final value theorems A.0.6 that

$$J_{\text{in}} = \frac{1}{G_{\text{in}}} \quad \text{and} \quad J_{\text{eq}} = \frac{1}{G_{\text{eq}}}. \tag{2.1.7}$$

2.1.2 Impulse response. Within the literature on acoustic wave propagation [Holm and Näsholm, 2011], the stress-strain relationship from figure 2.1 is described by its impulse response:

$$\epsilon(t) = \kappa(t) * \sigma(t),$$

or in the frequency domain

$$\widehat{\epsilon}(\omega) = \widehat{\kappa}(\omega)\widehat{\sigma}(\omega) \tag{2.1.8}$$

The impulse response $\kappa(t)$ is called the **generalized compressibility**. In view of (2.1.3) there exists a simple relationship between the compressibility $\kappa(t)$ and the creep compliance $J(t)$

$$\kappa(t) = D_t J(t) \tag{2.1.9}$$

From the fundamental relation (see property A.0.4)

$$\mathcal{F}\{D_t f(x); \omega\} = i\omega\widehat{F}(\omega) \tag{2.1.10}$$

it is clear that

$$\widehat{\kappa}(\omega) = (i\omega)\widehat{J}(s = i\omega). \tag{2.1.11}$$

Let us look at how the instantaneous (J_{in}) and equilibrium (J_{eq}) responses of the creep compliance relate to the generalized compressibility in the frequency domain. By the initial value theorem of the Laplace transform A.0.6 we have

$$J_{\text{in}} = \lim_{s\to\infty} s\widehat{J}(s)$$

$$J_{\text{eq}} = \lim_{s\to 0} s\widehat{J}(s)$$

Since the impulse response $\kappa(\omega)$ is causal, we know by Titchmarsch's theorem [Weaver and Pao, 1981] that it is analytic in the upper half complex plane. In light of this, the limit $\kappa(\omega \to \infty)$ must be the same for all directions in the complex ω plane. Using the fact that $s = i\omega$ we get

$$\kappa_\infty := \lim_{\omega\to\infty} \widehat{\kappa}(\omega) = \lim_{\omega\to\infty} \widehat{\kappa}(i\omega) = \lim_{s\to\infty} s\widehat{J}(s) = J_{\text{in}} \tag{2.1.13a}$$

$$\kappa_0 := \lim_{\omega\to 0} \widehat{\kappa}(\omega) = \lim_{s\to 0} s\widehat{J}(s) = J_{\text{eq}} \tag{2.1.13b}$$

These identifications make physically intuitive sense. The instantaneous response J_{in} is the compressibility experienced by infinitely quick movements. At this high frequency the viscoelastic creep has no time to set in. On the other hand the equilibrium J_{eq} is reached when there is no movement at all. This is the zero frequency.

2.1.3 Constitutive equations. Finally we may express the stress-strain relationship from figure 2.1 by a differential equation. According to the theory of linear viscoelasticity, these equations are given by $D_a\sigma = D_b\epsilon$, where D_a and D_b are differential operators on the form $a_0 + a_1\partial_t + a_2\partial_t^2 + \cdots$. Such an equation is called a **constitutive equation**. Some of the most common such constitutive equations are

Hooke's law	$\sigma(t) = a_0\epsilon(t)$
The Maxwell model	$[1 + a_1\partial_t]\,\sigma(t) = b_1\partial_t\epsilon(t)$
The Kelvin-Voigt model	$\partial_t\sigma(t) = [b_0 + b_1\partial_t]\,\epsilon(t)$
The Zener model	$[1 + a_1\partial_t]\,\sigma(t) = [b_0 + b_1\partial_t]\,\epsilon(t)$

These equations are rarely defined in terms of the constants a_0, b_0, a_1 and a_2 but with other Greek letters which all have different physical interpretations. We will further acquaint ourselves with the Zener model shortly. The two middle models of the table above are stated for reference – they are all invariably mentioned in standard introductions to linear viscoelasticity. The interested reader may learn more about them (and their fractional generalizations) in Mainardi and Spada [2011]. Hooke's law gives rise to an elastic medium where the waves never attenuate and lose energy. This is the basis of the section on scattering – chapter 3. We extend the Zener model to the fractional Zener model in chapter 4.

Let us spell out the details of Hooke's law. **Young's module** E_0 takes the place of a_0 in the generic form above, but often the reciprocal of E_0 is used instead; $\kappa_0 = \frac{1}{E_0}$, which is called the **compressibility modulus**. We get the following:

Constitutive equation	$\epsilon(t) = \kappa_0\sigma(t)$	
Generalized compressibility	$\kappa(t) = \kappa_0\delta(t)$	(2.1.14)
Creep compliance	$J(t) = \kappa_0 H(t)$, with $J_{\text{in}} = J_{\text{eq}} = \kappa_0$	

2.2 The Zener model

A viscoelastic body whose constitutive equation is the Zener model is alternatively called a **Standard Linear Solid (SLS)**. This is a term you may see in many of the papers referred to by this thesis, most notably the corner stone article Le and Burridge [1998]. The Zener constitutive equation is given by

$$[1 + \tau_\sigma \partial_t]\, \sigma(t) = \frac{1}{J_{\text{eq}}} [1 + \tau_\epsilon \partial_t]\, \epsilon(t). \tag{2.2.1}$$

It may be shown, indeed it is shown in section 4.1, that its creep compliance and relaxation modulus are given by

$$J(t; J_{\text{eq}}, \tau_\epsilon, \tau_\sigma) = J_{\text{eq}} \left\{ 1 - \left(1 - \frac{\tau_\sigma}{\tau_\epsilon} \right) \exp\left(-\frac{t}{\tau_\epsilon} \right) \right\} H(t) \tag{2.2.2}$$

$$G(t; G_{\text{eq}}, \tau_\epsilon, \tau_\sigma) = G_{\text{eq}} \left\{ 1 - \left(1 - \frac{\tau_\epsilon}{\tau_\sigma} \right) \exp\left(-\frac{t}{\tau_\sigma} \right) \right\} H(t). \tag{2.2.3}$$

Comparing these exponentially decaying expressions to the graphs in figure 2.2 (b) we gather the parameters τ_σ and τ_ϵ determine the rate of decay. In fact τ_ϵ is called the **retardation time** and τ_σ is called the **relaxation time**. These same graphs imply that we may take 6 different physical measurements: Two decay times (one for each test), $J_{\text{in}}, J_{\text{eq}}, G_{\text{in}}$ and G_{eq}. But within the linear viscoelastic regime it is evident by counting the number of constants in (2.2.1) that we only have three degrees of freedom. We find one dependency by calculating

$$J_{\text{in}} = J(0) = \frac{J_{\text{eq}} \tau_\sigma}{\tau_\epsilon},$$

and we have already found the remaining ones in (2.1.7). These dependencies explain how only 3 variables dictate 6 and reveals an inherent weakness of the linear viscoelastic theory. In section 4.1.1 we find that an equivalent restriction applies to the fractional case. Finally, since $J_{\text{in}} < J_{\text{eq}}$ we get

$$1 < \frac{J_{\text{eq}}}{J_{\text{in}}} = \frac{\tau_\epsilon}{\tau_\sigma}, \tag{2.2.4}$$

so we must have $\tau_\sigma < \tau_\epsilon$.

Let us finally find the generalized compressibility. By (2.1.9) and (2.1.4) we find that the generalized compressibility can also be split into

$$\kappa(t) = D_t J(t) = \underbrace{J_{\text{in}} \delta(t)}_{\substack{\text{Instantaneous} \\ \text{elastic compressibility}}} + \underbrace{H(t)(\partial_t \bar{J}(t))}_{\text{Viscoelastic compressibility}} \tag{2.2.5}$$

Differentiating (2.2.2) above we get

$$\kappa(t) = \underbrace{J_{\text{in}} \delta(t)}_{\substack{\text{Instantaneous} \\ \text{elastic compressibility}}} + \underbrace{J_{\text{in}} \left(\frac{1}{\tau_\sigma} - \frac{1}{\tau_\epsilon} \right) \exp\left(-\frac{t}{\tau_\epsilon} \right) H(t)}_{\text{Viscoelastic compressibility}}$$

Notice that (2.2.2) is the model used in Le and Burridge [1998, equation (13)], and that $\kappa(t)$ above is stated in Le and Burridge [1998, equation (16)].

2.3 The acoustic wave equation

Throughout this thesis we examine acoustic waves propagating through different types of media; some elastic with spatial structure, some viscoelastic, and some with both. This propels us not to find a single wave-equation that fits all environments, but rather establish a catalog of equations. In the following we will be particularly meticulous about making the underlying assumptions of each wave equation explicit, making this section a handy reference for the rest of the thesis. After reading this, the reader should be able to recognize basic wave equations when reading general acoustic literature.

Before we begin we introduce a few physical variables. $\rho(z)$ is the density of the medium, $u(z,t)$ is the particle displacement, $v(z,t)$ is the particle velocity field and $p(z,t)$ is the pressure field. Also note, in fluid mechanics, that stress (σ) is the same as negative pressure ($-p$). z is the spatial variable.

The acoustic wave equation predicates on these three ideas:

$$\begin{aligned} &\text{Constitutive equation} && \epsilon(z,t) = \kappa(z,t) * \sigma(z,t) && (2.3.1)\\ &\text{Conservation of mass} && \epsilon(z,t) = \partial_z u(z,t) && (2.3.2)\\ &\text{Conservation of momentum} && \partial_z \sigma(z,t) = \rho(z)\partial_t^2 u(z,t) && (2.3.3) \end{aligned}$$

The equation describing conservation of mass is a linear approximation putting our model into the realm of **linear acoustics**. The equation describing conservation of momentum is exact. Note that the constitutive equations may be reformulated as

$$D^\epsilon(z)\epsilon(z,t) = D^\sigma(z)\sigma(z,t) \tag{2.3.4}$$

2.3.1 Pressure-velocity system. As is customary within the acoustic literature we seek to describe the acoustic wave in a pressure-velocity system. We begin by observing that the velocity is simply the derivative of the displacement $v(z,t) = \partial_t u(z,t)$. Next, we use that $\sigma(z,t) = -p(z,t)$, and we may rewrite the conservation of momentum (2.3.3) equations as

$$\text{I.} \quad \partial_z p(z,t) = -\rho(z)\partial_t v(z,t) \tag{2.3.5}$$

This is the first of the two equations in our pressure-velocity system. We find the second equation by inserting the conservation of mass rule (2.3.2) into to the constitutive equation (2.3.1)

$$\partial_z u(z,t) = \kappa(z,t) * \sigma(z,t).$$

Finally we use that $\sigma(z,t) = -p(z,t)$ and differentiate both sides with respect to t. Remember from property (A.0.1) that the derivative of a convolution is the derivative of only one of the terms, and we get

$$\text{II.} \quad \partial_z v(z,t) = -\kappa(z,t) * \partial_t p(z,t). \tag{2.3.6}$$

Alternatively we may express it as

$$\text{IIalt.} \quad D^\epsilon(z)\partial_z v(z,t) = -D^\sigma(z)\partial_t p(z,t). \tag{2.3.7}$$

These two equations embody the general pressure-velocity system. We may take the Fourier transform of (2.3.5) and (2.3.6) using property A.0.4. And we get

$$\begin{aligned} \partial_z \widehat{p}(z,\omega) &= -i\omega\rho(z)\widehat{v}(z,\omega)\\ \partial_z \widehat{v}(z,\omega) &= -i\omega\widehat{\kappa}(z,\omega)\widehat{p}(z,\omega). \end{aligned}$$

Adopting the vector $\boldsymbol{v}(z,t)$ which contains both the pressure and velocity field

$$\boldsymbol{v}(z,t) = \begin{bmatrix} p(z,t) \\ v(z,t) \end{bmatrix}$$

we may summarize all of this in

Wave equation 2.3.1 (General pressure-velocity system)**.**

Time domain

$$\begin{aligned} \partial_z p(z,t) &= -\rho(z)\partial_t v(z,t) \\ \partial_z v(z,t) &= -\kappa(z,t) * \partial_t p(z,t) \end{aligned}$$

Frequency domain

$$\partial_z \widehat{\boldsymbol{v}}(z,\omega) = -i\omega M(z,\omega)\widehat{\boldsymbol{v}}(z,\omega), \quad M(z,\omega) = \begin{bmatrix} 0 & \rho(z) \\ \widehat{\kappa}(z,\omega) & 0 \end{bmatrix}$$

- General viscoelastic media with compressibility $\kappa(z,t)$

2.3.2 One-variable second-order equation. We may collapse our 2 variable system to a 1 variable equation by eliminating one of the variables. Let us make a wave equation in only p. For this we differentiate (2.3.5) with respect to z and (2.3.7) with respect to t.

$$\partial_z^2 p(z,t) = -\partial_z \left(\rho(z)\partial_t v(z,t)\right) \tag{2.3.8}$$

$$D^\epsilon(z)\partial_z\partial_t v(z,t) = -D^\sigma(z)\partial_t^2 p(z,t) \tag{2.3.9}$$

In order to advance, we must assume that ρ is constant. Then (2.3.8) becomes

$$-\partial_z^2 p(z,t) = \rho\partial_z\partial_t v(z,t)$$

We may solve this for $\partial_z\partial_t v(z,t)$ and insert it into (2.3.9) and get

$$D^\epsilon(z)\partial_z^2 p(z,t) - \rho D^\sigma(z)\partial_t^2 p(z,t) = 0 \tag{2.3.10}$$

One may easily rewrite it in terms of the generalized compressibility, as well as finding the frequency domain version.

Wave equation 2.3.2 (General 1-variable wave equation)**.**

Time domain

$$\begin{aligned} D^\epsilon(z)\partial_z^2 p(z,t) - \rho D^\sigma(z)\partial_t^2 p(z,t) &= 0, \quad \textit{or alternatively} \\ \partial_z^2 p(z,t) - \rho\kappa(z,t) * \partial_t^2 p(z,t) &= 0 \end{aligned}$$

Frequency domain

$$\partial_z^2 \widehat{p}(z,\omega) + \omega^2\rho\kappa(z,\omega)\widehat{p}(z,t) = 0$$

- General viscoelastic media with compressibility $\kappa(z,t)$
- Density ρ is constant

All wave equations presented in this section, as the one above, is joined by an explicit list of assumptions which the equation predicates on. One may always remove z-dependencies, but adding them is not allowed.

Note that that our system is symmetric in the sense that the exact same equation could be found for the velocity field $v(z,t)$, even the displacement $u(z,t)$.

2.3.3 Elastic wave equations. Let us now get specific about the choice of constitutive equation. These elastic wave equations come from Hooke's law, which pursuant to (2.1.14) means that $\kappa(z,t) = \kappa_0(z)\delta(t)$, where $\kappa_0(z)$ is the compressibility modulus. Inserting this into wave equation 2.3.1 we get the system

$$\begin{aligned} &\text{I. } \partial_z p(z,t) = -\rho(z)\partial_t v(z,t) \\ &\text{II.} \partial_z v(z,t) = -\kappa_0(z)\partial_t p(z,t) \end{aligned}$$

which may reformulate, again using the vector notation $\boldsymbol{v}(z,t)$, and get

Wave equation 2.3.3 (Elastic pressure-velocity system)**.**

Time domain

$$\partial_z \boldsymbol{v}(z,t) = -M(z)\partial_t \boldsymbol{v}(z,t), \quad \textit{where} \quad M(z) = \begin{bmatrix} 0 & \rho(z) \\ \kappa_0(z) & 0 \end{bmatrix}$$

Frequency domain

$$\partial_z \widehat{\boldsymbol{v}}(z,\omega) = -i\omega M(z)\widehat{\boldsymbol{v}}(z,t)$$

- Elastic medium; Hooke's law with compressibility $\kappa_0(z)$

When solving such systems of linear differential equations, mathematically speaking, it is common practice to diagonalize the matrix $M(z)$ from wave equation 2.3.3. By property (D.0.16) we can diagonalize $M(z)$ by

$$M(z) = E(z)\Lambda(z)E^{-1}(z), \tag{2.3.11}$$

$$\text{with } \Lambda(z) = \begin{bmatrix} \frac{1}{c(z)} & 0 \\ 0 & -\frac{1}{c(z)} \end{bmatrix}, E(z) = \frac{1}{\sqrt{2}} \begin{bmatrix} Z(z)^{1/2} & -Z(z)^{1/2} \\ Z(z)^{-1/2} & Z(z)^{-1/2} \end{bmatrix}. \tag{2.3.12}$$

Here $Z(z) = \sqrt{\frac{\rho(z)}{\kappa_0(z)}}$ is the **acoustic impedance** and $c(z) = \sqrt{\frac{1}{\kappa_0(z)\rho(z)}}$ is the speed of sound. By now, we have introduced many different physical variables, and the reader may use the in chart in appendix C to keep track. We may now consider a certain construction

$$\boldsymbol{w}(z,t) := E^{-1}(z)\boldsymbol{v}(z,t). \tag{2.3.13}$$

This is in accordance with the notation of the beginning of Burridge et al. [1993, equation (6)]. The vector $\boldsymbol{w}(z,t)$ contain two elements

$$\boldsymbol{w}(z,t) = \begin{bmatrix} R(z,t) \\ L(z,t) \end{bmatrix},$$

which are the **left- and right-going waves**. As in Burridge et al. [1993] they are also often called **modes**. We give a physical interpretation of them shortly. Expanding $M(z)$ in wave equation 2.3.3 to its diagonalization (2.3.11) we get

$$E^{-1}(z)\partial_z \boldsymbol{v}(z,t) = \Lambda(z)E^{-1}(z)\partial_t \boldsymbol{v}(z,t). \tag{2.3.14}$$

We would like to express our wave equation in terms of the left- and right-going waves. Since $E^{-1}(z)$ does not depend on t we may move it past the ∂_t on the right-hand side of the equation above. If we restrict ourselves to the case where E^{-1} does not depend on z either, we may do the same on the left hand side. By (2.3.13) we get

$$\partial_z \boldsymbol{w}(z,t) = -\Lambda(z)\partial_t \boldsymbol{w}(z,t).$$

Remember the definition of $E(z)$ from (2.3.11). It is clear that assuming that E is constant is that same as assuming that the acoustic impedance is constant. We may summarize.

Wave equation 2.3.4 (Elastic left- and right-system)**.**

Time domain

$$\partial_z \boldsymbol{w}(z,t) = -\Lambda(z)\partial_t \boldsymbol{w}(z,t), \quad \Lambda(z) = \begin{bmatrix} \frac{1}{c(z)} & 0 \\ 0 & -\frac{1}{c(z)} \end{bmatrix}, \quad c(z)^2 = \frac{1}{\rho(z)\kappa_0(z)}$$

Frequency domain

$$\partial_z \widehat{\boldsymbol{w}}(z,\omega) = -i\omega\Lambda(z)\widehat{\boldsymbol{w}}(z,\omega)$$

- Elastic medium; Hooke's law with compressibility modulus $\kappa_0(z)$
- Acoustic impedance Z is constant

So what exactly is the physical interpretation of the left- and right-going waves? By writing out all the components of the wave equation 2.3.4 we get

$$\partial_z R(z,t) = -\tfrac{1}{c}\partial_t R(z,t)$$
$$\partial_z L(z,t) = +\tfrac{1}{c}\partial_t L(z,t).$$

So the left- and right-going waves are decoupled and completely independent of each other. That is, if one of these waves change in amplitude or shape, the other is unaffected. These waves are also sometimes called up- and down-waves. This perspective is inherited from seismic applications where waves are shot downwards into the ground. Our use of z instead of x as the spatial variable is also a legacy to that origin.

In the end we look at a one variable formulation of the elastic wave equation. We simply take wave equation 2.3.2 with $\kappa(z,t) = \kappa_0(z)\delta(t)$ and get the classic wave equation:

Wave equation 2.3.5 (1 variable elastic equation)**.**

Time domain

$$\frac{\partial^2 p}{\partial z^2} - \frac{1}{c^2(z)}\frac{\partial^2 p}{\partial t^2} = 0, \quad c(z)^2 = \frac{1}{\rho\kappa_0(z)}$$

- Elastic medium; Hooke's law with compressibility modulus $\kappa_0(z)$
- Density ρ is constant

2.3.4 Viscoelastic wave equation from the Zener model. With all the previous preparation we may easily look at a wave equation building upon the Zener model. Remember from section 2.2 that the Zener model is given by $D^\sigma(z) = \kappa_0(z)(1 + \tau_\sigma(z)\partial_t)$ and $D^\epsilon(z) = 1 + \tau_\epsilon(z)\partial_t$. Applying this to (2.3.10) yields

$$(1 + \tau_\epsilon(z)\partial_t)\partial_z^2 p(z,t) - \rho\kappa_0(z)(1 + \tau_\sigma(z)\partial_t)\partial_t^2 p(z,t) = 0$$

Cleaning up this expression we get

Wave equation 2.3.6 (1 variable Zener wave equation)**.**

Time domain

$$\frac{\partial^2 p}{\partial z^2} - \frac{1}{c_0^2(z)}\frac{\partial^2 p}{\partial t^2} + \tau_\epsilon(z)\frac{\partial}{\partial t}\frac{\partial^2 p}{\partial z^2} - \frac{\tau_\sigma(z)}{c_0^2(z)}\frac{\partial^3 p}{\partial t^3} = 0, \quad c(z)^2 = \frac{1}{\rho\kappa_0(z)}$$

- Viscoelastic medium; Zener model with parameters $J_{eq}(z)$, $\tau_\sigma(z)$ and $\tau_\epsilon(z)$
- Density ρ is constant

By now we have built a catalog of wave equations. Hopefully our preparations will be paid back with interest.

2.4 The dispersion relation

In general, for an incoming wave $X(\omega)$ entering a medium at $z = 0$ and propagating through to depth $z = z_0$, we assume that the effect of the propagation is an LTI system

$$Y(\omega, z_0) = \mathfrak{T}(\omega, z_0)X(\omega). \tag{2.4.1}$$

Here $\mathfrak{T}(\omega)$ is called the **material transfer function**. Ultimately we seek to describe the transfer function of complex inhomogeneous media. By inhomogeneous media we specifically mean that the medium state variables (for instance κ_0 and ρ) depend on z. In this case there is no general solution to the wave equation, though in section 3 and section 5 we will make some simplifying assumptions which allows us to find good approximations. For now, let us describe the propagation through an homogeneous medium where all the medium state variables stay constant throughout the medium.

Consider a plane harmonic wave in the direction of the z space axis with amplitude $A(\omega)$

$$h(z, t) = A(\omega)e^{-i[\omega t - k(\omega)z]}. \tag{2.4.2}$$

Here $k(\omega)$ is the **wave number**. Inserting this into the general viscoelastic wave equation 2.3.2 we get

$$-k(\omega)^2 A(\omega) + \omega^2\rho\kappa(\omega)A(\omega) = 0.$$

Solving this for $k(\omega)$ gives us

$$k(\omega) = \omega\sqrt{\rho}\sqrt{\kappa(\omega)}. \tag{2.4.3}$$

This is the **dispersion relation** for an homogeneous viscoelastic body with generalized compressibility $\kappa(\omega)$. The dispersion relation is the spatiotemporal frequency domain description of the wave propagation. It defines the relationship between the spatial frequency k and the temporal frequency ω. Identifying the $A(\omega)e^{-i\omega t}$ of (2.4.2) as the incoming wave $X(\omega)$ of (2.4.1) gives us the material transfer function

$$\mathfrak{T}(\omega, z) = e^{ik(\omega)z}. \tag{2.4.4}$$

To further understand the effect of spatial propagation we should split the wave number up into its real and imaginary parts. These are respectively called the **dispersion** and **attenuation** of the propagating wave.

$$k(\omega) = \mathcal{D}(\omega) - i\mathcal{A}(\omega). \tag{2.4.5}$$

Inserting this into (2.4.4) yields

$$\mathfrak{T}(\omega, z) = \underbrace{e^{i\mathcal{D}(\omega)z}}_{\text{Phase shift}} \underbrace{e^{-\mathcal{A}(\omega)z}}_{\text{Attenuation}} . \tag{2.4.6}$$

Hence, we see that $\mathcal{A}(\omega)$ gives attenuation and $\mathcal{D}(\omega)$ gives only a phase shift. The dispersion relation of an homogeneous viscoelastic body as in (2.4.3) gives the dispersion and attenuation

$$\text{Attenuation :} \qquad \mathcal{A}_{\text{vis}}(\omega) = -\omega\sqrt{\rho}\,\mathfrak{Im}\,\sqrt{\kappa(\omega)} \tag{2.4.7}$$

$$\text{Dispersion :} \qquad \mathcal{D}_{\text{vis}}(\omega) = \omega\sqrt{\rho}\,\mathfrak{Re}\,\sqrt{\kappa(\omega)}. \tag{2.4.8}$$

Also, the speed of sound is given by

$$c(\omega) = \frac{\omega}{\mathcal{D}_{\text{vis}}(\omega)}. \tag{2.4.9}$$

We must require that the material transfer function $\mathfrak{T}(\omega, z_0)$ is causal – it makes no physical sense that any part of the signal arrives at $z = z_0$ before it is sent from $z = 0$. In fact, the **Kramers-Kronig relation** is a sufficient condition to guarantee a causal transfer function. The Kramers-Kronig relation is satisfied when $\mathfrak{Im}\,\mathfrak{T}(\omega, z_0)$ is the Hilbert-transform of $\mathfrak{Re}\,\mathfrak{T}(\omega, z_0)$ and vice versa [Weaver and Pao, 1981].

$$\mathfrak{Im}\,\mathfrak{T}(\omega) = -\frac{1}{\pi}\mathcal{P}\int_{-\infty}^{\infty} \frac{\mathfrak{Re}\,\mathfrak{T}(\omega')}{\omega' - \omega}\,d\omega', \quad \text{and} \quad \mathfrak{Re}\,\mathfrak{T}(\omega) = \frac{1}{\pi}\mathcal{P}\int_{-\infty}^{\infty} \frac{\mathfrak{Im}\,\mathfrak{T}(\omega')}{\omega' - \omega}\,d\omega'$$

Here $\mathcal{P}$ denotes the Cauchy principal value integral. Furthermore, this imposes a similar condition on the complex wave number $k(\omega)$. In fact, under the assumption that we have a finite speed in the infinite frequency limit

$$c_\infty = \lim_{\omega\to\infty} c(\omega)$$

we may express this condition as [Weaver and Pao, 1981, section III]

$$\mathfrak{Im}\,k(\omega) = -\frac{\omega}{\pi}\mathcal{P}\int_{-\infty}^{\infty}\left[\frac{\mathfrak{Im}\,k(\omega')}{\omega'} - \frac{1}{c_\infty}\right]\frac{d\omega'}{\omega' - \omega} + \mathfrak{Im}\,k(0) \tag{2.4.10a}$$

$$\mathfrak{Re}\,k(\omega) = \frac{\omega}{c_\infty} + \frac{\omega}{\pi}\mathcal{P}\int_{-\infty}^{\infty}\frac{\mathfrak{Im}\,k(\omega')}{\omega'}\frac{d\omega'}{\omega' - \omega} + \mathfrak{Re}\,k(0) \tag{2.4.10b}$$

In section 4.2 we will see that these relations apply to us since the fractional Zener (and the classic Zener) indeed has finite c_∞.

Finally let us find the dispersion relation in some concrete cases. By inserting the plane harmonic wave (2.4.2) into the elastic wave equation 2.3.5 we get

$$k(\omega)^2 - \frac{1}{c^2}\omega^2 = 0,$$

which gives us the dispersion relation for an elastic medium governed by Hooke's law:

$$k(\omega) = \frac{\omega}{c}. \tag{2.4.11}$$

It says that for a monochromatic wave the spatial frequency is proportional to the time frequency. We also see that it has no imaginary part, so by (2.4.6) the wave is

not attenuated. We may continue in the same fashion and find the dispersion relation of the Zener model. Again by inserting 2.4.2 into the wave equation 2.3.6 we get

$$k(\omega)^2 - \frac{1}{c_0^2}\omega^2 + i\omega\tau_\epsilon k(\omega)^2 - \frac{\tau_\sigma}{c_0^2} i\omega^3 = 0,$$

which we may solve and find the dispersion relation

$$k(\omega) = \frac{\omega}{c_0}\left(\frac{1 + i\tau_\sigma\omega}{1 + i\tau_\epsilon\omega}\right)^{1/2}. \tag{2.4.12}$$

2.5 Propagation of left- and right-going waves

In the previous section we sent plane waves through wave equations expressed by the pressure field alone. But what about the left- and right-going waves? As we learned in section 2.3 these are linear combinations of the pressure and velocity fields. Can we expect them to propagate in the same way? To answer this we simply solve the differential equation from wave equation 2.3.4:

$$\partial_z \widehat{\boldsymbol{w}}(z,\omega) = -i\omega\Lambda\widehat{\boldsymbol{w}}(z,\omega).$$

This is done by theorem E.0.22 and we get

$$\boldsymbol{w}(z,\omega) = e^{-i\omega\Lambda z}\boldsymbol{w}(0,\omega).$$

In other words, the system propagates by multiplication with the propagator

$$\widehat{P}(z,\omega) = e^{-i\omega\Lambda z}.$$

Since Λ (see (2.3.11)) is a diagonal matrix, the matrix exponential is

$$\widehat{P}(z,\omega) = \begin{bmatrix} e^{-i\frac{\omega}{c}z} & 0 \\ 0 & e^{i\frac{\omega}{c}z} \end{bmatrix}.$$

Recall that for an elastic medium we have $k = \omega/c$. From the above we see that the right- and left-going waves propagate in the same fashion as waves through the pressure field. Though much more importantly, we see that they travel independently. This is not the case with the pressure velocity system where the pressure and velocity fields are coupled.

Now we have the necessary tools to begin to tackle the issue of spatial variation. This is really where the preliminaries end and the interesting issues begin.

Chapter 3

Scattering

Throughout the natural sciences scattering has many different faces. Within the context of acoustics though, scattering refers to something very specific. When a wave propagates through a change in the acoustic impedance of the underlying media, the wave spreads in different direction. In this process, no energy is lost, only dispersed. Furthermore, *we* work solely within an idealized 1-dimensional world where the situation is simpler still. When a wave experiences a change in acoustic impedance it will be spread, but now we have only two possible directions: Some part of the wave continues straight ahead, and the rest bounces back. Yet as in many areas of mathematics, even if the basic rules are simple, they give rise to a plethora of rich and complex behavior. We seek to explore some of these phenomena in this chapter.

3.1 Discontinuous interfaces

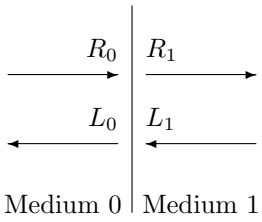

Figure 3.1: Scattering in a single interface

To understand scattering, we must begin by describing the simplest possible form, namely a wave hitting a discontinuous interface as depicted in figure 3.1. On each side of the interface we have a perfectly elastic constant medium. Indeed, throughout this entire chapter on scattering we are only dealing with elastic lossless media. To describe the right- and left-going waves, we must begin with the underlying physical pressure and velocity field. Let us imagine the interface occurs exactly at $z = z_{\text{int}}$. These waves, one for each side, must be equal at this interface to ensure continuity of the physical world; $\boldsymbol{v}_1(z_{\text{int}}, t) = \boldsymbol{v}_0(z_{\text{int}}, t)$. From (2.3.13) we get

$$\begin{aligned} E_1 \boldsymbol{w}_1(z_{\text{int}}, t) &= E_0 \boldsymbol{w}_0(z_{\text{int}}, t) \\ \boldsymbol{w}_1(z_{\text{int}}, t) &= E_1^{-1} E_0 \boldsymbol{w}_0(z_{\text{int}}, t). \end{aligned}$$

After some calculation, multiplication of $E_1^{-1}E_0$ gives the interface matrix $\mathcal{I}$:

$$\begin{bmatrix} R_1(z_{\text{int}},t) \\ L_1(z_{\text{int}},t) \end{bmatrix} = \mathcal{I} \begin{bmatrix} R_0(z_{\text{int}},t) \\ L_0(z_{\text{int}},t) \end{bmatrix}, \quad \text{where} \quad \mathcal{I} = \frac{1}{\mathcal{T}} \begin{bmatrix} 1 & \mathcal{R} \\ \mathcal{R} & 1 \end{bmatrix}. \tag{3.1.1}$$

And $\mathcal{R}$ and $\mathcal{T}$ are respectively the reflection and transmission coefficients

$$\mathcal{R} = \frac{Z_0 - Z_1}{Z_0 + Z_1}, \quad \text{and} \quad \mathcal{T} = \frac{2\sqrt{Z_0 Z_1}}{Z_0 + Z_1}.$$

One may easily check from the above definition that

$$\mathcal{R}^2 + \mathcal{T}^2 = 1,$$

from which we immediately see, as will be used later, that the determinant of J is

$$\det J = \frac{1 - \mathcal{R}^2}{\mathcal{T}^2} = 1. \tag{3.1.2}$$

The interface matrix $\mathcal{I}$ describes how the wave is affected by propagation past the interface. If we start with the left and right waves on the left-hand side of the interface $\boldsymbol{w}_0(z_{\text{int}},t)$, we simply multiply by $\mathcal{I}$ to find $\boldsymbol{w}_1(z_{\text{int}},t)$ on the other side. There is another way of capturing the same information. We could rearrange (3.1.1) using Property D.0.17 such that the left and right side of the equation contains respectively the incoming and outgoing waves. This gives a much more intuitive description of what happens (the reader is advised to carry out the matrix multiplication and compare with figure 3.1).

$$\begin{bmatrix} R_1 \\ L_0 \end{bmatrix} = \begin{bmatrix} \mathcal{T} & \mathcal{R} \\ -\mathcal{R} & \mathcal{T} \end{bmatrix} \begin{bmatrix} R_0 \\ L_1 \end{bmatrix} \tag{3.1.3}$$

3.2 Goupillaud medium and the exact solution

We will now stack up many thin layers in a row which gives us many consecutive discontinuous interfaces. This is what we call a **stratified medium**. The **Goupillaud medium** is the simplest medium of this kind. It is a stratified medium where each interface is spaced by an equal travel time $\tau_0/2$ apart. That is, it takes τ_0 seconds for the waves to travel across one layer and back. The layers are also perfectly elastic, and the underlying physical properties (density, acoustic impedance etc.) are constant within each layer.

Look at figure 3.2 to see a picture of how the wave propagates through our stratified medium. The releasing factor of our analysis is the fact that each interface is spaced apart by an equal travel time τ_0. It is apparent from figure 3.2 that we only need to keep track of what happens *at* the interfaces. If we have N interfaces, our state space consists of the left and right going waves at each location. As a mental exercise, try to envision what would happen if the travel times of the layers were different. In this case the number of wave fronts would increase indefinitely, and the mathematical state space describing the exact solution would become increasingly complex.

In the following calculations we largely follow the exposition of chapter 8 in Claerbout [1976]. Note from the top of 3.2 that apostrophe annotates which side of the layer the wave is at. From (3.1.1) we have then

$$\begin{bmatrix} R(t) \\ L(t) \end{bmatrix}_{k+1} = \mathcal{I}_k \begin{bmatrix} R(t) \\ L(t) \end{bmatrix}'_k. \tag{3.2.1}$$

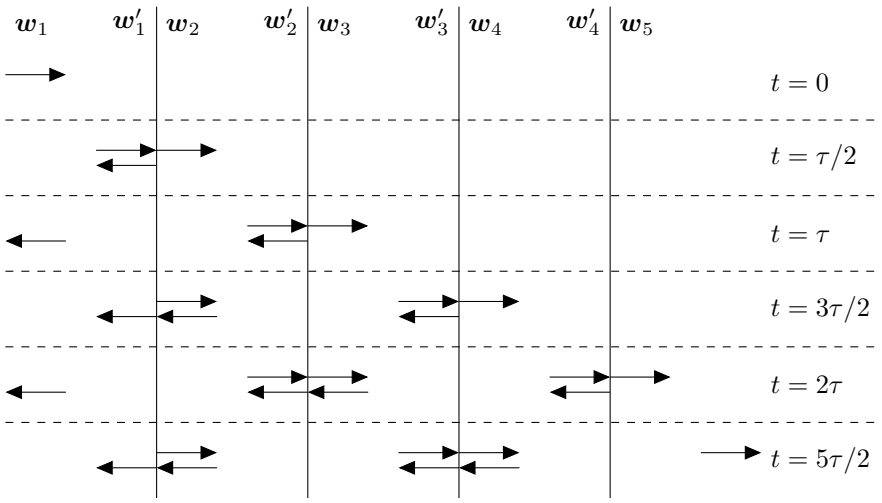

Figure 3.2: Scattering in multiple layers

We will analyze this in the frequency domain, or in fact the z-transform. To distinguish between the spatial variable z and the variable of the z-transform, we use ξ for the latter. Formally we have multiple layers of different thickness Δz_j and different speed c_j. The layers are spaced such that the travel time equals $\Delta z_j/c_j = \tau_0/2$ for all layers. Remember further from section 2.4 that propagating across a distance Δz in the frequency domain is the same as multiplying the wave by $e^{-ik_j\Delta z_j}$. Each such propagator becomes

$$e^{-ik_j\Delta z_j} = e^{-i\frac{\omega}{c_j}\Delta z_j} = e^{-i\omega\tau_0/2} \tag{3.2.2}$$

The fact that this is equal for all layers is the essence of the Goupillaud medium. It is clear from figure 3.2 that, with $\xi = e^{-i\omega\tau_0}$, propagation across a layer is described by

$$\begin{bmatrix} \widehat{R}(\xi) \\ \widehat{L}(\xi) \end{bmatrix}_k' = \begin{bmatrix} \xi^{-1/2} & 0 \\ 0 & \xi^{1/2} \end{bmatrix} \begin{bmatrix} \widehat{R}(\xi) \\ \widehat{L}(\xi) \end{bmatrix}_k. \tag{3.2.3}$$

Inserting this into (3.2.1) we get the recursive propagation relation

$$\begin{aligned} \begin{bmatrix} \widehat{R}(\xi) \\ \widehat{L}(\xi) \end{bmatrix}_{k+1} &= \frac{1}{\mathcal{T}_k} \begin{bmatrix} 1 & \mathcal{R}_k \\ \mathcal{R}_k & 1 \end{bmatrix} \begin{bmatrix} \xi^{-1/2} & 0 \\ 0 & \xi^{1/2} \end{bmatrix} \begin{bmatrix} \widehat{R}(\xi) \\ \widehat{L}(\xi) \end{bmatrix}_k \\ &= \widehat{J}_k(\xi) \begin{bmatrix} \widehat{R}(\xi) \\ \widehat{L}(\xi) \end{bmatrix}_k \end{aligned}$$

where $\widehat{J}_k(\xi)$ is the effect of propagating across layer k and then hitting interface k:

$$\widehat{J}_k(\xi) = \mathcal{I}_k\widehat{P}_k(\xi) = \frac{\sqrt{\xi}}{\mathcal{T}_k} \begin{bmatrix} \xi^{-1} & \mathcal{R}_k \\ \mathcal{R}_k\xi^{-1} & 1 \end{bmatrix}.$$

Trivially, we have that

$$\begin{bmatrix} \widehat{R}(\xi) \\ \widehat{L}(\xi) \end{bmatrix}_{k+1} = \widehat{J}_k(\xi)\widehat{J}_{k-1}\cdots\widehat{J}_1(\xi)\begin{bmatrix} \widehat{R}(\xi) \\ \widehat{L}(\xi) \end{bmatrix}_1. \tag{3.2.4}$$

What does the cumulative product $K_k(\xi) := \widehat{J}_k(\xi)\widehat{J}_{k-1}\cdots\widehat{J}_1(\xi)$ look like? By induction, one can easily demonstrate it is on the form

$$K_k(\xi) = \frac{\sqrt{\xi}^k}{\prod_{i=1}^k \mathcal{T}_i}\begin{bmatrix} \xi^{-k}F_k(\frac{1}{\xi}) & G_k(\xi) \\ \xi^{-k}G_k(\frac{1}{\xi}) & F_k(\xi) \end{bmatrix}. \tag{3.2.5}$$

First note it is obviously true for $K_1 = J_1$, in which case $F_1(\xi) = 1$ and $G_1(\xi) = \mathcal{R}_1$. Furthermore

$$\begin{aligned} K_{k+1}(\xi) &= J_{k+1}(\xi)K_k(\xi) \\ &= \frac{\sqrt{\xi}}{\mathcal{T}_{k+1}}\begin{bmatrix} \xi^{-1} & \mathcal{R}_{k+1} \\ \mathcal{R}_{k+1}\xi^{-1} & 1 \end{bmatrix}\frac{\sqrt{\xi}^k}{\prod_{i=1}^k \mathcal{T}_i}\begin{bmatrix} \xi^{-k}F_k(\frac{1}{\xi}) & G_k(\xi) \\ \xi^{-k}G_k(\frac{1}{\xi}) & F_k(\xi) \end{bmatrix} \\ &= \frac{\sqrt{\xi}^{k+1}}{\prod_{i=1}^{k+1} \mathcal{T}_i} \\ &\quad \times \begin{bmatrix} \xi^{-k-1}F_k(\frac{1}{\xi}) + \mathcal{R}_{k+1}\xi^{-k}G_k(\frac{1}{\xi}) & \xi^{-1}G(\xi) + \mathcal{R}_{k+1}F_k(\xi) \\ \mathcal{R}_{k+1}\xi^{-k-1}F_k(\frac{1}{\xi}) + \xi^{-k}G_k(\frac{1}{\xi}) & \mathcal{R}_{k+1}\xi^{-1}G_k(\xi) + F_k(\xi) \end{bmatrix} \end{aligned}$$

which upon reflection is indeed on the form of (3.2.5). This gives us a recursive definition of our unknown polynomials $F_k(\xi)$ and $G_k(\xi)$:

$$F_{k+1}(\xi) = F_k(\xi) + \mathcal{R}_{k+1}\xi^{-1}G_k(\xi) \tag{3.2.6}$$

$$G_{k+1}(\xi) = \mathcal{R}_{k+1}F_k(\xi) + \xi^{-1}G_k(\xi). \tag{3.2.7}$$

By increasing k up to N we see immediately from (3.2.4) that we can describe the action of all layers at once as

$$\begin{bmatrix} \widehat{R}_N(\xi) \\ \widehat{L}_N(\xi) \end{bmatrix} = K_N(\xi)\begin{bmatrix} \widehat{R}_1(\xi) \\ \widehat{L}_1(\xi) \end{bmatrix}. \tag{3.2.8}$$

Remember that the closed form of $K_N(\xi)$ is given by (3.2.5). By noting that $\det K_N(\xi) = \det\prod_{i=1}^k J_k(\xi) = \prod_{i=1}^k \det J_k = 1$ we can apply the switch around Property D.0.17 to (3.2.8) and get

$$\begin{bmatrix} \widehat{R}_{N+1}(\xi) \\ \widehat{L}_1(\xi) \end{bmatrix} = \frac{\prod_{i=1}^N \mathcal{T}_i}{\sqrt{\xi}^N F_N(\xi)}\begin{bmatrix} 1 & \frac{\sqrt{\xi}^N G_N(\xi)}{\prod \mathcal{T}_i} \\ -\frac{G(\frac{1}{\xi})}{\sqrt{\xi}^N \prod \mathcal{T}_i} & 1 \end{bmatrix}\begin{bmatrix} \widehat{R}_1(\xi) \\ \widehat{L}_{N+1}(\xi) \end{bmatrix}$$

We have made this into a statement of outgoing waves as a function of incoming waves. If we now assume that our input signal is $\widehat{R}(\xi)_1$ and then set $L_{N+1}(\xi) = 0$, i.e. there is no wave being sent through the opposite way at the same time, we can now express the output signal

$$\widehat{R}_{N+1}(\xi) = \widehat{\mathfrak{T}}(\xi)\widehat{R}_1(\xi), \quad \text{and} \quad \widehat{L}_1(\xi) = \widehat{\mathfrak{R}}(\xi)\widehat{R}_1(\xi)$$

where

$$\widehat{\mathfrak{T}}(\xi) = \frac{\prod_i^N \mathcal{T}_i}{\sqrt{\xi}^N F_N(\xi)}, \quad \text{and} \quad \widehat{\mathfrak{R}}(\xi) = -\frac{G_N(\frac{1}{\xi})}{\xi^N F_N(\xi)} \tag{3.2.9}$$

are respectively the material transfer function of the medium, and the material reflection function. This gives the exact solution to the problem. Here we can even see by the $\sqrt{\xi}^{-N}$ term the time delay of the initial wave front that comes through the whole slab of material. It should also hold that $F_N(\xi)$ is minimum phase. Clearly $F_1(\xi) = 1$ is minimum phase. If we again use the fact that $\det K_N(\xi) = 1$ we get from (3.2.5) that

$$F_N(\xi)F_N(\tfrac{1}{\xi}) - G_N(\xi)G_N(\tfrac{1}{\xi}) = \prod \mathcal{T}_i^2 > 0 \tag{3.2.10}$$

meaning that the spectrum of $F_N(\xi)$ is greater than the spectrum of $G_N(\xi)$. We can then use the "addition of small noise to a minimum phase filter" property A.0.10 and see from (3.2.6) that $F_k(\xi)$ is minimum phase (note that since $|\mathcal{R}_{k+1}| < 1$ the spectrum of $\mathcal{R}_{k+1}\xi^{-1}G_k(\xi)$ is even smaller than the spectrum of $G_k(\xi)$). In the preceding ξ is assumed on the unit-circle. For such circumstances the spectrum of F is $|F(\xi)|^2 = F(\xi)F(\xi)^* = F(\xi)F(\frac{1}{\xi})$.

One more important observation is due. Let us investigate if there is energy lost inside the slab of medium by adding up the power exiting at both ends.

$$|\widehat{\mathfrak{T}}(\xi)|^2 + |\widehat{\mathfrak{R}}(\xi)|^2 = \frac{\prod \mathcal{T}_i^2 + |G(\xi)|^2}{|F_N(\xi)|^2} = 1 \tag{3.2.11}$$

The last equality is by (3.2.10). We see then that no energy is lost inside the slab – that is if one is willing to wait long enough. The wave is bouncing back and forth within the slab, so in reality one would have to wait for eternity for all energy to escape. Though the parts which arrive very late – the parts which have bounced back and forth many times – are in general so small they can be justifiably ignored.

In general the complete analytical description of $F_N(\xi)$ is not tractable, but for certain specific scenarios it is possible to gain more explicit theoretical expressions. This can for instance be done for a medium with alternating layers called Briggs resonance. See chapter 3 of Fouque et al. [2007] for details.

3.3 The O'Doherty-Anstey approximation

We will now devise the famous O'Doherty-Anstey approximation. It was first presented in O'Doherty and Anstey [1971], and it gives an approximate description of the transfer function of a Goupillaud medium. We will follow a different route than is done in the original paper O'Doherty and Anstey [1971] building directly on the work we have already done, though parallels are drawn to the original article when important milestones in the argument are reached.

By looking at (3.2.9) we have the transfer function

$$\widehat{\mathfrak{T}}(\xi) = \frac{\prod_i^N \mathcal{T}_i}{\sqrt{\xi}^N F_N(\xi)}.$$

At the heart of the ODA theory lies the assumption that the reflection coefficients are small. In light of this are able to approximate $F_N(\xi)$ and $G_N(\xi)$. We begin with

the observation that they have the general form

$$F_k(\xi) = 1 + \sum_{1 \le i < j \le k} \mathcal{R}_i \mathcal{R}_j \xi^{i-j} + F_k^\dagger(\xi) \tag{3.3.1}$$

$$G_k(\xi) = \sum_{i=1}^{k} \mathcal{R}_i \xi^{i-k} + G_k^\dagger(\xi) \tag{3.3.2}$$

where $F_k^\dagger(\xi)$ and $G_k^\dagger(\xi)$ only contain higher order terms of reflection coefficients, or to be precise, 3 or more reflection coefficients multiplied together. Again, this trivially holds true for $F_1(\xi) = 1$ and $G_1(\xi) = \mathcal{R}_1$. By inserting (3.3.1) and (3.3.2) into (3.2.6) and (3.2.7) one can confirm, after some computation, that the form is indeed correct. Note that since the $\mathcal{R}_i$'s are small $F_N(\xi)$ is close to 1. Using the Taylor expansion $\frac{1}{x} \approx 2 - x$ around 1 we get

$$\begin{aligned} \widehat{\mathfrak{T}}(\xi) &\approx (2 - F_N(\xi)) \frac{\prod \mathcal{T}_i}{\sqrt{\xi}^N} \\ &\approx (1 - \sum_{1 \le i < j \le N} \mathcal{R}_i \mathcal{R}_j \xi^{i-j}) \frac{\prod \mathcal{T}_i}{\sqrt{\xi}^N}. \end{aligned} \tag{3.3.3}$$

In the last approximation we have ignored $F_N^\dagger(\xi)$ since it only contains higher multiples of something small. Furthermore we can find what really lies behind the sum

$$\sum_{1 \le i < j \le N} \mathcal{R}_i \mathcal{R}_j \xi^{i-j} = \sum_{k=1}^{N-1} \left(\sum_{1=1}^{N-k} \mathcal{R}_i \mathcal{R}_{i+k} \right) \xi^{-k}. \tag{3.3.4}$$

From this we may define the sample autocorrelation function

$$\phi_{\mathcal{R}}[k] := \frac{1}{N} \sum_{i=1}^{\max(N-|k|,0)} \mathcal{R}_i \mathcal{R}_{i+|k|}. \tag{3.3.5}$$

Let us remind ourselves that the spectrum of a function is given by the transform (here to the z-domain) of the autocorrelation function

$$S_{\mathcal{R}}(\xi) = \mathcal{Z}\left\{\phi_{\mathcal{R}}[k]; \xi\right\}.$$

We need the autocorrelation of only positive lags

$$\phi_{\mathcal{R}}^+[k] := \begin{cases} \phi_{\mathcal{R}}[k] & \text{for } k \ge 1 \\ 0 & \text{otherwise,} \end{cases}$$

and its corresponding spectrum of only positive lags $S_{\mathcal{R}}^+(\xi) := \mathcal{Z}\left\{\phi_{\mathcal{R}}^+[k]; \xi\right\}$. Note that they are used in the appendix of O'Doherty and Anstey [1971] under the names $a(l) = N\phi_{\mathcal{R}}[l]$, $-m(l) = N\phi_{\mathcal{R}}^+[l]$ and $-M(\xi) = NS_{\mathcal{R}}^+(\xi)$. We may define $\phi_{\mathcal{R}}^-[k]$ and $S_{\mathcal{R}}^-(\xi)$ in the obvious way and get

$$S_{\mathcal{R}}(\xi) = S_{\mathcal{R}}^+(\xi) + S_{\mathcal{R}}^-(\xi) + \phi_{\mathcal{R}}[0]. \tag{3.3.6}$$

Looking at (3.3.4) we may now rewrite it as

$$\sum_{1 \le i < j \le N} \mathcal{R}_i \mathcal{R}_j \xi^{i-j} = NS_{\mathcal{R}}^+(\omega),$$

and finally observe that

$$\sum \mathcal{R}_i^2 = N\phi_{\mathcal{R}}[0].$$

Putting all this to use together with a repeated application of $e^x \approx 1 + x$ we can finish the approximation we started in (3.3.3):

$$\begin{aligned}\widehat{\mathfrak{T}}(\xi) &\approx \sqrt{\xi}^{-N}(1 - NS_{\mathcal{R}}^+(\xi))\prod_{i=1}^{N}\sqrt{1-\mathcal{R}_i^2} \\ &\approx \sqrt{\xi}^{-N}\exp\left\{-NS_{\mathcal{R}}^+(\xi)\right\}\prod_{i=1}^{N}\exp\left\{-\frac{1}{2}\mathcal{R}_i^2\right\}\end{aligned}$$

which gives us an approximation of the material transfer function

$$\widehat{\mathfrak{T}}(\xi) \approx \sqrt{\xi}^{-N}e^{-N[\frac{1}{2}\phi_{\mathcal{R}}[0]+S_{\mathcal{R}}^+(\xi)]} \tag{3.3.7}$$

This is exactly expression (12) in the appendix of O'Doherty and Anstey [1971], though they have a factor 2 since they go back and forth, but we go through the medium only once. Again, the $\sqrt{\xi}^{-N}$ in the equation above represents the initial wave front. The following exponential describes the part of the signal which arrives later, after having bounced back and forth inside the slab. This is often referred to as the wave **coda**. We may further find the attenuation of the material transfer function

$$\begin{aligned}|\widehat{\mathfrak{T}}(\xi)|^2 &= \widehat{\mathfrak{T}}^*(\xi)\widehat{\mathfrak{T}}(\xi) \\ &\approx |\xi|^{-N}e^{-N[\frac{1}{2}\phi_{\mathcal{R}}[0]+S_{\mathcal{R}}^+(\xi)^*]}e^{-N[\frac{1}{2}\phi_{\mathcal{R}}[0]+S_{\mathcal{R}}^+(\xi)]} \\ &= |\xi|^{-N}e^{-N[\phi_{\mathcal{R}}[0]+S_{\mathcal{R}}^+(\xi)^*+S_{\mathcal{R}}^+(\xi)]}.\end{aligned} \tag{3.3.8}$$

Let us define the arrival time $T = N\tau_0/2$ which is the time it takes to cross the entire slab of material. If the reflection coefficients are small, the variation in impedance is small, and in turn, the speed of sound is nearly constant. For now let us call this the "average" speed $\bar{c}$. Then intuitively $T\bar{c} = L$, and we get $N = \frac{2L}{\tau_0\bar{c}}$. Furthermore, since $\phi_{\mathcal{R}}[k] = \phi_{\mathcal{R}}[-k]$ we get that, on the unit-circle $|\xi| = 1$, $S_{\mathcal{R}}^+(\omega)^* = S_{\mathcal{R}}^-(\omega)$. Inserting all this into (3.3.8) and using $\xi = e^{-i\omega\tau_0}$ as well as (3.3.6) we get

$$|\widehat{\mathfrak{T}}(\omega)| \approx e^{-\frac{1}{\tau_0\bar{c}}S_{\mathcal{R}}(\omega\tau_0)L} \tag{3.3.9}$$

What we have now discovered is quite grand. We have found that we can describe our material transfer function from the reflection coefficients alone! Indeed, this is the **O'Doherty-Anstey-approximation (ODA)**. It is a key result that we will refer to time and time again. We call this attenuation

$$\mathcal{A}_{\text{scat}}(\omega) = \frac{1}{\tau_0\bar{c}}S_{\mathcal{R}}(\omega\tau_0) \tag{3.3.10}$$

for the **apparent attenuation**. It is *so* called since no energy is really lost. Remember from (3.2.11) that the rest of the energy is reflected back. Finally, another significant strength of the ODA theory is that the approximate transfer function (3.3.7) is known to be causal [Banik et al., 1985].

We should be more specific about our definition of $\bar{c}$. The total travel time is given by

$$T = \int_0^L \frac{1}{c(z)}dz = L\left\langle \tfrac{1}{c(z)} \right\rangle.$$

We may then define the average speed in the obvious way $\bar{c} = L/T$:

$$\bar{c} = \left\langle \tfrac{1}{c(z)} \right\rangle^{-1}$$

This is also called the homogenized speed [Fouque et al., 2007].

Comparing (3.3.9) to (1.0.1) and (1.0.2) we see that the only missing piece on our quest to explain power-law attenuation as described in the introduction, is for $S_{\mathcal{R}}(\omega)$ to resemble the power-law relation (1.0.2) with exponent $\gamma \in (0, 2)$. This is exactly what we will explore in the next section.

3.4 Spatially fractional media with power-law attenuation

Recall that in the introduction we saw examples of media with power-law attenuation with $\gamma \in (0, 2)$. Especially in medical applications we saw an exponent close to 1. By comparing (3.3.9) to our original sentiment (1.0.1) and (1.0.2) it is clear that the attenuation is described by the spectrum of the reflection coefficients. Thus we would like to be able to model reflection coefficients with a power-law spectrum with exponents in the $(0, 2)$ range. Let us remember where the reflection coefficients come from. We have the following chain of physical concepts.

$$\underbrace{\rho, \kappa_0}_{\substack{\text{Physical variables of} \\ \text{the underlying medium}}} \implies \underbrace{Z = \sqrt{\frac{\rho}{\kappa_0}}}_{\text{Acoustic impedance}} \implies \underbrace{\mathcal{R}_i = \frac{Z_i - Z_{i+1}}{Z_i + Z_{i+1}}}_{\text{Reflection coefficient}} \tag{3.4.1}$$

We see that if we endow the physical parameters ρ and/or κ_0 with a spatial structure, their structure percolate up and finally give rise to spatial structure in the reflection coefficients. We will now look at how the spectrum of the acoustic impedance and the reflection coefficients relate to each other.

Let us parametrize the acoustic impedance not by the spatial z variable, but by the travel time τ. Since τ_0 is the time to cross two layers, we would have $Z(\tau) = Z_{\lceil 2\tau/\tau_0 \rceil}$, where $\lceil . \rceil$ is the ceiling function. Likewise, the reflection coefficients by travel time is $\mathcal{R}(\tau) = \mathcal{R}_{\lceil 2\tau/\tau_0 \rceil}$. We may then reformulate the reflection coefficients as

$$\mathcal{R}(\tau) = \mathcal{R}_i = \frac{Z_i - Z_{i+1}}{Z_i + Z_{i+1}} \approx \frac{\tau_0}{2} \frac{\partial_\tau Z(\tau)}{2Z(\tau)} = \frac{\tau_0}{4} \partial_\tau \log Z(\tau), \text{ where } i = \lceil 2\tau/\tau_0 \rceil \tag{3.4.2}$$

Using theorem A.0.11 we get

$$\tfrac{1}{\tau_0} S_{\mathcal{R}}(\omega\tau_0) = \tfrac{1}{N} |\mathcal{F}\{\mathcal{R}_i; \omega\tau_0\}|^2 \approx \tfrac{1}{N} \left| \mathcal{F}\left\{ \tfrac{1}{\tau_0} \mathcal{R}_{\lceil \tau/\tau_0 \rceil}; \omega \right\} \right|^2. \tag{3.4.3}$$

Note that $\mathcal{R}_i$ is a discrete series and $\mathcal{R}_{\lceil \tau/\tau_0 \rceil}$ is continuous in τ. Hence the second approximation approximates the sum on the left by the integral on the right. See definition A.0.1. Furthermore, we may calculate

$$\begin{aligned}
\tfrac{1}{N} \left| \mathcal{F}\left\{ \tfrac{1}{\tau_0} \mathcal{R}_{\lceil \tau/\tau_0 \rceil}; \omega \right\} \right|^2 &\approx \tfrac{1}{N} \left| \mathcal{F}\left\{ \tfrac{1}{4} \partial_\tau \log Z(\tau/2); \omega \right\} \right|^2 && \text{by (3.4.2)} \\
&= \tfrac{1}{N} \left| \mathcal{F}\left\{ \tfrac{1}{2} \partial_\tau \log Z(\tau); 2\omega \right\} \right|^2 && \text{by (A.0.2)} \\
&= \tfrac{1}{N} \left| \mathcal{F}\left\{ \tfrac{1}{2} (i2\omega) \log Z(\tau); 2\omega \right\} \right|^2 && \text{by property } A.0.4 \\
&= \tfrac{1}{2} \omega^2 S_{\log Z(\tau)}(2\omega). && \text{by theorem } A.0.11
\end{aligned}$$

All in all this gives us the relation

$$\tfrac{1}{\tau_0} S_{\mathcal{R}}(\omega\tau_0) = \tfrac{1}{2}\omega^2 S_{\log Z(\tau)}(2\omega)$$

which is precisely the relation found in Banik et al. [1985, equation (16)] and the apparent attenuation becomes

$$\mathcal{A}_{\text{scat}}(\omega) = \frac{1}{2\bar{c}}\omega^2 S_{\log Z(\tau)}(2\omega). \tag{3.4.4}$$

It is apparent then that if we can create a spatial structure such that

$$S_{\log Z(\tau)}(\omega) \;\propto\; 1/\omega^{\alpha}, \quad \text{then} \quad \mathcal{A}_{\text{scat}}(\omega) \;\propto\; \omega^{2-\alpha}. \tag{3.4.5}$$

If we are able to chose $\alpha \in (0, 2)$ we reach our ambition to model attenuation with exponent $\gamma \in (0, 2)$. But how do we put this spatial structure into operation?

First we may intuit that $z(\tau) \approx \tau\bar{c}$, though in reality, sometimes the wave is in front of this "average" wavefront, and sometimes it is behind. But since we assume that the spatial variations are small, the variations in speed are negligible. Within this context, whether we talk about the spectrum as experienced by the travel time or as spanned spatially is only a simple scaling. Since $Z(z) \approx Z(\tau = z/\bar{c})$ we get by A.0.2 that

$$S_{\log Z(z)}(\omega) = \bar{c}^2 S_{\log Z(\tau)}(\bar{c}\omega).$$

We would like to model the spatial structure through the fundamental physical variables ρ and κ_0 that constitute the media. Let us assume that ρ is constant and that $\kappa_0(z)$ has a spatial structure as in Burridge et al. [1993, equation 91]. Then we have

$$\kappa_0(z) = \bar{\kappa}_0 e^{-\sigma\nu(z)}, \tag{3.4.6}$$

where $\nu(z)$ is a spatially varying process with zero mean. If we move up the chain of (3.4.1) we get that

$$Z(z) = \sqrt{\frac{\rho}{\bar{\kappa}_0}} e^{\sigma\nu(z)},$$

and,

$$\log(Z(z)) = \log\sqrt{\frac{\rho}{\kappa_0}} + \sigma\nu(z),$$

which has the spectrum

$$S_{\log(Z)}(\omega) = \sigma^2 S_{\nu}(\omega) + \left(\log\sqrt{\frac{\rho}{\bar{\kappa}_0}}\right)^2 \delta(\omega).$$

So we have successfully reduced our mission to finding a process $\nu(z)$ with a power-law spectrum with exponent $\alpha \in (-2, 0)$. This is exactly what we investigate in the next sections. We will examine several theoretical sources of such processes and discuss briefly how to simulate them. Finally from section 3.4.8 and onwards, we discuss the physical feasibility and interpretation of the different theoretical models.

Obviously there are many ways of operationalizing spatial structure: One could equally well model spatial variation in ρ. Currently we focus our attention on the classic approach of implementing spatial structure in the instantaneous response (κ_0 or J_{in}) which is the approach embraced in Le and Burridge [1998] and Burridge et al. [1993]. Though in chapter 6 we investigate the possibility of spatial variation in the remaining viscoelastic state variables τ_σ and τ_ϵ.

3.4.1 ARMA approximations. Let us investigate the possibility of creating an ARMA filter with a $1/\omega^\alpha$ spectrum. To begin we attempt to illustrate that this can not be done (for all frequencies at once). We begin by factorizing the $1/\omega^\alpha$ spectrum and find the filter

$$H(s = i\omega) = \frac{1}{s^{\alpha/2}}$$

The next step is to discretize it. The standard method here is the Tustin transformation

$$s = \frac{\xi - 1}{\xi + 1}.$$

Inserting this into the filter above gives us

$$H(\xi) = \frac{(\xi + 1)^{\alpha/2}}{(\xi - 1)^{\alpha/2}}.$$

In an ARMA model we can only accept integer powers of z (which corresponds to integer delays in time domain). We may try to approximate $(\xi - 1)^{\alpha/2}$ by a Taylor expansion. It is clear that this expansion must work on the unit-circle $|z| = 1$ for us to achieve the desired spectral properties. Also it must be a real expansion since we can not have imaginary coefficients in our ARMA model. This leaves us with $z = \pm 1$. But if we try to expand $(\xi - 1)^{\alpha/2}$ around $z = 1$, which corresponds to expanding $f(x) = x^{\alpha/2}$ around 0, we see that $f'(0) = \infty$. In other words, we need to approach infinitely many powers of x to approach the original expression. Thus, we need to approach infinitely many state variables in our ARMA model to approach the $1/\omega^\alpha$ spectrum. The case of expanding around $z = -1$ meets the same destiny for the numerator of the filter above.

Though the case for ARMA approximations seems hopeless we will look at two ingenious methods for approximating the $1/\omega^\alpha$ spectrum within the ARMA regime. This method concentrates the impact of the ARMA coefficients such that the spectrum quickly converges to $1/\omega^\alpha$ in a small frequency band, rather than trying to converge for all frequencies at once. Both of these methods build upon the notion of a **relaxation process**. The autocorrelation function of a relaxation process with relaxation time τ is

$$\phi_{\text{rel}}(z; \tau) = e^{-\tau|z|},$$

and it has the corresponding Lorenzian spectrum

$$S_{\text{rel}}(\omega; \tau) = \frac{2\tau}{\tau^2 + \omega^2} \tag{3.4.7}$$

which is obviously

$$S_{\text{rel}}(\omega; \tau) \sim \frac{1}{\omega^2} \quad \text{as } \omega \to \infty.$$

So it follows $1/\omega^2$ for large frequencies, and one may easily show that it becomes white approximately below $\omega = \tau$. The spectral factorization is given by

$$H_{\text{rel}}(s = i\omega; \tau) = \frac{\sqrt{2\tau}}{s + \tau}. \tag{3.4.8}$$

It is clear then that we can create a relaxation process by filtering white noise through the above filter. Also, this filter will nicely discretize by the aforementioned Tustin transform. In the first approximation method, due to van der Ziel, many uncorrelated

relaxation processes are added in parallel. In the second method, due to Keschner, one stream of random noise is fed through many filters of the kind (3.4.8). See the excellent book Wornell [1996, section 3.3.1] for a more in depth analysis and further references to the works of van der Ziel and Keschner.

According to the theory of van der Ziel, we can add a continuum of relaxation processes in parallel and get the resulting effective spectrum

$$S_{\text{effective}}(\omega;\alpha) = \int_0^\infty S_{\text{rel}}(\omega;\tau) f(\tau;\alpha) d\tau. \tag{3.4.9}$$

This is an integral weighted by the density function $f(\tau;\alpha) = \tau^{-\alpha}$, i.e. we want more of the processes with low relaxation time, and few of the ones with long relaxation time. If we make the substitution $x = \frac{\tau}{\omega}$ we may rewrite (3.4.9) and get

$$S_{\text{effective}}(\omega;\alpha) = \frac{2}{\omega^\alpha} \int_0^\infty x^{1-\alpha} \frac{1}{1+x^2} dx \propto \frac{1}{\omega^\alpha},$$

and we have shown that it indeed follows the desired power-law. Furthermore, integral (3.4.9) may be approximated in the obvious way by choosing exponentially spaced relaxation times $\tau_n = \Delta^n$ for $n \in \mathbb{Z}$:

$$S_{\text{effective}}(\omega;\alpha) \approx \sum_{n=-\infty}^{\infty} \Delta S_{\text{rel}}(\omega;\Delta^n) f(\Delta^n;\alpha) = \sum_{n=-\infty}^{\infty} \frac{\Delta^{(2-\alpha)n}}{\omega^2 + \Delta^{2n}}.$$

See figure 3.3 where we have calculated the above sum by truncating it to runs from $-N$ to N. We see that it converges quickly and that $N = 7$ is enough to approximate $1/\omega^{0.8}$ over about 6 decades.

We swiftly move on to the next method due to Keschner by attempting to put filters of the kind (3.4.8) in series [Plaszczynski, 2007, section 2.2]. This time we use a variation of (3.4.7)

$$S_{\text{rel}}(\omega;\omega_0,\omega_1) = \frac{\omega^2 + \omega_1^2}{\omega^2 + \omega_0^2}.$$

This spectrum is different from (3.4.7) in that it is white approximately above ω_1 and below ω_0. It only admits the $1/\omega^2$ in a band between them. Again it easily factorizes to

$$H_{\text{rel}}(s = i\omega;\omega_0,\omega_1) = \frac{s+\omega_1}{s+\omega_0}. \tag{3.4.10}$$

Again let us define our target. We want to approximate

$$S_{\text{target}}(\omega;\alpha,\omega_0,\omega_1) = |S_{\text{rel}}(\omega;\omega_0,\omega_1)|^{\alpha/2}.$$

Since $S_{\text{rel}}(\omega;\omega_0,\omega_1)$ admits $1/\omega^2$ between ω_0 and ω_1, taking it to the power of $\alpha/2$ gives us the desired exponent of α. Furthermore, we numerically verify, that if we if we use N filters, and choose the variables $\{\omega_{0,n}\}_{n=1}^N$ and $\{\omega_{1,n}\}_{n=1}^N$ wisely, the target may be approximated by

$$S_{target}(\omega;\alpha,\omega_0,\omega_1) \approx \prod_{n=0}^{N} \frac{\omega^2 + \omega_{1,n}^2}{\omega^2 + \omega_{0,n}^2}.$$

Plaszczynski [2007, section 2.2] recommends placing the parameters at

$$\begin{aligned} \omega_{0,n} &= \Delta^{n+\frac{1}{2}(1-\frac{\alpha}{2})}\omega_0 \\ \omega_{1,n} &= \omega_{0,n}\Delta^{\frac{\alpha}{2}} \end{aligned}$$

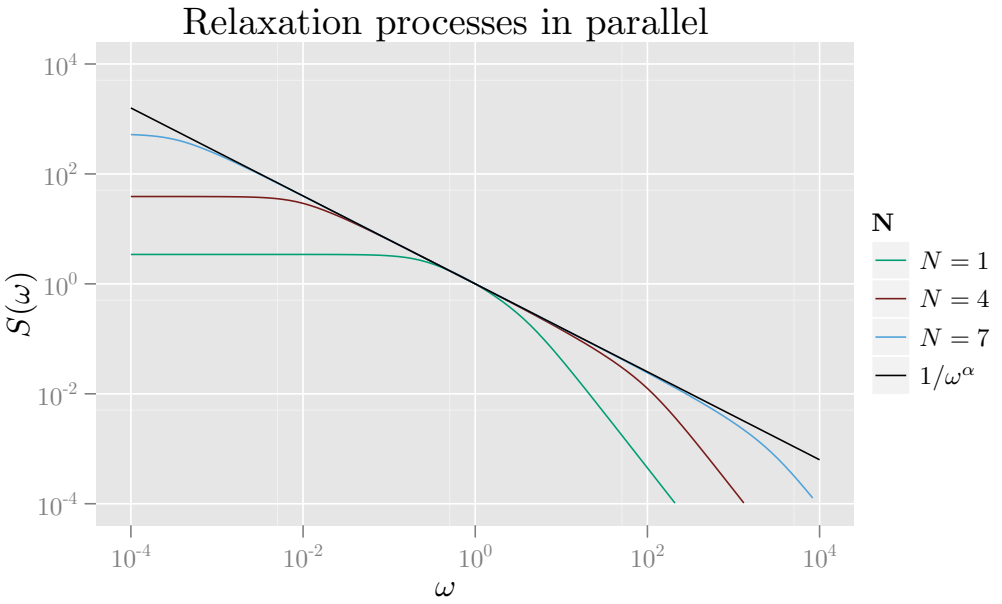

Figure 3.3: Relaxation processes in parallel with $\Delta = 3$ and $\alpha = 0.8$

with

$$\Delta = \sqrt[N]{\frac{\omega_1}{\omega_0}}.$$

See figure 3.4 for a demonstration of its convergence. We see again that $N = 7$ renders it indistinguishable from $1/\omega^{0.8}$ over about 6 decades.

In the end we have demonstrated the ARMA models can in fact approximate a $1/\omega^\alpha$ spectrum quite well in a limited frequency band.

3.4.2 Long-range and short-range dependence. We are about to introduce several different processes that may serve to model the physical properties of a medium through (3.4.6). However, these processes fall into two categories which require separate theoretical treatment. We must distinguish between processes with short-range dependence and long-range dependence.

A process exhibits **short-range dependence (SRD)** if its autocorrelation function decays fast enough that it is absolutely summable:

$$\int_0^\infty |\phi(z)|dz < \infty$$

Such processes are also sometimes called **mixing**. In contrast, a process exhibits **long-range dependence (LRD)** if its autocorrelation function is not absolutely summable:

$$\int_0^\infty |\phi(z)|dz = \infty \tag{3.4.11}$$

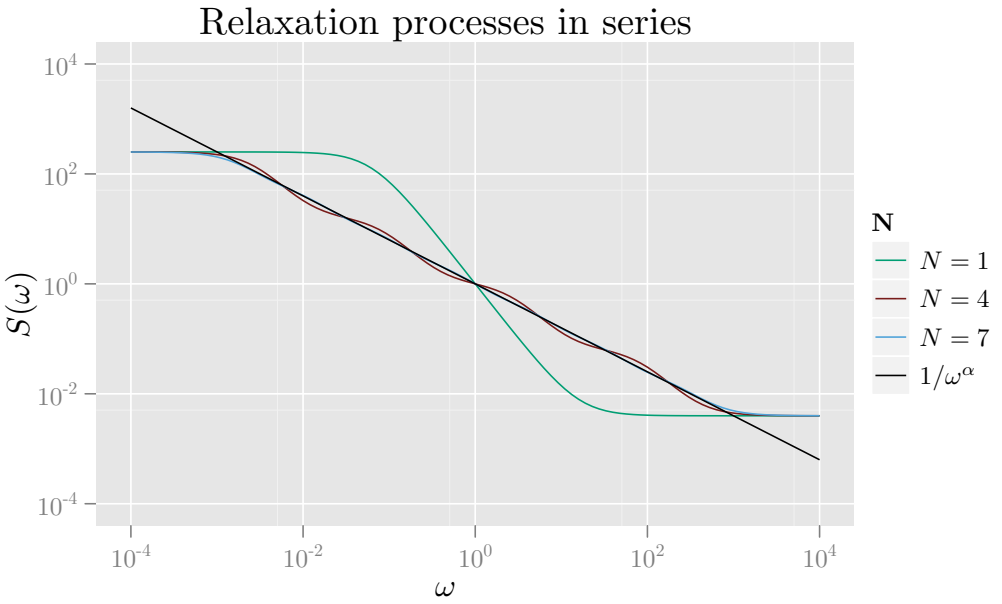

Figure 3.4: Relaxation processes in series with $\omega_0 = 10^{-3}$, $\omega_1 = 10^3$ and $\alpha = 0.8$

In Garnier and Sølna [2010] we find a more concrete description of short range dependence

$$\phi_{\text{SRD}}(z) \underset{|z|\to 0}{\sim} \phi(0)\left(1 - a|z|^{\beta_S} + O(|z|)\right), 0 < \beta_S < 1.$$

A well established alternative to the definition (3.4.11) of long range dependence [Beran, 1994; Lim and Muniandy, 2003] is

$$\phi_{\text{LRD}}(z) \underset{|z|\to\infty}{\sim} a\frac{1}{|z|^{\beta_L}}, \qquad 0 < \beta_L < 1.$$

Within this context SRD processes are associated with spectra on the form [Garnier and Sølna, 2010]

$$S_{\text{SRD}}(\omega) \underset{|\omega|\to\infty}{\sim} \frac{1}{\omega^{\alpha_S}}, \qquad 1 < \alpha_S = \beta_S + 1 < 2$$

and the LRD processes are associated with spectra on the form [Beran, 1994; Lim and Muniandy, 2003]

$$S_{\text{LRD}}(\omega) \underset{|\omega|\to 0}{\sim} \frac{1}{\omega^{\alpha_L}}, \qquad 0 < \alpha_L = 1 - \beta_L < 1$$

The first lesson to learn from this is that in the SRD case the behavior of the spectrum as the frequency approaches infinity is dictated by the behavior of the autocorrelation function around 0. In the LRD case the opposite is true. The behavior of the spectrum around 0 is dictated by the behavior of the autocorrelation as the lag approaches

infinity. In view of (3.4.5) we get in the SRD and LRD case the total scattering exponent γ

$$\gamma_S = 2 - \alpha_S \in (0, 1)$$

and

$$\gamma_L = 2 - \alpha_L \in (1, 2).$$

It is an established fact that the SRD case is covered by the classic ODA theory [Garnier and Sølna, 2010]. The last point we make about SRD and LRD is qualitatively dealt with, but this must not detract from its importance. In the short-range setting the function described in (3.3.5) will quickly converge to the true autocorrelation function. The result is a deterministic scattering which inherits its properties from the statistical second moment autocorrelation description of the medium. In this case we may think of the spectrum of (3.3.10) and (3.4.4) as the true spectrum.

However, in the LRD case, the sample autocorrelation function (3.3.5) will converge extremely slowly. In fact, we have just seen that in this case the power-law behavior of the spectrum close to 0 comes from the behavior of the autocorrelation function at arbitrarily large lags. No matter how far the wave propagates through such a medium, it will never average out and inherit only the statistical properties of the autocorrelation between points arbitrarily far apart. In this regime the classic ODA theory fails. There is a large modern body of literature describing the necessary extensions. See Fouque et al. [2007] for a thorough introduction and see Garnier and Sølna [2010] which is especially relevant to power-law spectra. In the following we will focus on SRD processes and therefore stay within the boundary of the classic ODA theory.

3.4.3 Fractional Brownian motion (fBm), fractional white noise and fractional Gaussian noise (fGn). The fractional Brownian motion is in most treaties the starting point for describing processes with a power-law spectrum. The fractional Brownian motion is the unique process which

1. Is Gaussian: $(\nu(z_1), \nu(z_2), ..., \nu(z_n)) \sim \mathcal{N}(0, \Sigma(z_1, z_2, ..., z_n))$
2. Is self-similar (with similarity parameter H): $\nu(az) \sim a^H \nu(z), \quad 0 < H < 1$
3. Has stationary increments: Distribution of $\nu(z_1) - \nu(z_2)$ only depends on $z_1 - z_2$.

Furthermore, an fBm has the autocorrelation function

$$\phi_{\text{fBm}}(z_1, z_2; H) = \tfrac{1}{2}\left[|z_1|^{2H} + |z_2|^{2H} - |z_1 - z_2|^{2H}\right],$$

from which we see that it is not stationary. Hence, the fBm does not have a spectrum, but in a generalized sense it may be seen to have a power-law spectrum [Wornell, 1996, chapter 3]. For historical reasons, H is called the Hurst parameter. Each sample path, seen as a graph in the plane, is itself a fractal with Hausdorff-Besicovitch fractal dimension

$$D = 2 - H$$

Hence, the fractional Brownian motion is the process which unites the ideas of statistical self-similarity, fractality and a power-law spectrum.

From the fBm we may generate other interesting processes. Just as white noise can be seen as the "derivative" of Brownian motion, we may define fractional white

noise (fwn) [Garnier and Sølna, 2010] by differencing a fractional Brownian motion process

$$\nu_{\mathrm{fGn}}(z;H) = \frac{\sigma}{l^H}(\nu_{\mathrm{fBm}}(z+l;H) - \nu_{\mathrm{fBm}}(z;H))$$

which has the autocorrelation function

$$\phi_{\mathrm{fwn}}(z;H) = \frac{\sigma^2}{2l^{2H}}(|z+l|^{2H} + |z-l|^{2H} - 2|z|^{2H}).$$

This may be seen to have the the SRD property for $H \in (0, 1/2)$ and LRD property for $H \in (1/2, 1)$ [Garnier and Sølna, 2010].

3.4.4 Fractional Ornstein-Uhlenbeck (fOU1) from Lamperti transformation. It is a rudimentary fact that Gaussian white noise is stationary, but the Brownian motion is not. The classic Ornstein-Uhlenbeck process is therefore typically the first Gaussian process one is introduced to with a more interesting correlation structure than the trivial white noise case. The classic Ornstein-Uhlenbeck is derived from Brownian motion in two different ways: Through the Lamperti transformation, or through the Langevin differential equation. We will following the same school of thought here, only in a fractional setting. Due to Lim and Muniandy [2003] we will experience that, unlike in the classic situation, this will lead to two different processes.

We begin with the Lamperti transformation. The Lamperti transformation, simply put, provides a one-to-one correspondence between the self-similar processes $(X_{\mathrm{ss}}(t))$ and the stationary processes $(X_{\mathrm{st}}(t))$. It is defined as

$$X_{\mathrm{st}}(t) = e^{-cHt}X_{\mathrm{ss}}(e^{ct}),$$

with $t \in \mathbb{R}, c \in \mathbb{R}$, or conversely,

$$X_{\mathrm{ss}}(t) = t^H X_{\mathrm{st}}(b \log t),$$

with $t > 0, b > 0$ and $X_{\mathrm{st}}(0) = 0$. Since we know that the fractional Brownian motion is self-similar, we may use the first of these transformations to create a stationary process. This is our first attempt at a fractional Ornstein-Uhlenbeck:

$$\nu_{\mathrm{fOU1}}(z;H) = \frac{e^{-2Hz/l}}{\sqrt{4H/l}}\nu_{\mathrm{fBm}}(e^{2z/l};H).$$

Again $0 < H < 1$, and one may show [Lim and Muniandy, 2003] that this fractional Ornstein-Uhlenbeck process has autocorrelation function

$$\phi_{\mathrm{fOU1}}(z;H) = \frac{l}{4H}\left[\cosh(2Hz/l) - 2^{2H-1}(\sinh(z/l))^{2H}\right]$$

and spectrum

$$S_{\mathrm{fOU1}}(\omega;H) = c(H,l)\frac{|\Gamma(1-H+\frac{1}{2}i\omega l)|^2}{|\Gamma(\frac{1}{2}+\frac{1}{2}i\omega l)|^2(H^2+\frac{1}{4}\omega^2 l^2)}$$

And from the asymptotic properties of the Γ-function F.0.3 one may show that

$$S_{\mathrm{fOU1}}(\omega;H) \sim \frac{1}{|\omega|^{2H+1}}, \quad \text{as } \omega \to \infty, 0 < H < 1$$

This process has the SRD property.

3.4.5 Fractional Ornstein-Uhlenbeck (fOU2) from a "fractional" Langevin equation. Next we will look at the Langevin equation which is given by

$$\partial_z Y(z) + aY(z) = bX(z), \quad \text{for } a > 0, b > 0.$$

In the classic derivation of the Ornstein-Uhlenbeck, Brownian motion is fed in as the input X(z) and the resulting process Y(z) is called the Ornstein-Uhlenbeck process. Notice that the right side of the Langevin equation is on average 0. Then the left side of the equation implies that the derivative $\partial_z Y(z)$ and $Y(z)$ have opposite signs. This gives the Ornstein-Uhlenbeck its so-called mean reverting quality. When it strays too far from the equilibrium, the derivative pulls it back in. This is the often used qualitative illustration of why the Ornstein-Uhlenbeck is stationary.

In this context it is important to voice a caveat: These arguments are not especially satisfying within the modern apparatus of stochastic calculus. The Ornstein-Uhlenbeck is not even differentiable, so the Langevin equation above isn't even well defined. Furthermore, in our next step we will "fractionalize" the Langevin equation. This too is not within the modern formulation of fractional calculus. Though this we will be formally acquainted with in chapter 4.

Let us fractionalize the Langevin equation [Lim and Muniandy, 2003] in the following way

$$(\partial_z + a)^{H+1/2} Y(z) = X(z). \tag{3.4.12}$$

Here we could expand the power expression as

$$(\partial_z + a)^{H+1/2} = \sum_{k=0}^{\infty} \binom{H+1/2}{k} a^k \partial_z^k,$$

with

$$\binom{H+1/2}{k} = \frac{\Gamma(H+1/2+1)}{\Gamma(k+1)\Gamma(H+1/2-k+1)}.$$

Using the fact that taking the n-th derivative is the same as multiplying by $(i\omega)^n$ in the frequency domain (see property A.0.5), we can take the Fourier-transform of both sides of (3.4.12).

$$\begin{aligned} \sum_{k=0}^{\infty} \binom{H+1/2}{k} a^k (i\omega)^k Y(\omega) &= X(\omega) \\ (i\omega + a)^{H+1/2} \widehat{Y}(\omega) &= \widehat{X}(\omega) \end{aligned}$$

So we have the impulse response

$$H(\omega) = \frac{1}{(i\omega + a)^{H+1/2}}$$

with the corresponding spectrum

$$S_{\text{fOU2}}(\omega) = H(\omega)H^*(\omega) = \frac{1}{(a^2 + \omega^2)^{H+0.5}},$$

which can be shown to have the autocorrelation function

$$\phi_{\text{fOU2}}(z) = \frac{1}{\sqrt{\pi} 2^H a^{2H} \Gamma(H+0.5)} |az|^H K_H(|az|),$$

where K_H is the modified Bessel function of second kind of order H. If we feed the system with white noise we get a process with the desired spectrum. It is clear that

$$S_{\text{fOU2}}(\omega) \sim \frac{1}{|\omega|^{2H+1}} \quad \text{for } |\omega| \to \infty.$$

3.4.6 A third fractional Ornstein-Uhlenbeck (fOU3) process. The last formulation of fractional Ornstein-Uhlenbeck is due to Garnier and Sølna [2010]. They define it as the stationary, zero mean, Gaussian process

$$\nu_{\text{fOU3}}(z; H, l) = \frac{\sigma}{\sqrt{H\Gamma(2H)}l^H}\left(\nu_{\text{fBm}}(z; H) - \frac{1}{l}\int_{-\infty}^{z} e^{(x-z)/l}\nu_{\text{fBm}}(x; H)dx\right)$$

It has the autocorrelation function

$$\phi_{\text{fOU3}}(z; H, l) = \frac{\sigma^2}{H\Gamma(2H)l^{2H}}\left[\frac{1}{4l}\int_{-\infty}^{\infty} e^{-|x|/l}|z+x|^{2H}dx - \frac{1}{2}|z|^{2H}\right] \tag{3.4.13}$$

It has the SRD property for $H \in (0, 1/2)$ and the LRD property for $H \in (1/2, 1)$ [Garnier and Sølna, 2010]. Lastly, in all the three cases of the fractional Ornstein-Uhlenbeck we recover the classical OU process when $H = 1/2$.

3.4.7 Von Kármán. Next we look at a correlation function which is used to describe the fractal nature of the upper crust from petrophysical logs [Dolan et al., 1998]. The von Kármán correlation function is given by

$$\phi_{\text{VK}}(z; H) = \frac{1}{2^{H-1}\Gamma(H)}\left|\frac{z}{a}\right|^H K_H\left(\left|\frac{z}{a}\right|\right),$$

where $K_H(x)$ is the modified Bessel-function of order H, and a is the correlation length. Furthermore, its spectrum is given by

$$S_{\text{VK}}(\omega; H) = 2\sqrt{\pi a}\frac{\Gamma(H+0.5)}{(1+\omega^2a^2)^{H+0.5}\Gamma(H)} \underset{|\omega|\to\infty}{\sim} \frac{1}{|\omega|^{2H+1}}. \tag{3.4.14}$$

In general, a process is not fully described by its correlation structure, though Gaussian processes are. So we could define a Gaussian process with the Von Kármán correlation function, and have a fully-fledged stochastic process. Otherwise we could spectrally factorize (3.4.14) and get

$$H_{\text{VK}}(\omega; H) = \sqrt[4]{\pi a}\sqrt{\frac{2\Gamma(H+0.5)}{\Gamma(H)}}\frac{1}{(1+i\omega a)^{H+0.5}}. \tag{3.4.15}$$

By feeding some kind of uncorrelated noise through this filter we would get the desired spectrum.

3.4.8 Discussion of $1/\omega^\alpha$ processes. The purpose of introducing so many different processes with $1/\omega^\alpha$ spectrum is decidedly not to confuse or bewilder the reader. It is on the contrary to make vivid the point that if our only criterion for a process is that it has a power-law spectrum, there are many ways to achieve this. It is meant to make the reader immune to any proselytizing from any one source claiming that power-laws originate from one specific place. There are even more such examples

out there, such as for instance jump processes [Garnier and Sølna, 2010] and wavelet descriptions [Wornell, 1996].

Knowing that there are many possible processes which will produce the desired outcome, which one should we use? The fractional Ornstein-Uhlenbeck process is immediately physically appealing since it is stationary. This is intuitively a property we would like our medium to possess. But what about the Gaussian premise underlying this model? Does this correspond to the real structure of say sedimentary layers? Dolan et al. [1998] successfully fits the Von Kármán autocorrelation function to petrophysical logs, and Walden and Hosken [1985] investigates the linear ARMA autocorrelation structure of rock sequences from seismic wells. However, it seems they do not question the Gaussianity premise.

Finally, remember from the introduction that in medical ultrasound one often encounters attenuation which follows a power-law with an exponent close to $\gamma = 1$. Looking back to (3.4.5) this amounts to a process ν whose spectrum is $1/\omega^\alpha$ with $\alpha = 1$. Looking at the spectra of the SRD processes of section 3.4.4, 3.4.5, 3.4.6 and 3.4.7 this corresponds to $H = 0$. However, inspecting their autocorrelation functions reveals that they collapse at $H = 0$. In fact, H must be strictly larger than 0. Thus it seems that the best we can do is to get very close to $\gamma = 1$ either through one of the SRD processes laid out in the previous sections, or through an ARMA approximation as explained in section 3.4.1.

As a closing thought, let us think about how the fractal structure of the earth's crust came to be. Of course, this is an open question not likely to have an easy answer, but it is interesting nonetheless. Is there anything in the process of the formation of geological structures, or in the formation of biological tissue, which could inform us to choose the right process?

3.4.9 Simulation. There are many ways of simulating $1/\omega^\alpha$ processes, but we quickly mention two methods here. First, we have explained how to create such processes using ARMA approximations. Second, notice that in the case of Gaussian processes we have a complete probabilistic description of the multivariate distribution of any collection of points. Formally, if we wish to simulate the processes along the x-axis at the discrete points $\{x_i\}_{i=0}^N$, then we in fact know the exact distribution of the entire vector $(\nu(x_1), \nu(x_2), ..., \nu(x_N))$. Simulating a sample path is then reduced to sampling one sample of this vector from the correct distribution. See section H.2 for a complete numerical recipe. Otherwise, read Plaszczynski [2007] for a long list of options.

3.4.10 Mathematical lessons for later use. Notice especially two ways of creating $1/\omega^\alpha$ processes which we will see analogies to in the next chapter. We have seen that a $1/\omega^\alpha$ process can emerge from a fractionalized differential equation. In the next chapter on viscoelasticity we formally introduce fractional calculus. Lastly, we have seen that such processes can be constructed by adding a certain weighted sum of $1/\omega^2$ filters either in series or in parallel.

Chapter 4

Fractional viscoelasticity

We will now extend the linear viscoelastic Zener model by introducing fractional derivatives. At first sight the fractional derivative seems quite obscure, though in the frequency domain the generalization is easy to grasp. Our choice of fractional derivative operator is the Caputo derivative

$$(D_C^\alpha f)(x) = \frac{1}{\Gamma(n-\alpha)} \int_0^x \frac{f^{(n)}(t)}{(x-t)^{\alpha-n+1}} dt, \qquad n = \lfloor \alpha \rfloor + 1, \tag{4.0.1}$$

where $\lfloor \alpha \rfloor$ is the integral part of α. The first thing to notice, where the fractional derivative stands in contrast to the classic derivative, is that it is not local. In fact, it depends on the the entire history of the function.

See appendix B for the most formal definition. In addition we must mention the possibly more common operator which is the Riemann-Liouville fractional derivative. This is also listed in appendix B. There are several variations of these also concerning the limits of the integrals – whether they should start at $-\infty$ or at zero as the one above. See Podlubny [1998] and Mathai et al. [2010, chapter 3] for a thorough theoretical introduction to the subject. All that we will mention in this context is that the reader is hereby informed that there are several available fractional derivative operators and that the choice of operator *does* make a difference: Different choices may lead to different results. But as shown simply and elegantly in Bagley [2007], the solution to our specific problem – the fractional Zener model – the Riemann-Liouville derivative and the Caputo derivative produces identical results. One may show that the Laplace and Fourier transform of the Caputo derivative is [Mathai et al., 2010, chapter 3]

$$\text{Laplace:} \qquad \mathcal{L}\left\{(D_C^\alpha f)(x); s\right\} = s^\alpha \widehat{F}(s) - \sum_{k=0}^{\lceil \alpha \rceil - 1} s^{\alpha-k-1} f^{(k)}(0^+) \tag{4.0.2}$$

$$\text{Frequency:} \quad \mathcal{F}\left\{(D_C^\alpha f)(x); \omega\right\} = (i\omega)^\alpha \widehat{F}(\omega). \tag{4.0.3}$$

We see that initial values are included in the same way as in the Laplace transform of the classic derivative. The natural choice of operator is the Caputo derivative, not only for its handle on initial conditions, but also for the attractive quality that the fractional derivative of a constant is zero;

$$D_C^\alpha A = 0.$$

This can be easily seen just by glancing at its definition B.0.14. Notice the $f^{(n)}(x)$ inside the integral which is just the conventional derivative. This kills the constant. In contrast one may show that the Riemann-Liouville derivative of a constant is

$$(D^{\alpha}_{RL}A)(x) = \frac{Ax^{-\alpha}}{\Gamma(1-\alpha)}$$

We are now ready to state our fractional Zener constitutive equation.

$$\sigma(t) + \tau^{\alpha}_{\sigma} D^{\alpha}_{C}\sigma(t) = \frac{1}{J_{\text{eq}}}\left(\epsilon(t) + \tau^{\beta}_{\sigma} D^{\beta}_{C}\epsilon(t)\right). \tag{4.0.4}$$

This is similar to the fractional Zener model as stated in Holm and Näsholm [2011, equation (6)], though the τ_σ and τ_ϵ have switched place. This is done to make it consistent with Le and Burridge [1998, equation (12)] and Mainardi and Spada [2011]. As a preliminary reality check we may make the following thought experiment. Imagine that we have a stress test such that $\sigma(t) = H(t)$. Imagine the system has reached its equilibrium such that nothing is changing. Since the Caputo derivative kills constants, all we are left with from (4.0.4) is $\epsilon = J_{\text{eq}}$, which is exactly what we want.

The goal for the next section is to solve (4.0.4) by finding its creep compliance $J(t)$ and compressibility $\kappa(t)$. To do this, we must move to the Laplace domain. Taking the Laplace transform of (4.0.4) we get

$$\widehat{\sigma}(s) + \tau^{\alpha}_{\sigma} s^{\alpha}\widehat{\sigma}(s) - \tau^{\alpha}_{\sigma} s^{\alpha-1}\sigma(0^+) = \frac{1}{J_{\text{eq}}}\left(\widehat{\epsilon}(s) + \tau^{\beta}_{\epsilon} s^{\beta}\widehat{\epsilon}(s) - \tau^{\beta}_{\epsilon} s^{\beta-1}\epsilon(0^+)\right) \tag{4.0.5}$$

Using the fact that $\epsilon(0^+) = J_{\text{in}}\sigma(0^+)$ (this one may intuit from reading section 2.1.1 or read Mainardi and Spada [2011]), after some rearrangement we get

$$(1 + \tau^{\alpha}_{\sigma} s^{\alpha})\widehat{\sigma}(s) = \frac{1}{J_{\text{eq}}}(1 + \tau^{\beta}_{\epsilon} s^{\beta})\widehat{\epsilon}(s) + \tau^{\alpha}_{\sigma} s^{\alpha-1}\sigma(0^+) - \frac{1}{J_{\text{eq}}}\tau^{\beta}_{\epsilon} s^{\beta-1} J_{\text{in}}\sigma(0^+) \tag{4.0.6}$$

The question now becomes: How can we make the initial condition terms

$$\tau^{\alpha}_{\sigma} s^{\alpha-1}\sigma(0^+) - \frac{1}{J_{\text{eq}}}\tau^{\beta}_{\epsilon} s^{\beta-1} J_{\text{in}}\sigma(0^+) = 0 \tag{4.0.7}$$

vanish? If $\alpha = \beta$ we may choose

$$J_{\text{in}} = J_{\text{eq}}\left(\frac{\tau_\sigma}{\tau_\epsilon}\right)^{\beta},$$

and after rearranging (4.0.6) we get

$$\widehat{\epsilon}(s) = J_{\text{eq}}\frac{1}{s}\frac{1 + (\tau_\sigma s)^{\beta}}{1 + (\tau_\epsilon s)^{\beta}}\widehat{\sigma}(s),$$

Again we find, as we did in section 2.2, that within the universe of LTI, the choice of instantaneous creep is done for us. We do not have a separate state variable only for that purpose. Note that if we set $\alpha = \beta = 1$ we get the transfer function of the classic Zener model.

If $\alpha \neq \beta$ there is no choice of initial conditions that make the initial condition terms of (4.0.7) disappear. From the point of view of initial conditions it is therefore unclear whether the fractional Zener model with two different exponents has sufficient theoretical grounding. In fact, many sources discount this model [Mainardi and Spada, 2011; Bagley, 2007], though since it is relevant to other key sources [Holm and Näsholm, 2011] we will keep it still.

4.1 Material functions of the fractional Zener model

We will now find the creep compliance of the fractional Zener model. This will be done by taking the inverse Laplace transform

$$\widehat{J}(s) = \frac{J_{\text{eq}}}{s}\frac{1+(\tau_\sigma s)^\alpha}{1+(\tau_\epsilon s)^\beta}. \tag{4.1.1}$$

There are ready look up-tables that would do the job for us; see for instance the lucid paper Mainardi and Spada [2011]. However, the ambition for this section is slightly higher. The aim is to expound a mathematical procedure for computing the inverse Laplace transform above. With any luck, the reader will be empowered to solve difficult fractional differential equations. The basic strategy for solving any fractional differential equation is to transform the equation to the Laplace domain, as we did in the previous section, and then follow the instructions in this section. This narrative is inspired heavily by Schiessel et al. [1995], though not exactly equal. In any case, the aforementioned article resorts, at times, to phrases like "we find ... after some tedious calculations". Here we will strive to expose the process in its entirety.

By way of introduction, as a preparation of what is ahead, one may tell the following story. The solution to fractional differential equations can often be expressed in the Fox-H functions. This is a wide class of functions which contains many other functions as special cases; the Meijer-G function, the generalized Mittag-Leffler function, the hypergeometric function, the generalized Wright function, the beta function and the Bessel function just to name a few. The Fox-H function is excellently examined in Mathai et al. [2010]. This book cannot be recommended enough for its clear exposition and its off the shelf ready-to-apply ideas.

Furthermore, The Fox-H functions are expressed by so-called Mellin-Barnes type integrals (F.0.4). These Mellin-Barnes type integrals also occur in the inverse Mellin transform. Therefore, as seen in Schiessel et al. [1995], the Mellin transform seems the appropriate milieu to produce these integrals. For those unfamiliar with the Mellin transform it is introduced in appendix F which only includes, unfortunately, the bare minimum of what is needed for this discussion.

To kick off, let $\psi(t) = e^{-t}$. The Mellin transform of $\psi(t)$ is

$$\mathcal{M}\left\{\psi(t);u\right\} = \int_0^\infty e^{-t}t^{u-1}dt = \Gamma(u). \tag{4.1.2}$$

The Mellin transform, as the Laplace transform, throughout literature, employs s as its parameter. Since we are employing both at once, the Mellin transform variable shall be u. The Laplace transform $J(s)$ is

$$\mathcal{L}\left\{J(t);s\right\} = \int_0^\infty J(t)e^{-st}dt.$$

We observe that using the multiplicative convolution notation as seen in appendix F we can express the Laplace transform in an unusual way

$$\widehat{J}(s) \equiv \mathcal{L}\left\{J(t);s\right\} = (J(t) \vee \psi(t))(s).$$

By the multiplicative convolution property of the Mellin transform seen in Prop-

erty F.0.26 we get

$$\begin{aligned}\mathcal{M}\left\{\widehat{J}(s);u\right\} &= \mathcal{M}\left\{(J\vee\psi)(s);u\right\}\\ &= \mathcal{M}\left\{J(t);1-u\right\}\mathcal{M}\left\{\psi(t);u\right\}\\ &= \mathcal{M}\left\{J(t);1-u\right\}\Gamma(u).\end{aligned}$$

Rearranging this we get the important identity

$$\mathcal{M}\left\{J(t);u\right\} = \frac{\mathcal{M}\left\{\widehat{J}(s);1-u\right\}}{\Gamma(1-u)}. \tag{4.1.3}$$

This is important because we have managed to take the inverse Laplace transform in the Mellin domain. On the right hand side we begin with the Mellin transform of $\widehat{J}(s)$ in the Laplace domain, then we divide by a gamma-function, and we end up with the Mellin transform of $J(t)$ in the time domain. It is apparent then that to make use of (4.1.3) we need first is to compute $\mathcal{M}\left\{\widehat{J}(s);u\right\}$. To meet this end we must make some preparations. Let us introduce the function

$$f(z) = \frac{1}{1+z}.$$

Note that $f(z)$ only has one simple pole at $z=-1$. This allows us to find its Mellin transform using Property F.0.25

$$\begin{aligned}\mathcal{M}\left\{f(z);u\right\} &= -\frac{\pi e^{-\pi u i}}{\sin\pi u}\sum\mathfrak{Res}\left\{z^{u-1}f(z);\text{at the poles of } f(z)\right\}\\ &= -\frac{\pi e^{-\pi u i}}{\sin\pi u}\,\mathfrak{Res}\left\{z^{u-1}f(u);z=-1\right\}\\ &= -\frac{\pi(-1)^u}{\sin\pi u}\lim_{z\to-1}(1+z)z^{u-1}f(z)\\ &= \frac{\pi}{\sin\pi u}\end{aligned}$$

Through the relation (F.0.1) we find the Mellin transform of $f(z)$

$$\mathcal{M}\left\{f(z);u\right\} = \Gamma(u)\Gamma(1-u), \tag{4.1.4}$$

which, by the way, is just the beta function $B(u,1-u)$. Now we are ready to attack the creep compliance. We begin by expressing it as

$$\begin{aligned}\widehat{J}(s) &= \frac{J_{\text{eq}}}{s}\frac{1+(s\tau_\sigma)^\alpha}{1+(s\tau_\epsilon)^\beta}\\ &= J_{\text{eq}}s^{-1}f\left[(s\tau_\epsilon)^\beta\right] + J_{\text{eq}}\tau_\sigma^\alpha s^{\alpha-1}f\left[(s\tau_\epsilon)^\beta\right].\end{aligned}$$

Using Property F.0.26 we get

$$\begin{aligned}\mathcal{M}\left\{\widehat{J}(s);u\right\} &= J_{\text{eq}}\mathcal{M}\left\{s^{-1}f\left[(s\tau_\epsilon)^\beta\right];u\right\} + J_{\text{eq}}\tau_\sigma^\alpha\mathcal{M}\left\{s^{\alpha-1}f\left[(s\tau_\epsilon)^\beta\right];u\right\}\\ &= \tfrac{J_{\text{eq}}}{\beta}\tau_\epsilon^{-(u-1)}\mathcal{M}\left\{f(z);\tfrac{u-1}{\beta}\right\} + \tau_\sigma^\alpha\tfrac{J_{\text{eq}}}{\beta}\tau_\epsilon^{-(u+\alpha-1)}\mathcal{M}\left\{f(z);\tfrac{u+\alpha-1}{\beta}\right\}.\end{aligned}$$

Putting this into (4.1.3) we get

$$\mathcal{M}\{J(t);u\} = \frac{J_{\text{eq}}\tau_\epsilon^u}{\beta\Gamma(1-u)}\left[\mathcal{M}\left\{f(z);-\tfrac{u}{\beta}\right\} + \left(\frac{\tau_\sigma}{\tau_\epsilon}\right)^\alpha \mathcal{M}\left\{f(z);\tfrac{\alpha-u}{\beta}\right\}\right].$$

By distributing the Gamma function inside the parenthesis we can rewrite this as

$$\mathcal{M}\{J(t);u\} = \frac{J_{\text{eq}}}{\beta}\left[\Theta_1(u) + \left(\frac{\tau_\sigma}{\tau_\epsilon}\right)^\alpha \Theta_2(u)\right]\left(\frac{1}{\tau_\epsilon}\right)^{-u}, \tag{4.1.5}$$

where $\Theta_1(s)$ and $\Theta_2(s)$ are Mellin-Barnes type functions

$$\Theta_1(u) = \frac{\mathcal{M}\left\{f(z);-\frac{u}{\beta}\right\}}{\Gamma(1-u)} = \frac{\Gamma(-\frac{1}{\beta}u)\Gamma(1+\frac{1}{\beta}u)}{\Gamma(1-u)}$$

and

$$\Theta_2(u) = \frac{\mathcal{M}\left\{f(z);\frac{\alpha-u}{\beta}\right\}}{\Gamma(1-u)} = \frac{\Gamma(\frac{\alpha}{\beta}-\frac{1}{\beta}u)\Gamma(1-\frac{\alpha}{\beta}+\frac{1}{\beta}u)}{\Gamma(1-u)}.$$

Finally we can apply the inverse Mellin transform to 4.1.5 and get

$$\bar{J}(t) = \frac{J_{\text{eq}}}{\beta}\left[\int_{c-i\infty}^{c+i\infty}\Theta_1(u)\left(\tfrac{t}{\tau_\epsilon}\right)^{-u}du + \left(\frac{\tau_\sigma}{\tau_\epsilon}\right)^\alpha\int_{c-i\infty}^{c+i\infty}\Theta_2(u)\left(\tfrac{t}{\tau_\epsilon}\right)^{-u}du\right].$$

After a careful reading of the definition of the Fox-H function in appendix F we arrive at the expression

$$\bar{J}(t) = \frac{J_{\text{eq}}}{\beta}H_{12}^{11}\left[\frac{t}{\tau_\epsilon}\middle|\begin{matrix}(1,\frac{1}{\beta})\\(1,\frac{1}{\beta}),(0,1)\end{matrix}\right] + \left(\frac{\tau_\sigma}{\tau_\epsilon}\right)^\alpha\frac{J_{\text{eq}}}{\beta}H_{12}^{11}\left[\frac{t}{\tau_\epsilon}\middle|\begin{matrix}(1-\frac{\alpha}{\beta},\frac{1}{\beta})\\(1-\frac{\alpha}{\beta},\frac{1}{\beta}),(0,1)\end{matrix}\right].$$

By applying Property F.0.27 we can rewrite it as

$$\begin{aligned}\bar{J}(t) =& \frac{J_{\text{eq}}}{\beta}\left(\frac{t}{\tau_\epsilon}\right)^\beta H_{12}^{11}\left[\frac{t}{\tau_\epsilon}\middle|\begin{matrix}(0,\frac{1}{\beta})\\(0,\frac{1}{\beta}),(-\beta,1)\end{matrix}\right]\\ &+\left(\frac{\tau_\sigma}{\tau_\epsilon}\right)^\alpha\frac{J_{\text{eq}}}{\beta}\left(\frac{t}{\tau_\epsilon}\right)^{\beta-\alpha}H_{12}^{11}\left[\frac{t}{\tau_\epsilon}\middle|\begin{matrix}(0,\frac{1}{\beta})\\(0,\frac{1}{\beta}),(\alpha-\beta,1)\end{matrix}\right].\end{aligned}$$

Again, by applying Property F.0.28 we can rewrite it as

$$\begin{aligned}\bar{J}(t) =& J_{\text{eq}}\left(\tfrac{t}{\tau_\epsilon}\right)^\beta H_{12}^{11}\left[\left(\tfrac{t}{\tau_\epsilon}\right)^\beta\middle|\begin{matrix}(0,1)\\(0,1),(-\beta,\beta)\end{matrix}\right]\\ &+J_{\text{eq}}\left(\frac{\tau_\sigma}{\tau_\epsilon}\right)^\alpha\left(\tfrac{t}{\tau_\epsilon}\right)^{\beta-\alpha}H_{12}^{11}\left[\left(\tfrac{t}{\tau_\epsilon}\right)^\beta\middle|\begin{matrix}(0,1)\\(0,1),(\alpha-\beta,\beta)\end{matrix}\right].\end{aligned}$$

Finally applying (F.0.7) we arrive at the final expression

$$\bar{J}(t) = J_{\text{eq}} \left(\tfrac{t}{\tau_\epsilon}\right)^\beta E_{\beta,\beta+1}\left(-\left(\tfrac{t}{\tau_\epsilon}\right)^\beta\right) + J_{\text{eq}} \left(\tfrac{\tau_\sigma}{\tau_\epsilon}\right)^\alpha \left(\tfrac{t}{\tau_\epsilon}\right)^{\beta-\alpha} E_{\beta,\beta-\alpha+1}\left(-\left(\tfrac{t}{\tau_\epsilon}\right)^\beta\right) \tag{4.1.6}$$

where $E_{\alpha,\beta}(z)$ is the two-parameter Mittag-Leffler function as described in Appendix F. This is indeed the creep compliance of the fractional Zener constitutive equation. Look-up tables may be found in Mathai et al. [2010] to convert Fox-H functions to other known functions, but in this case let us finish the calculation by hand. Consider the H-function

$$H_{12}^{11}\left[z\middle|\begin{array}{l}(0,1)\\(0,1)(1-\beta,\alpha)\end{array}\right] = \frac{1}{2\pi i}\int_{\gamma-i\infty}^{\gamma+i\infty} \frac{\Gamma(s)\Gamma(1-s)}{\Gamma(\beta-\alpha s)} z^{-s} ds \tag{4.1.7}$$

This equality is simply the definition of the Fox-H function (see again (F.0.4) for the definition). Notice especially that the path of integration is one that separates the poles of $\Gamma(s)$ and $\Gamma(1-s)$. We may then evaluate the integral (4.1.7) by summing up the residues at the poles of either $\Gamma(s)$ or $\Gamma(1-s)$; say $\Gamma(s)$. Appendix F states that the poles of the Γ-function are located at $z = 0, -1, -2, \ldots$. Its residues are listed in (F.0.2). The integral in (4.1.7) becomes

$$\begin{aligned}\int_{\gamma-i\infty}^{\gamma+i\infty} \frac{\Gamma(s)\Gamma(1-s)}{\Gamma(\beta-\alpha s)} z^{-s} ds &= \frac{1}{2\pi i}\sum_{k=0}^{\infty} \mathfrak{Res}\left\{\frac{\Gamma(s)\Gamma(1-s)}{\Gamma(\beta-\alpha s)} z^{-s}; -k\right\} \\ &= \sum_{k=0}^{\infty} \frac{\Gamma(1+k)z^k}{\Gamma(\beta+\alpha k)} \mathfrak{Res}\left\{\Gamma(z); -k\right\} \\ &= \sum_{k=0}^{\infty} \frac{k! z^k}{\Gamma(\beta+\alpha k)} \frac{(-1)^k}{k!} = E_{\alpha,\beta}(-z)\end{aligned}$$

The exact same process may be pursued with a general integration kernel (F.0.5). In that case one would have to sum up the residues of the poles at each of the m different $\Gamma(b_j - B_j s)$ or each of the n different $\Gamma(1 - a_j + A_j s)$ functions. This is the so-called **computable form**. It represents the Mellin-Barnes integral (F.0.4) as an infinite sum. See Appendix A.6 of Mathai et al. [2010] for details.

Before we wrap this section up we should allow ourselves a short respite and glance at figure 4.1 to recapitulate the entire process.

4.1.1 The generalized compressibility of the fractional Zener. As an immediate consequence of the definition of the Mittag-Leffler function, we have that $E_{a,b}(0) = \frac{1}{\Gamma(b)}$. From this we find from (4.1.6) J_{in}

$$\begin{aligned}J_{\text{in}} = \lim_{t\to 0} J(t) &= J_{\text{eq}} \frac{1}{\Gamma(\beta+1)} * 0 + J_{\text{eq}} \left(\frac{\tau_\sigma}{\tau_\epsilon}\right)^\alpha \frac{1}{\Gamma(\beta-\alpha+1)} \lim_{t\to 0}\left(\frac{t}{\tau_\epsilon}\right)^{\beta-\alpha} \\ &= \begin{cases} 0 & \text{for } \alpha < \beta \\ J_{\text{eq}}\left(\frac{\tau_\sigma}{\tau_\epsilon}\right)^\beta & \text{for } \alpha = \beta \end{cases}\end{aligned} \tag{4.1.8}$$

So it is evident that for the case $\alpha < \beta$ there is no instantaneous creep compliance, where there *is* one for $\alpha = \beta$. Beginning with the case $\alpha < \beta$, we find from (2.2.5) the generalized compressibility

$$\kappa(t) = D_t J(t) = J_{\text{in}}\delta(t) + H(t)(\partial_t \bar{J}(t)).$$

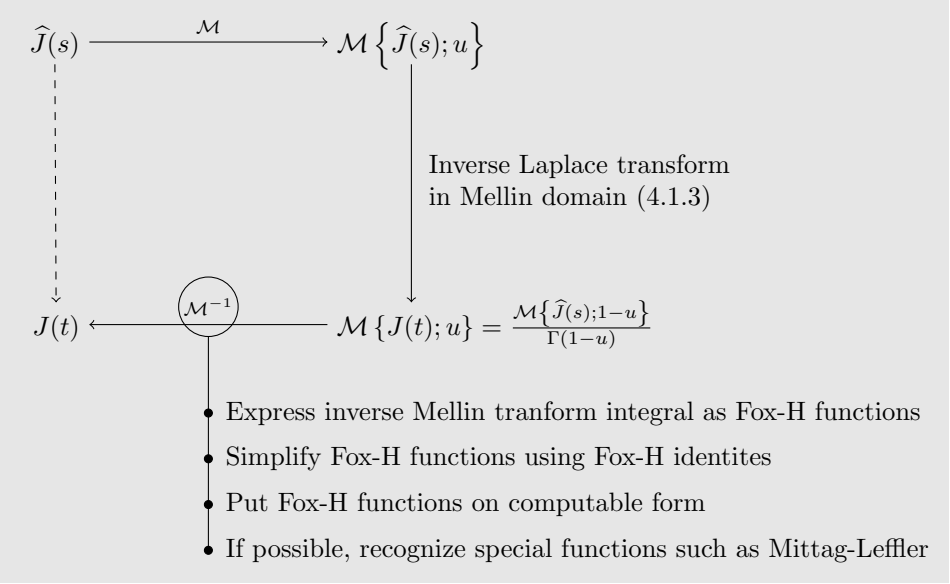

Figure 4.1: Process of transferring the material functions from the Laplace domain to the time domain

But for $\alpha < \beta$ we have $J_{\text{in}} = 0$. We may find the derivative of $\bar{J}(t)$ by applying the Mittag-Leffler differentiation rule F.0.31 to (4.1.6) and get

$$\kappa_{\alpha<\beta}(t) = \frac{J_{\text{eq}} t^{\beta-1}}{\tau_\epsilon^\beta} \left\{ E_{\beta,\beta}\left(-\left(\tfrac{t}{\tau_\epsilon}\right)^\beta\right) + \left(\frac{\tau_\sigma}{t}\right)^\alpha E_{\beta,\beta-\alpha}\left(-\left(\tfrac{t}{\tau_\epsilon}\right)^\beta\right) \right\} H(t)$$

It may be shown that the creep compliance given by (4.1.6) is not monotonely increasing for $\alpha < \beta$. One may find the necessary references in Holm and Näsholm [2011]. This has lead many, again, to discount it as a physically viable alternative. In addition to this, we have just seen that the Zener model with $\alpha < \beta$ has no instantaneous response J_{in}. Since we are ultimately interested in theory explaining how scattering and viscoelasticity interact, the $\alpha < \beta$ is of no further interest to us. Hence, for the rest of this thesis we will deal *only* with the case $\alpha = \beta$, and we will adopt β as the single exponent of the fractional Zener model. In this case we may simplify (4.1.6) quite a lot by applying F.0.30

$$\bar{J}(t) = J_{\text{eq}} \left\{ 1 - E_\beta\left(-\left(\tfrac{t}{\tau_\epsilon}\right)^\beta\right) \right\} + J_{\text{eq}} \left(\tfrac{\tau_\sigma}{\tau_\epsilon}\right)^\beta E_{\beta,1}\left(-\left(\tfrac{t}{\tau_\epsilon}\right)^\beta\right)$$

Using the fact that $E_{\beta,1}(z) = E_\beta(z)$ we get the final expression for the creep compliance

$$J(t) = J_{\text{eq}} \left\{ 1 - \left(1 - \left(\tfrac{\tau_\sigma}{\tau_\epsilon}\right)^\beta\right) E_\beta\left(-\left(\tfrac{t}{\tau_\epsilon}\right)^\beta\right) \right\} H(t). \tag{4.1.9}$$

After all this mathematics things have worked out quite beautifully. Comparing this to (2.2.2) we immediately see that we recover the classic Zener creep compliance for

$\beta = 1$ since $E_1(z) = e^z$ (see the definition of the Mittag-Leffler function (F.0.6)). Finally, we use again (2.2.5) and find its generalized compressibility

$$\kappa_{\alpha=\beta}(t) = J_{\text{in}}\delta(t) + J_{\text{eq}}\left(1 - \left(\tfrac{\tau_\sigma}{\tau_\epsilon}\right)^\beta\right)\frac{t^{\beta-1}}{\tau_\epsilon^\beta}E'_\beta\left(-\left(\tfrac{t}{\tau_\epsilon}\right)^\beta\right)$$

Rewriting it using $J_{\text{in}} = J_{\text{eq}}\left(\tfrac{\tau_\sigma}{\tau_\epsilon}\right)^\beta$ we get

$$\boxed{\kappa_{\alpha=\beta}(t) = J_{\text{in}}\delta(t) + J_{\text{in}}\left(\frac{1}{\tau_\sigma^\beta} - \frac{1}{\tau_\epsilon^\beta}\right)\beta t^{\beta-1}E'_\beta\left(-\left(\tfrac{t}{\tau_\epsilon}\right)^\beta\right)H(t).} \qquad (4.1.10)$$

Finally we may look at the generalized compressibility in the frequency domain. We remember the relationship between creep compliance $J(\omega)$ and $\kappa(\omega)$ from (2.1.11) which gives from (4.1.1)

$$\widehat{\kappa}(\omega) = J_{\text{eq}}\frac{1 + (i\omega\tau_\sigma)^\beta}{1 + (i\omega\tau_\epsilon)^\beta}. \qquad (4.1.11)$$

From this one may confirm, in accordance with (2.1.13a), that

$$J_{\text{in}} = \lim_{\omega\to\infty}\widehat{\kappa}(\omega) = J_{\text{eq}}\left(\frac{\tau_\sigma}{\tau_\epsilon}\right)^\beta.$$

To conclude, it is worth directing attention to the fact that the fractional Zener model is indeed causal. No extra work is needed to establish this as it is obvious from our explicit expression (4.1.10).

4.2 Power-law attenuation of the fractional Zener model

We are about to complete the second branch of this thesis by showing that that the fractional Zener model gives rise to power-law attenuation. Recall from (2.4.7) that the attenuation in a viscoelastic body with compressibility $\kappa(\omega)$ is given by

$$\mathcal{A}_{\text{vis}}(\omega) = -\omega\sqrt{\rho}\,\mathfrak{Im}\,\sqrt{\kappa(\omega)}. \qquad (4.2.1)$$

For the purpose of clarity let us repeat from (4.1.11) the compressibility in the frequency domain for the fractional Zener model

$$\kappa(\omega) = \kappa_0\frac{1 + (i\omega\tau_\sigma)^\beta}{1 + (i\omega\tau_\epsilon)^\beta}. \qquad (4.2.2)$$

Here we have used (2.1.13) which says that we may interchange J_{eq} and κ_0.

Our main theme is familiar by now. In accordance with the empirical evidence presented in the introduction, we are looking for power-laws with an exponent in the range of $\gamma \in (0, 2)$. We will show that the fractional Zener can indeed accomplish this, though with a caveat at $\gamma = 1$. In fact, the fractional Zener model yields power-law attenuation in three different bands, which at first can be seen in figure 4.2. Here we see a plot of the attenuation $\mathcal{A}_{\text{vis}}(\omega)$ in the log-log plane normalized such that $\mathcal{A}_{\text{vis}}(\omega = \frac{1}{\tau_\epsilon}) = 1$. Especially notice that the middle range stretches from $\ln\omega = -\ln\tau_\epsilon$ to $\ln\omega = -\ln\tau_\sigma$.

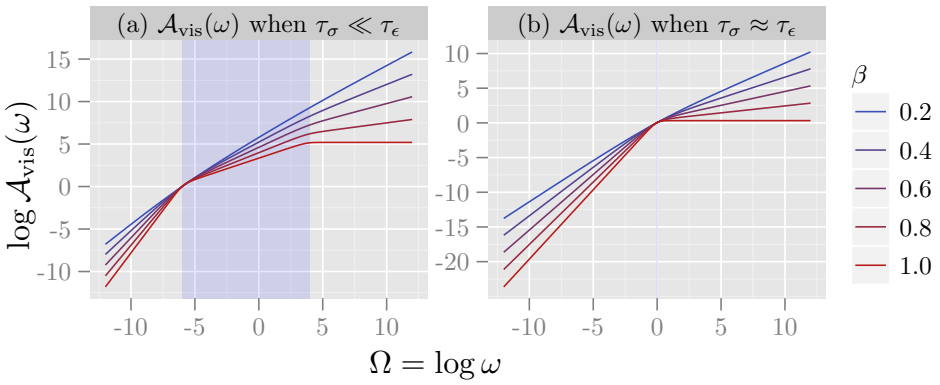

Figure 4.2: Attenuation of fractional Zener normalized such that $\mathcal{A}_{\text{vis}}(\omega = 1/\tau_\epsilon) = 1$. The light blue area is the mid-range $-\log \tau_\epsilon < \log(\omega) < -\log(\tau_\sigma)$, with $\tau_\epsilon = 10^6$s and $\tau_\sigma = 10^{-3}$s in (a), and $\tau_\epsilon \approx \tau_\sigma \approx 1$s in (b).

In the following we will trace the arguments of Holm and Näsholm [2011]. Note that compared to Holm and Näsholm [2011], we have swapped the place of τ_ϵ and τ_σ to be consistent with Le and Burridge [1998]. Let us find the approximate power-laws in the three bands. For low frequencies we observe that both $(\omega\tau_\epsilon)^\beta \ll 1$ and $(\omega\tau_\sigma)^\beta \ll 1$ and we may approximate $\mathcal{A}_{\text{vis}}(\omega)$ by simple Taylor expansions

$$\begin{aligned}
\mathcal{A}_{\text{vis}}(\omega) &\approx -\frac{\omega}{c_0}\,\mathfrak{Im}\left\{\left(1+\tfrac{1}{2}(i\omega\tau_\sigma)^\beta\right)\left(1-\tfrac{1}{2}(i\omega\tau_\epsilon)^\beta\right)\right\} \\
&= -\tfrac{\omega}{c_0}\sqrt{\rho\kappa_0}\,\mathfrak{Im}\left\{1-\tfrac{1}{2}(\tau_\epsilon^\beta - \tau_\sigma^\beta)(i\omega)^\beta\right\} \\
&= \tfrac{1}{2c_0}(\tau_\epsilon^\beta - \tau_\sigma^\beta)\sin(\tfrac{\pi}{2}\beta)\omega^{1+\beta}
\end{aligned}$$

where $c_0 = 1/\sqrt{\kappa_0\rho}$. We could follow the same procedure in the other bands. In the mid-range we would start by observing that $(\tau_\sigma\omega)^\beta \ll 1 \ll (\tau_\epsilon\omega)^\beta$, and in the high-range, we would observe that both are much greater than one. Then we would apply the appropriate Taylor approximations, and the interested reader may see these calculations in Holm and Näsholm [2011]. All in all the three bands are approximated by the following power-laws.

$$c_0\mathcal{A}_{\text{vis}}(\omega) \approx \begin{cases} \frac{1}{2}(\tau_\epsilon^\beta - \tau_\sigma^\beta)\sin\left(\frac{\pi}{2}\beta\right)\omega^{1+\beta} & \text{Low-range} \\ \tau_\sigma^{-\beta/2}\sin\left(\frac{\pi}{4}\beta\right)\left\{1-\frac{1}{4}\left(\frac{\tau_\epsilon}{\tau_\sigma}\right)^\beta\right\}\omega^{1-\frac{1}{2}\beta} & \text{Mid-range} \\ \frac{1}{2}\frac{\tau_\sigma}{\tau_\epsilon}^{\beta/2}(\tau_\sigma^{-\beta} - \tau_\epsilon^{-\beta})\sin\left(\frac{\pi}{2}\beta\right)\omega^{1-\beta} & \text{High-range} \end{cases} \tag{4.2.3}$$

When $\beta = 1$ we get the classic Zener model, from which we see in the algebraic expressions above, that the attenuation will be proportional to ω^2, $\omega^{1/2}$ and ω^0. This can be confirmed by glancing at figure 4.2. In other words, the classic Zener model *does* produce power-law attenuation, but can only, if we look away from the mid-range band, model ω^2 dampening. The fractional Zener however, if we choose $\beta \in (0, 1)$, successfully gives dampening, by (4.2.3), proportional to ω^γ with γ in the desired $(0, 2)$ range.

According to Holm and Näsholm [2011] empirical evidence suggest that τ_ϵ and τ_σ are often very close together, thus the mid-range can be largely ignored. They give two examples of this. One is attenuation in oxygen at 20°C, 0% relative humidity and 1 atmosphere, and the other is in fluorine at 102°C and 1 atmosphere. These are thought to measure respectively $\tau_\epsilon/\tau_\sigma \approx 1.0007$ and $\tau_\epsilon/\tau_\sigma \approx 1.043$.

Again, by looking at the exponents in (4.2.3), if we set $\beta = 0$ we should get the sought after ω^1 attenuation which is so often seen in medical applications. But if we insert $\beta = 0$ into (4.2.2) we get a real number, which by (4.2.1) gives no attenuation at all. By the same token, if we set $\tau_\sigma = \tau_\epsilon$ attenuation disappears again. So we are faced with two empirically relevant, but degenerate limit cases, which we need to understand. To meet this end we will deviate from Holm and Näsholm [2011] and introduce a technical tool which allows us to explain what happens very close to these singularities, i.e in the limits $\tau_\sigma \to \tau_\epsilon$ and $\beta \to 0$. The following result gives us the necessary equipment.

Lemma 4.2.1. *Let $f(z) = \frac{A(z)}{B(z)}$ be a fraction of two complex valued functions $A(z)$ and $B(z)$. Then we have:*

1. $\mathfrak{Im}\,\sqrt{f(z)} = \frac{\mathfrak{Im}\,A\overline{B}}{|B|\sqrt{2(|A||B|+\mathfrak{Re}\,A\overline{B})}}$
2. $\ln \operatorname{sign}(\,\mathfrak{Im}\,A\overline{B})\;\mathfrak{Im}\,\sqrt{f(z)} = -\frac{1}{2}\left(\ln 2 + \ln\frac{|B|^2}{|\,\mathfrak{Im}\,A\overline{B}|} + \operatorname{arcsinh}\frac{\mathfrak{Re}\,A\overline{B}}{|\,\mathfrak{Im}\,A\overline{B}|}\right)$

Proof. We begin by looking at the square root of a complex number $z = a + bi$ expressed in Cartesian coordinates, namely

$$\sqrt{z} = \sqrt{\frac{|z|+a}{2}} + \operatorname{sign}(b)\sqrt{\frac{|z|-a}{2}}i.$$

The imaginary part is thus

$$\begin{aligned}\mathfrak{Im}\,\sqrt{z} &= \operatorname{sign}(b)\sqrt{\frac{(|z|-a)(|z|+a)}{2(|z|+a)}} \\ &= \frac{b}{\sqrt{2(|z|+a)}}\end{aligned}$$

The first result comes from substituting a and b with the real and imaginary parts of the function $f(z)$:

$$f(z) = \frac{A(z)}{B(z)}\frac{\overline{B}(z)}{\overline{B}(z)} = \frac{\mathfrak{Re}\,A\overline{B}}{|B|^2} + \frac{\mathfrak{Im}\,A\overline{B}}{|B|^2}i. \tag{4.2.4}$$

The second result follows by multiplying the above expression for $\mathfrak{Im}\,\sqrt{z}$ equation with $\operatorname{sign}(b)$, dividing the numerator and denominator by $\sqrt{|b|}$ and then taking the logarithm. □

The expressions become more manageable in the log-log domain, so we begin by introducing the function

$$\psi(\Omega) := \frac{1 + e^{i\frac{\pi}{2}}e^{\beta(\Omega-\frac{1}{2}\Delta)}}{1 + e^{i\frac{\pi}{2}}e^{\beta(\Omega+\frac{1}{2}\Delta)}} \equiv \frac{A(\Omega)}{B(\Omega)}$$

where $\Delta := \ln \frac{\tau_\epsilon}{\tau_\sigma} = \ln \tau_\epsilon - \ln \tau_\sigma$ is the width of the mid-range in the log-log domain. We can then express the compressibility as

$$\breve{\kappa}(\omega) = \psi(\Omega), \quad \text{where} \quad \Omega = \ln \omega + \tfrac{1}{2} \ln \tau_\epsilon \tau_\sigma = \ln \sqrt{\tau_\epsilon \tau_\sigma}\omega.$$

Here we use $\breve{\kappa}(\omega)$ as the dimensionless compressibility such that $\kappa(\omega) = \kappa_0 \breve{\kappa}(\omega)$. Note that $\psi(\Omega)$ revolves around the mid-point of the mid-range; $\ln \omega = -\frac{1}{2} \ln \tau_\epsilon \tau_\sigma$. Clearly $\breve{\kappa}(-\frac{1}{2} \ln \tau_\epsilon \tau_\sigma) = \psi(0)$. In the language of Lemma 4.2.1 we need these quantities.

$$|A(\Omega)|^2 = 2e^{\beta(\Omega - \frac{1}{2}\Delta)} \left(\cosh \beta(\Omega - \tfrac{1}{2}\Delta) + \cos \tfrac{\pi}{2}\beta\right) \tag{4.2.5a}$$

$$|B(\Omega)|^2 = 2e^{\beta(\Omega + \frac{1}{2}\Delta)} \left(\cosh \beta(\Omega + \tfrac{1}{2}\Delta) + \cos \tfrac{\pi}{2}\beta\right) \tag{4.2.5b}$$

$$\mathfrak{Re}\, A\overline{B}(\Omega) = 2e^{\beta\Omega} \left(\cosh \beta\Omega + \cosh \tfrac{1}{2}\beta\Delta \cos \tfrac{\pi}{2}\beta\right) \tag{4.2.5c}$$

$$\mathfrak{Im}\, A\overline{B}(\Omega) = -2e^{\beta\Omega} \sinh \tfrac{1}{2}\beta\Delta \sin \tfrac{\pi}{2}\beta. \tag{4.2.5d}$$

We will begin by examining what happens as $\beta \to 0$. As we already mentioned, the exponents of (4.2.3) implies that as $\beta \to 0$, $\mathcal{A}_{\text{vis}}(\omega)$ should approach a straight line. Trouble is that the $\sin \frac{\pi}{2}\beta$ coefficients imply that $\mathcal{A}_{\text{vis}}(\omega) \to 0$. We will now see that both statements are true simultaneously. In fact, it behaves like a line whose slope goes to zero. We begin by observing

$$\lim_{\beta \to 0} |A|^2 = \lim_{\beta \to 0} |B|^2 = \lim_{\beta \to 0} \mathfrak{Re}\, A\overline{B} = 4$$

Also note that $\sinh x$ obeys the same famous limit as $\sin x$:

$$\lim_{x \to 0} \frac{\sin x}{x} = \lim_{x \to 0} \frac{\sinh x}{x} = 1.$$

By using the first point of Lemma 4.2.1 we can see that $\mathcal{A}_{\text{vis}}(\omega)$ behaves like the line $\frac{1}{16}\frac{1}{c_0}\Delta\pi\beta^2\omega$.

$$\begin{aligned}
\lim_{\beta \to 0} \frac{\mathcal{A}_{\text{vis}}(\omega)}{\frac{1}{16}\frac{1}{c_0}\Delta\pi\beta^2\omega} &= \lim_{\beta \to 0} \frac{-\,\mathfrak{Im}\,\sqrt{\psi(\Omega = \ln \sqrt{\tau_\epsilon \tau_\sigma}\omega)}}{\frac{1}{16}\Delta\pi\beta^2} \\
&= \lim_{\beta \to 0} \frac{-\,\mathfrak{Im}\, A\overline{B}}{|B|\sqrt{2(|A||B| + \mathfrak{Re}\, A\overline{B})}\frac{1}{16}\Delta\pi\beta^2} \\
&= \frac{1}{2 * \sqrt{2(2*2+4)}} \lim_{\beta \to 0} \left(\frac{2}{\frac{1}{4}} * \frac{\sinh \frac{1}{2}\beta\Delta}{\frac{1}{2}\beta\Delta} * \frac{\sin \frac{\pi}{2}\beta}{\frac{\pi}{2}\beta} \right) = 1.
\end{aligned}$$

From this we conclude that observations of exponents γ close to 1 is only feasible if Δ is large, that is, if $\tau_\epsilon \gg \tau_\sigma$, as this would counteract the smallness of β^2. Though this goes against the empirical suggestions we have already established. Under the assumption that τ_ϵ is close to τ_σ, the fractional Zener model seems to struggle with modeling power-laws with exponents close to $\gamma = 1$. In any case, the fractional Zener model cannot model attenuation at γ exactly 1.

Now let us deal with the case $\tau_\sigma \to \tau_\epsilon$ or in other words $\Delta \to 0$. For this we introduce the approximate attenuation

$$\mathcal{A}_{\text{vis}}^{\text{approx}}(\omega) = -\tfrac{1}{2}\omega\sqrt{\rho\kappa_0}\, \mathfrak{Im}\, \breve{\kappa}(\omega). \tag{4.2.6}$$

The closed form of this, without the $\mathfrak{Im}$ operator, is much easier to find since $\kappa(\omega)$ is freed from its square root. Way find after some calculation that

$$\mathcal{A}_{\text{vis}}^{\text{approx}}(\omega) = \frac{\omega}{2c_0}\left\{1 - \left(\frac{\tau_\sigma}{\tau_\epsilon}\right)^\beta\right\}\frac{\sin(\frac{\pi}{2}\beta)}{(\omega\tau_\epsilon)^{-\beta} + 2\cos(\frac{\pi}{2}\beta) + (\omega\tau_\epsilon)^\beta} \tag{4.2.7}$$

which may be easily seen to have the asymptotic power-law expressions

$$\begin{aligned}\mathcal{A}_{\text{vis}}^{\text{approx}}(\omega) &\underset{\omega\to 0}{\sim} \frac{1}{2c_0}\left\{1 - \left(\tfrac{\tau_\sigma}{\tau_\epsilon}\right)^\beta\right\}\sin(\tfrac{\pi}{2}\beta)\tau_\epsilon^\beta\omega^{1+\beta}\\ \mathcal{A}_{\text{vis}}^{\text{approx}}(\omega) &\underset{\omega\to\infty}{\sim} \frac{1}{2c_0}\left\{1 - \left(\tfrac{\tau_\sigma}{\tau_\epsilon}\right)^\beta\right\}\sin(\tfrac{\pi}{2}\beta)\tau_\epsilon^{-\beta}\omega^{1-\beta}.\end{aligned}$$

So how does this relate to $\Delta \to 0$? Let us attempt to evaluate

$$\lim_{\Delta\to 0}\frac{\mathcal{A}_{\text{vis}}^{\text{approx}}(\omega)}{\mathcal{A}_{\text{vis}}(\omega)} = \lim_{\Delta\to 0}\frac{1}{2}\frac{\mathfrak{Im}\,\psi(\Omega)}{\mathfrak{Im}\,\sqrt{\psi(\Omega)}}. \tag{4.2.8}$$

Observe first that

$$\lim_{\Delta\to 0}\frac{\mathfrak{Re}\,A\overline{B}}{|B|^2} = \lim_{\Delta\to 0}\frac{|A|^2}{|B|^2} = 1$$

Then recall from (4.2.4) that

$$\mathfrak{Im}\,\psi(\Omega) = \frac{\mathfrak{Im}\,A\overline{B}}{|B|^2}.$$

Applying all this, and finally the first part of Lemma 4.2.1, to (4.2.8) we get

$$\begin{aligned}\lim_{\Delta\to 0}\frac{\mathcal{A}_{\text{vis}}^{\text{approx}}(\omega)}{\mathcal{A}_{\text{vis}}(\omega)} &= \lim_{\Delta\to 0}\frac{1}{2} * \frac{\mathfrak{Im}\,A\overline{B}}{|B|^2} * \frac{|B|\sqrt{2(|A||B| + \mathfrak{Re}\,A\overline{B})}}{\mathfrak{Im}\,A\overline{B}}\\ &= \lim_{\Delta\to 0}\frac{1}{2} * \sqrt{2\left(\frac{|A|}{|B|} + \frac{\mathfrak{Re}\,A\overline{B}}{|B|^2}\right)} = 1.\end{aligned}$$

What we have now found is quite satisfying. If τ_ϵ and τ_σ are of roughly the same size, we may approximate the attenuation by the expression (4.2.7). Recall from (2.2.4) that $\tau_\epsilon > \tau_\sigma$. We see in (4.2.7) that when $\tau_\sigma/\tau_\epsilon$ is slightly less than one, the attenuation becomes very small. In fact, in the next chapter we will deal only with small viscoelastic absorptive attenuation, and we will use this result then.

Finally, should one be faced with an application where understanding the details of the mid-range is desirable, we should mention another modest advantage that Lemma 4.2.1 gives. If we now take the logarithm of the $\mathcal{A}_{\text{vis}}(\omega)$ and use the variable $\Omega = \ln\left(\sqrt{\tau_\epsilon\tau_\sigma}\omega\right)$, or inversely $\omega = \frac{1}{\sqrt{\tau_\epsilon\tau_\sigma}}e^\Omega$ we have made it to the log-log domain.

$$\ln\mathcal{A}_{\text{vis}}\left(\tfrac{1}{\sqrt{\tau_\epsilon\tau_\sigma}}e^\Omega\right) = \ln\left\{-\tfrac{1}{c_0\sqrt{\tau_\epsilon\tau_\sigma}}e^\Omega\,\mathfrak{Im}\,\sqrt{\psi(\Omega)}\right\}$$

Lemma 4.2.1 we can now give us a complete expression for the attenuation in the general case in the $\ln\mathcal{A}_{\text{vis}}$-$\Omega$ domain:

$$\ln\mathcal{A}_{\text{vis}}\left(\tfrac{1}{\sqrt{\tau_\epsilon\tau_\sigma}}e^\Omega\right) = \Omega - \tfrac{1}{2}\ln\tfrac{|B|^2}{|\,\mathfrak{Im}\,A\overline{B}|} - \tfrac{1}{2}\operatorname{arcsinh}\tfrac{\mathfrak{Re}\,A\overline{B}}{|\,\mathfrak{Im}\,A\overline{B}|} - \tfrac{1}{2}\ln 2 - \ln\left(c_0\sqrt{\tau_\sigma\tau_\epsilon}\right) \tag{4.2.9}$$

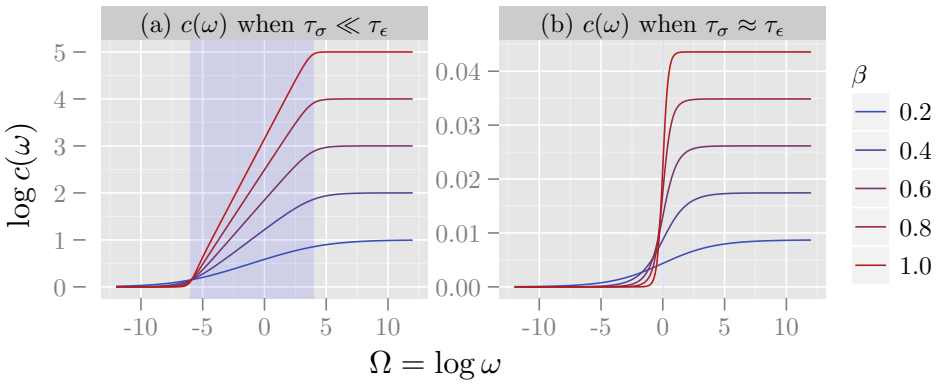

Figure 4.3: Speed of sound of fractional Zener normalized such that $c(0) = 1$ m/s. The light blue area is the mid-range $-\log \tau_\epsilon < \log(\omega) < -\log(\tau_\sigma)$, with $\tau_\epsilon = 10^6$s and $\tau_\sigma = 10^{-3}$s in (a), and $\tau_\epsilon \approx \tau_\sigma \approx 1$s in (b).

Looking back at (4.2.5) we see that this involves taking logarithms of $\cosh x$ functions. Upon some reflection (just write out the definition of $\cosh x$) one sees immediately that the logarithm of $\cosh x$ behaves very much like $|x|$. Asymptotically we have

$$\lim_{x\to\pm\infty} \frac{\ln\left[2a\left(\cosh x + b\right)\right]}{x} = \lim_{x\to\pm\infty} \frac{\operatorname{arcsinh}\left[a(\cosh x + b)\right]}{x} = |x| + \ln a \qquad (4.2.10)$$

These functions are for the most part very close to $|x|$ except for a short and smooth transition around 0 between the two branches of $|x|$ around $x = 0$. However, if ab is large, the transition becomes longer – like a flat suspension bridge:

$$\operatorname{arcsinh}\left[a(\cosh x + b)\right] \approx \begin{cases} -x + \ln a & \text{for } x < -\phi \\ \text{constant} = \operatorname{arcsinh} a(1+b) & \text{for } |x| < \phi \\ x + \ln a & \text{for } x > \phi \end{cases} \qquad (4.2.11)$$

Here ϕ denotes the limit between the mid-range suspension bridge behavior and the high- and low-range $|x|$ behavior. Though we will not pursue these details further, we have found an explicit expression in (4.2.9) for the attenuation in the log-log domain. With the tools presented above one could for instance examine the details of the transitions between the three bands. Remember that the slope of the line in the log-log domain is really the exponent. One could for instance establish three bands where one guarantees that the slope is within a certain specified error bar of the three slopes $1 + \beta$, $1 - \frac{1}{2}\beta$ and $1 + \beta$ from (4.2.3). One would also discover that claiming that the limits between the bands are exactly $\ln \omega = -\ln \tau_\epsilon$ and $\ln \omega = -\ln \tau_\sigma$ is a simplification.

To conclude let us look at the speed of sound in the fractional Zener model. This is given by (2.4.9) as

$$c(\omega) = \frac{\omega}{\mathcal{D}_{\text{vis}}(\omega)} = \frac{1}{\sqrt{\rho}\,\mathfrak{Re}\,\sqrt{\kappa(\omega)}}$$

which can be seen in figure 4.3. It is clear from the above that

$$c(\omega \to 0) = c_0, \quad \text{and} \quad c(\omega \to \infty) = c_0 \left(\frac{\tau_\epsilon}{\tau_\sigma}\right)^{\beta/2}.$$

We see that when $\tau_\epsilon \approx \tau_\sigma$ (Δ is small) there is very little variation in the speed of sound throughout the spectrum. This also suggests a method of measuring the size of the fraction $\frac{\tau_\sigma}{\tau_\epsilon}$ by measuring $c(0)/c(\infty)$. In fact, this is exactly how Holm and Näsholm [2011] argue that the fraction is almost equal to 1. In this respect, the fractional Zener model appears almost elastic.

4.3 Loss operator

For practical engineering purposes, say in medical ultrasound, one is often satisfied with a model which coincides with empirical evidence, even though the model is not understood from first physical principles. If the solution to the chosen differential equation stands the test of confrontation with real measurements of attenuation through the liver, do we really need to know why?

Following this philosophy we may take a look at the one variable viscoelastic wave equation 2.3.6. We see that it takes the form of the classic elastic wave equation 2.3.5 with some extra derivative terms. This inspires us the make the following ansatz about the wave propagation

$$\partial_z^2 p - \frac{1}{c_0^2}\partial_t^2 p + Lp = 0.$$

Here L is a **loss operator**. As in Holm and Sinkus [2010] we could attempt with $L = \tau^\beta D_C^\beta \partial_z^2$ which would give the equation

$$\partial_z^2 p - \frac{1}{c_0^2}\partial_t^2 p + \tau^\beta D_C^\beta \partial_z^2 p = 0$$

Assuming a plane harmonic wave $p(z,t) = e^{-(\omega t - kz)}$ we may apply the Fourier-transform (recall the Fourier-transform of fractional derivatives (4.0.3)) and get

$$k^2 - \frac{1}{c_0^2}\omega^2 + \tau^\beta (i\omega)^\beta k^2 = 0,$$

which yields the dispersion relation

$$k = \frac{\omega}{c_0}\sqrt{\frac{1}{1 + (i\omega\tau)^\beta}}.$$

Remember that the attenuation is given by the negative of the imaginary part of the wave number (2.4.5). (It may be shown from Holm and Sinkus [2010] that the attenuation follows $\omega^{1+\beta}$ for low frequencies and $\omega^{1-\beta/2}$ for high-frequencies.) We see then that the question of designing a wave equation which corresponds to measurements becomes a question of choosing the right loss operator L. The loss operator, however, can not be chosen freely. Pursuant to section 2.4, causality of the wave equation sets restrictions on the dispersion relation. A sufficient condition is that the dispersion relation satisfies the Kramers-Kronig relation.

4.4 Alternatives to fractional calculus

In contrast to the previous section, we will now ask the bigger questions. We have succeeded in modeling viscoelastic attenuation with a power-law exponent $\gamma \in (0, 2)$ using the formalism of fractional calculus, but what does it mean? What is the physical interpretation of a fractional derivative?

First we may mention a phenomenological explanation found in some sources. Since the attenuation is given by $\mathcal{A}_{\text{vis}}(\omega) = -\omega\sqrt{\rho}\,\mathfrak{Im}\,\sqrt{\kappa(\omega)}$ it inherits its behavior from $\kappa(\omega)$. Remember that $\kappa(\omega)$ is just the impulse response of Figure 2.1. This transfer mechanism is often modeled by dashpots and springs in series and/or parallel. Furthermore, it can be shown [Schiessel et al., 1995] that an infinite hierarchy of carefully chosen dashpots and springs may give rise to a fractional constitutive equation.

A more physically appealing approach which is clearly analogous to what we learned in section 3.4.1 (A $1/\omega^\alpha$ process may be constructed from adding up a weighted sum of $1/\omega^2$ processes) is this. Nachman et al. [1990] describes a wave equation with so called **relaxation losses**. This wave equation predicates on thermodynamics and other first principles of acoustic. Note especially that these physical origins are different from the linear viscoelastic principles set out in chapter 2. The relaxation losses are similar to that of the classic Zener model in that it follows ω^2 for low frequencies before it flattens out and becomes constant for high frequencies [Nachman et al., 1990, equation (47) and (49)]. Visually it resembles figure 4.2(b) with $\beta = 1$. In Näsholm and Holm [2011] it is shown that the fractional Zener model of arbitrary exponent β can be made from a weighted sum of relaxation process. This is perhaps a more physically appealing argument for the fractional Zener model as relaxation models are thought to be firmly physically grounded.

We will continue down the same path and show that we can indeed get the fractional Zener model with arbitrary β from a weighted sum of classic Zener-models. This idea is due to Mainardi and Spada [2011], but here we spell out the mathematics. There is a well known integral representation of the Mittag-Leffler function $E_\beta(-z^\beta)$ [Mainardi and Spada, 2011, equation (3.7)]

$$E_\beta(-t^\beta) = \int_0^\infty e^{-\frac{1}{x}t} f(x;\beta)dx, \quad \text{where} \quad f(x;\beta) = \frac{1}{x\pi}\frac{\sin(\beta\pi)}{x^\beta + 2\cos(\beta\pi) + x^{-\beta}},$$

which is valid for $0 < \beta \leq 1$. As a reference this may be found in appendix F. The astute reader will notice than the x in the exponent is placed slightly differently than in Mainardi and Spada [2011, equation (3.7)], though the change can be made by a simple variable substitution. One may confirm that $f(x;\beta)$ on $x \in [0, \infty)$ is indeed a distribution by

$$1 = E_\beta(0) = \int_0^\infty f(x;\beta)dx.$$

We will now sum up a family of classic Zener models (2.2.2) parametrized by

$$J_{\text{Zener}}(t; J_{\text{eq}}, x\tau_\epsilon, \tfrac{x\tau_\sigma^\beta}{\tau_\epsilon^{\beta-1}}).$$

We integrate over this family with the weights $f(x;\beta)$ and get the effective creep

compliance

$$\begin{aligned}
J_{\text{effective}}(t;\beta) &= \int_0^\infty J_{\text{Zener}}(t; J_{\text{eq}}, x\tau_\epsilon, \tfrac{x\tau_\sigma^\beta}{\tau_\epsilon^{\beta-1}}) f(x;\beta)dx \\
&= \int_0^\infty J_{\text{eq}} \left\{ 1 - \left(1 - \left(\tfrac{\tau_\sigma}{\tau_\epsilon} \right)^\beta \right) \exp\left(-\tfrac{1}{x} \tfrac{t}{\tau_\epsilon} \right) \right\} f(x;\beta)dx \\
&= J_{\text{eq}} \left\{ \int_0^\infty f(x;\beta)dx - \left(1 - \left(\tfrac{\tau_\sigma}{\tau_\epsilon} \right)^\beta \right) \int_0^\infty \exp\left(-\tfrac{1}{x} \tfrac{t}{\tau_\epsilon} \right) f(x;\beta)dx \right\} \\
&= J_{\text{eq}} \left\{ 1 - \left(1 - \left(\tfrac{\tau_\sigma}{\tau_\epsilon} \right)^\beta \right) E_\beta \left(- \left(\tfrac{t}{\tau_\epsilon} \right)^\beta \right) \right\},
\end{aligned}$$

which is exactly the creep compliance of the fractional Zener model (4.1.9).

Chapter 5

Combination model: Propagation through media with both microstructure and viscoelasticity

We have finally arrived at the milestone where we combine the ideas from fractional viscoelasticity with fractal spatial structure. To achieve this we will lay out the theory of the two articles Burridge et al. [1993] and Le and Burridge [1998]. However, we will make two important simplifications. First, Burridge et al. [1993] deals with 3 dimensions, but we stick to our idealized 1-dimensional case. Second, Burridge et al. [1993] implements spatial structure both in the form of discontinuous jumps *and* continuous variations in between these jumps. As this gives no real conceptual benefit we include continuous variations only. Furthermore, we will divide our discussion into three parts. The first section is a preparation which will qualify us to understand where the articles in question begin. In the second section we explicate the main argument of Burridge et al. [1993]. And finally, in the last section we extend this to the fractional case – both to the fractional Zener model as well as fractal spatial structure.

5.1 Preparing a wave equation with separate elastic and viscoelastic components

Concretely, we will now establish the theory necessary to understand Burridge et al. [1993, section I&IIA]. To begin let us formalize the split from (2.2.5)

$$\kappa(t) = J_{\text{in}}\delta(t) + H(t)\partial_t \bar{J}(t)$$

by defining $\kappa_{\text{vis}} := H(t)\partial_t \bar{J}(t)$. In this language we may rewrite this as

$$\kappa(t) = \underbrace{\kappa_\infty \delta(t)}_{\text{elastic part}} + \underbrace{\kappa_{\text{vis}}(t)}_{\text{viscoelastic part}} . \tag{5.1.1}$$

Recall again from (2.1.13a) that the instantaneous creep compliance J_{in} is the same as the generalized compressibility at infinitely high frequency κ_∞. Looking at this in the frequency domain is perhaps more informative. We take the Fourier-transform of (5.1.1) and get

$$\widehat{\kappa}(\omega) = \kappa_\infty + \widehat{\kappa}_{\text{vis}}(\omega),$$

or

$$\widehat{\kappa}_{\text{vis}}(\omega) = \widehat{\kappa}(\omega) - \kappa_\infty. \tag{5.1.2}$$

So $\widehat{\kappa}_{\text{vis}}(\omega)$ is simply the generalized compressibility minus the compressibility at the limit of infinite frequency. We will now endow this instantaneous response with a spatial structure $\kappa_\infty(z)$. This spatial variation of the underlying medium is what Burridge et al. [1993] means with **microstructure**. This is a continuous version of the stratified spatial variation we saw in section 3. We learned then that spatial variation in acoustic impedance gives rise to scattering and apparent attenuation, which we will confirm again to be true in this chapter.

It is clear from (4.1.8), that if $\kappa_\infty(z)$ varies with z, so must one of the other variables κ_0, τ_σ or τ_ϵ. Clearly these variables are featured in $\kappa_{\text{vis}}(z,t)$, so $\kappa_{\text{vis}}(z,t)$ must itself depend on z. There is a lesson to be learned from this: Within the linear viscoelastic regime, it is impossible to isolate spatial structure in the instantaneous behavior of the generalized compressibility $\kappa(z,t)$ without also inducing spatial structure in its long term behavior.

Let us formulate a new wave equation based on the compressibility split (5.1.1). By inserting this into our original pressure-velocity system in wave equation 2.3.1 we get

$$\begin{aligned}\partial_z p(z,t) &= -\rho(z)\partial_t v(z,t)\\ \partial_z v(z,t) &= -\kappa_\infty(z)p(z,t) + \kappa_{\text{vis}}(z,t) * \partial_t p(z,t),\end{aligned}$$

which we may, in accordance with section 2.3 write on matrix form.

Wave equation 5.1.1 (Separated pressure-velocity system)**.**

Time domain

$$\partial_z \boldsymbol{v}(z,t) + M_{in}(z)\partial_t \boldsymbol{v}(z,t) + \partial_t M_{vis}(z,t) * \boldsymbol{v}(z,t) = 0$$

$$M_{in}(z) = \begin{bmatrix} 0 & \rho(z) \\ \kappa_\infty(z) & 0 \end{bmatrix}, \text{ and } M_{vis}(z,t) = \begin{bmatrix} 0 & 0 \\ \kappa_{vis}(z,t) & 0 \end{bmatrix}.$$

- General viscoelastic medium; compressibility $\kappa(z,t) = \kappa_\infty(z)\delta(t) + \kappa_{vis}(t)$

This is exactly on the form of Burridge et al. [1993, equation (3)] where $M_{\text{in}}(z)$ contains the elastic response with its spatial structure and $M_{\text{vis}}(z,t)$ describes the viscoelastic effect. We need to rewrite the wave equation system 5.1.1 in terms of left- and right-going waves. As we did for wave equation 2.3.4 we begin by finding the spectral decomposition of $M_{\text{in}}(z)$:

$$M_{\text{in}}(z) = E(z)\Lambda(z)E^{-1}(z), \tag{5.1.3}$$

$$\text{with } \Lambda(z) = \begin{bmatrix} \frac{1}{c(z)} & 0 \\ 0 & -\frac{1}{c(z)} \end{bmatrix}, E(z) = \frac{1}{\sqrt{2}} \begin{bmatrix} Z(z)^{1/2} & -Z(z)^{1/2} \\ Z(z)^{-1/2} & Z(z)^{-1/2} \end{bmatrix}. \tag{5.1.4}$$

This is exactly the same decomposition as (2.3.11) except now the acoustic impedance and speed of sound are given by

$$Z(z) = \sqrt{\frac{\rho(z)}{\kappa_\infty(z)}}, \quad \text{and} \quad c(z) = \sqrt{\frac{1}{\kappa_\infty(z)\rho(z)}}.$$

There is a subtle difference here. They are no longer defined by the compressibility modulus κ_0 from Hooke's law, but instead by the instantaneous part $\kappa_\infty = J_{\text{in}}$ of the viscoelastic response system described in figure 2.2. One may also note that the actual speed of sound is given by (2.4.9). We assume however, as will be made explicit soon, that $\kappa_{\text{vis}}(z,t)$ is very small which implies that $\kappa_0 \approx \kappa_\infty$ and our rheological model is nearly elastic. Within this context this speed of sound as stated above is a good approximation.

Analogous to (2.3.13) we define the left- and right-going waves

$$\boldsymbol{w}(z,t) := E(z)^{-1}\boldsymbol{v}(z,t) \tag{5.1.5}$$

We should perhaps give all these entities $E(z)$, $\Lambda(z)$, $Z(z)$, $c(z)$ and $\boldsymbol{w}(z,t)$ the subscript "in" to remind us that these predicate only on the instantaneous (or infinite frequency) behavior of our viscoelastic system. But we will suppress this not to get lost in too much notation. On the same note, we will sometimes suppress the dependencies of our variables to make the equations easier to read. Just to be clear, $E(z)$, $M_{\text{in}}(z)$, $M_{\text{vis}}(z)$, $\Lambda(z)$, $\kappa_{\text{vis}}(z,t)$ and $\boldsymbol{w}(z,t)$ all depend on z, though the five first of the aforementioned variables pertain only to the spatial structure of the elastic response, so they do not depend on time.

By swapping around (5.1.5) we get $\boldsymbol{v}(z,t) = E(z)\boldsymbol{w}(z,t)$. We now insert this into wave equation 5.1.1.

$$\begin{aligned} 0 &= \partial_z(E\boldsymbol{w}) + M_{\text{in}}\partial_t(E\boldsymbol{w}) + \partial_t M_{\text{vis}} * (E\boldsymbol{w}) \\ &= (\partial_z E)\boldsymbol{w} + E(\partial_z \boldsymbol{w}) + M_{\text{in}}E(\partial_t \boldsymbol{w}) + \partial_t M_{\text{vis}} E * \boldsymbol{w} \end{aligned}$$

Finally, by applying $M_{\text{in}}(z)E(z) = E(z)\Lambda(z)$ by (5.1.5) we get

$$(\partial_z E)\boldsymbol{w} + E(\partial_z \boldsymbol{w}) + E\Lambda(\partial_t \boldsymbol{w}) + \partial_t M_{\text{vis}} E * \boldsymbol{w} = 0$$

If we multiply throughout by E^{-1} and rearrange the terms we get

$$\partial_z \boldsymbol{w} + \Lambda\partial_t \boldsymbol{w} = -\underbrace{E^{-1}(\partial_z E)\boldsymbol{w}}_{Microstructure} - \underbrace{E^{-1}(\partial_t M_1)E * \boldsymbol{w}}_{Viscoelasticity}. \tag{5.1.6}$$

This is Burridge et al. [1993, equation (14)]. As a reality check we may conduct the following thought experiment. Suppose now that there is no microstructure, i.e. the acoustic impedance (and in turn E) is not dependent on z such that $\partial_z E = 0$. Then the microstructure term disappears. Likewise, if there is no viscoelastic behavior, i.e. $M_{\text{vis}} = 0$, the viscoelastic term vanishes. If both go away we are left with $\partial_z \boldsymbol{w} + \Lambda\partial_t \boldsymbol{w} = 0$ which is simply the wave equation 2.3.4.

As in Burridge et al. [1993, equation (18a&b)], let us define the two matrices

$$\begin{aligned} \boldsymbol{A}_{\text{Bur}}(z) &:= E^{-1}(z)(\partial_z E(z)) \\ \boldsymbol{B}_{\text{Bur}}(z,t) &:= E^{-1}(z)(\partial_t M_{\text{vis}}(z,t))E(z) \end{aligned}$$

which allows us to write our wave equation on a more compact form

$$\partial_z \boldsymbol{w}(z,t) + \Lambda(z)\partial_t \boldsymbol{w}(z,t) = -\boldsymbol{A}_{\mathrm{Bur}}(z)\boldsymbol{w}(z,t) - \boldsymbol{B}_{\mathrm{Bur}}(z,t) * \boldsymbol{w}(z,t) \tag{5.1.7}$$

Finally we may compute our two matrices $\boldsymbol{A}_{\mathrm{Bur}}(z)$ and $\boldsymbol{B}_{\mathrm{Bur}}(z,t)$ and find, after some calculation

$$\boldsymbol{A}_{\mathrm{Bur}}(z) = \frac{1}{2}\partial_z \log Z(z) \begin{bmatrix} 0 & -1 \\ -1 & 0 \end{bmatrix} \tag{5.1.8}$$

$$\boldsymbol{B}_{\mathrm{Bur}}(z,t) = \frac{1}{2}\partial_t \kappa_{\mathrm{vis}}(z,t) Z(z) \begin{bmatrix} 1 & -1 \\ 1 & -1 \end{bmatrix}. \tag{5.1.9}$$

5.1.1 Reparametrizing by travel time. Instead of the spatial variable z we seek to reparametrize our functions in terms of the travel time

$$\tau(z) = \int_0^z \frac{1}{c(s)} ds.$$

To change the z-axis into a τ-axis one may think of the z-axis as being made of a soft rubber band. Then stretch the parts where the wave is slow and compress the parts where the wave is fast until the wave ends up traveling with constant speed along the τ-axis. In terms of the Goupillaud medium, this means that all the interfaces end up being equidistant along the τ-axis. In fact the ODA theory of section 3.3 uses this point of view. The spectrum of the reflection coefficients is computed not along its spatial placement, but along the travel time τ axis where they are equidistant. We may reparametrize our wave equation (5.1.7) by the basic chain rule

$$\frac{\partial}{\partial z} = \frac{\partial \tau}{\partial z}\frac{\partial}{\partial \tau} = \frac{1}{c(z)}\frac{\partial}{\partial \tau} = \frac{1}{c(\tau)|_{\tau=\tau(z)}}\frac{\partial}{\partial \tau}$$

Applying this to (5.1.7) we get

$$\frac{1}{c(\tau)}\partial_\tau \boldsymbol{w}(\tau,t) + \Lambda(\tau)\partial_t \boldsymbol{w}(\tau,t) = -\boldsymbol{A}_{\mathrm{Bur}}(\tau)\boldsymbol{w}(\tau,t) - \boldsymbol{B}_{\mathrm{Bur}}(\tau,t) * \boldsymbol{w}(\tau,t).$$

Multiplying by $c(z)$ gives

$$\partial_\tau \boldsymbol{w}(\tau,t) + \bar{\Lambda}\partial_t \boldsymbol{w}(\tau,t) = -\boldsymbol{A}(\tau)\boldsymbol{w}(\tau,t) - \boldsymbol{B}(\tau,t) * \boldsymbol{w}(\tau,t) \tag{5.1.10}$$

when we define the variables

$$\boldsymbol{A}(\tau) = A(\tau)\begin{bmatrix} 0 & -1 \\ -1 & 0 \end{bmatrix}, \quad \text{where} \quad A(\tau) = \frac{1}{2}\partial_\tau \log Z(\tau) \tag{5.1.11}$$

$$\boldsymbol{B}(\tau) = B(\tau)\begin{bmatrix} 1 & -1 \\ 1 & -1 \end{bmatrix}, \quad \text{where} \quad B(\tau) = \frac{1}{2}\partial_t \kappa_{\mathrm{vis}}(\tau,t) Z(\tau) c(\tau) \tag{5.1.12}$$

$$\bar{\Lambda} = \begin{bmatrix} 1 & 0 \\ 0 & -1 \end{bmatrix} \tag{5.1.13}$$

The astute reader may wonder how we got

$$c(\tau)\partial_z \log Z(\tau) = c(\tau)\frac{1}{c(\tau)}\partial_\tau \log Z(\tau) = \partial_\tau \log Z(\tau).$$

Really $\boldsymbol{w}(\tau,t)$ is abuse of notation as it could be seen as $\boldsymbol{w}(z,t)|_{z=\tau}$, but it is not. It is really a new function $\boldsymbol{w}_{\text{new}}(\tau,t) := \boldsymbol{w}_{\text{old}}(z(\tau),t)$. The same remark goes for all the other reparametrized quantities. In the frequency domain we get

$$\partial_\tau \widehat{\boldsymbol{w}}(\tau,\omega) + i\omega\bar{\Lambda}\widehat{\boldsymbol{w}}(\tau,\omega) = -\boldsymbol{A}(\tau)\widehat{\boldsymbol{w}}(\tau,\omega) - \widehat{\boldsymbol{B}}(\tau,\omega)\widehat{\boldsymbol{w}}(\tau,\omega),$$

or alternatively

$$\widehat{\mathcal{W}}\widehat{\boldsymbol{w}} = -\boldsymbol{A}(\tau)\widehat{\boldsymbol{w}} - \widehat{\boldsymbol{B}}(\tau,\omega)\widehat{\boldsymbol{w}}$$

where we have introduced the differential operator $\mathcal{W} = \partial_\tau + \bar{\Lambda}\partial_t$ which is $\widehat{\mathcal{W}} = \partial_\tau + i\omega\bar{\Lambda}$ in the frequency domain.

5.2 Burridge et al.'s model: Microstructure small, viscoelastic absorption even smaller

We have already gone through the main ideas of Burridge et al. [1993, section I&IIA]. In the following section we expound the calculations of Burridge et al. [1993, section IIB&C]. Since the differential equation (5.1.10) can not be solved exactly we must make some simplifying assumptions. The quintessence of Burridge et al. [1993] is that we begin with a medium without neither microstructure nor viscoelasticity

$$\mathcal{W}\boldsymbol{w}(\tau,t) = 0,$$

and then perturb it by adding them in small quantities. More precisely we approximate the solution to the equation

$$\widehat{\mathcal{W}}\widehat{\boldsymbol{w}}(\tau,t) = -\varepsilon\boldsymbol{A}(\tau)\widehat{\boldsymbol{w}}(\tau,t) - \varepsilon^2\widehat{\boldsymbol{B}}(\tau,\omega)\widehat{\boldsymbol{w}}(\tau,t) \tag{5.2.1}$$

for small ε. Moreover, the separation of scales, i.e. that the viscoelastic element is much smaller than the spatial inhomogeneities, is also of key importance. This allows us at times to ignore the viscoelastic effects while still considering microstructure. As is usual in perturbation of differential equations, in accordance with Burridge et al. [1993, equation (32)] we assume the solution can be approximated by

$$\boldsymbol{w}(\tau,t) = \boldsymbol{w}^{(0)}(\tau,t) + \varepsilon\boldsymbol{w}^{(1)}(\tau,t) + \varepsilon^2\boldsymbol{w}^{(2)}(\tau,t) \tag{5.2.2}$$

in an neighborhood of $(\tau_1,0)$. Remember from (2.3.13) that $\boldsymbol{w}(\tau,t)$ is really a vector containing the left- and right-going waves $R(\tau,t)$ and $L(\tau,t)$. In addition we assume, without loss of generality, that

$$R^{(1)}(\tau_1,t) = R^{(2)}(\tau_1,t) = 0, \tag{5.2.3}$$

which immediately leads to

$$R(\tau_1,t) = R^{(0)}(\tau_1,t). \tag{5.2.4}$$

Let us put our approximate solution into the two first $\boldsymbol{w}$'s of (5.2.1).

$$\widehat{\mathcal{W}}\widehat{\boldsymbol{w}}^{(0)} + \varepsilon(\widehat{\mathcal{W}}\widehat{\boldsymbol{w}}^{(1)} + \boldsymbol{A}\widehat{\boldsymbol{w}}^{(0)}) + \varepsilon^2(\widehat{\mathcal{W}}\widehat{\boldsymbol{w}}^{(2)} + \boldsymbol{A}\widehat{\boldsymbol{w}}^{(1)} + \widehat{\boldsymbol{B}}\widehat{\boldsymbol{w}}^{(0)}) + O(\varepsilon^3) = 0$$

If we ignore higher order terms we get a second degree polynomial in ε. In order for this to be exactly 0 for all ε close to 0, each coefficient must be zero, and we get a new set of equations:

$$\widehat{\mathcal{W}}\widehat{\boldsymbol{w}}^{(0)} = 0 \tag{5.2.5}$$
$$\widehat{\mathcal{W}}\widehat{\boldsymbol{w}}^{(1)} = -\boldsymbol{A}\widehat{\boldsymbol{w}}^{(0)} \tag{5.2.6}$$
$$\widehat{\mathcal{W}}\widehat{\boldsymbol{w}}^{(2)} = -\boldsymbol{A}\widehat{\boldsymbol{w}}^{(1)} - \widehat{\boldsymbol{B}}\widehat{\boldsymbol{w}}^{(0)} \tag{5.2.7}$$

Finally we write down a restriction on our left-going waves. Our setup is again akin to figure 3.2 where we send a right-going wave through the slab of material that begins at $z = 0$ and ends at $z = L$. If T is the arrival time – the time it takes to cross the whole slab, this corresponds to beginning at $\tau = 0$ and ending at $\tau = T$. Since we are not simultaneously sending another signal through the material in the opposite direction, it is clear that there is no left-going wave at the other end of the slab. This gives us $L(\tau, t) = 0$ for all t and $\tau > T$. Since this should be true for all ε we have

$$L^{(0)}(\tau, t) = L^{(1)}(\tau, t) = L^{(2)}(\tau, t) = 0, \text{ for all } t, \text{ and } \tau > T. \tag{5.2.8}$$

Armed with these initial conditions and a set of differential equations, we are ready for some mathematical accounting. We begin by solving (5.2.5), which by theorem E.0.22 is simply

$$\widehat{\boldsymbol{w}}^{(0)}(\tau, \omega) = e^{-i\omega\bar{\Lambda}\tau}C = \begin{bmatrix} e^{-i\omega\tau} & 0 \\ 0 & e^{+i\omega\tau} \end{bmatrix} \begin{bmatrix} c_1 \\ c_2 \end{bmatrix}$$

By initial condition (5.2.8) we must choose $c_2 = 0$ and by (5.2.4) we get $c_1 = e^{i\omega\tau_1}R(\tau_1, t)$, so we have

$$\widehat{\boldsymbol{w}}^{(0)}(\tau, \omega) = e^{-i\omega(\tau-\tau_1)}\widehat{R}(\tau_1, \omega) \begin{bmatrix} 1 \\ 0 \end{bmatrix}, \tag{5.2.9}$$

which is just an elastic right-going wave. Solving equations (5.2.6) and (5.2.7) is slightly trickier. We start with (5.2.6). To solve this inhomogeneous system we must by theorem E.0.23 first find the fundamental matrix for the homogeneous equation $\widehat{\mathcal{W}}\boldsymbol{w}^{(1)} = 0$. By theorem E.0.22 the fundamental matrix is simply $Y = e^{-i\omega\bar{\Lambda}\tau}$. Theorem E.0.23 gives

$$\begin{aligned}
D(\tau) &= \int_0^\tau Y^{-1}(s)G(s)ds \\
&= -\int_0^\tau e^{i\omega\bar{\Lambda}s}\boldsymbol{A}(s)\widehat{\boldsymbol{w}}^{(0)}(s, \omega)ds \\
&= \int_0^\tau e^{i\omega\bar{\Lambda}s}A(s) \begin{bmatrix} 0 & 1 \\ 1 & 0 \end{bmatrix} \widehat{\boldsymbol{w}}^{(0)}(s, \omega)ds \\
&= \int_0^\tau A(s) \begin{bmatrix} e^{+i\omega s} & 0 \\ 0 & e^{-i\omega s} \end{bmatrix} \begin{bmatrix} 0 & 1 \\ 1 & 0 \end{bmatrix} \begin{bmatrix} 1 \\ 0 \end{bmatrix} e^{-i\omega(s-\tau_1)}\widehat{R}(\tau_1, \omega)ds \\
&= \widehat{R}(\tau_1, \omega) \int_0^\tau A(s)e^{-i\omega s}e^{-i\omega(s-\tau_1)}ds \begin{bmatrix} 0 \\ 1 \end{bmatrix} \\
&= \widehat{R}(\tau_1, \omega)e^{i\omega\tau_1} \int_0^\tau A(s)e^{-2i\omega s}ds \begin{bmatrix} 0 \\ 1 \end{bmatrix}
\end{aligned}$$

Furthermore, by theorem E.0.23 we have the general solution

$$\begin{aligned}\widehat{\boldsymbol{w}}^{(1)}(\tau,\omega) &= Y(\tau)(D(\tau)+C)\\ &= \begin{bmatrix} e^{-i\omega\tau} & 0 \\ 0 & e^{+i\omega\tau}\end{bmatrix}\left\{\widehat{R}(\tau_1,\omega)e^{i\omega\tau_1}\int_0^\tau A(s)e^{-2i\omega s}ds\begin{bmatrix}0\\1\end{bmatrix}+\begin{bmatrix}c_1\\c_2\end{bmatrix}\right\}\\ &= \widehat{R}(\tau_1,\omega)e^{i\omega\tau_1}e^{i\omega\tau}\int_0^\tau A(s)e^{-2i\omega s}ds\begin{bmatrix}0\\1\end{bmatrix}+\begin{bmatrix}c_1e^{-i\omega\tau}\\c_2e^{+i\omega\tau}\end{bmatrix}\end{aligned}$$

Again we remember that the two components of $\boldsymbol{w}^{(1)}$ have names $(R^{(1)}, L^{(1)})$. To satisfy initial condition (5.2.3) we immediately see that $c_1 = 0$. To satisfy initial condition (5.2.8) c_2 must satisfy the equation

$$0 = \widehat{L}^{(1)}(T,\omega) = \widehat{R}(\tau_1,\omega)e^{i\omega\tau_1}e^{i\omega T}\int_0^T A(s)e^{-2i\omega s}ds + c_2e^{i\omega T},$$

giving

$$c_2 = -\widehat{R}(\tau_1,\omega)e^{i\omega\tau_1}\int_0^T A(s)e^{-2i\omega s}ds.$$

and finally

$$\begin{aligned}\widehat{\boldsymbol{w}}^{(1)}(\tau,\omega) &= -\widehat{R}(\tau_1,\omega)e^{i\omega\tau_1}e^{i\omega\tau}\int_\tau^T A(s)e^{-2i\omega s}ds\begin{bmatrix}0\\1\end{bmatrix}\\ &= -\widehat{R}(\tau_1,\omega)e^{i\omega\tau_1}e^{i\omega\tau}\Psi(\tau)\begin{bmatrix}0\\1\end{bmatrix}.\end{aligned} \tag{5.2.10}$$

Here we have introduced $\Psi(\tau)$

$$\Psi(\tau) = \int_\tau^T A(s)e^{-2i\omega s}ds$$

to save space in the arguments to come. The expression for $\boldsymbol{w}^{(1)}$ is intuitively meaningful. $\boldsymbol{w}^{(0)}$ was just a right going elastic wave, but now it has bounced back as $\boldsymbol{w}^{(1)}$ which is a purely left-going wave. We can see how the wave is now affected by the microstructure through $\Psi(\tau)$ which is just some kind of box-car-cut Fourier transform of $A(\tau)$.

Though revealing the end of a good story is detrimental to storytelling suspense, I do it here for the purpose of motivating the reader to endure the following mathematics. In our last move of the chess piece the wave will bounce yet again; this time back to the right. Now it will be affected by microstructure again giving rise to a "microstructure squared" term which is roughly the spectral density of $\log Z$. This will fit in nicely with Banik et al. [1985] which we studied in section 3.4. Finally, the wave also picks up effects from the viscoelasticity.

We begin by applying the wave operator to (5.2.2)

$$\widehat{\mathcal{W}}\widehat{\boldsymbol{w}} = \widehat{\mathcal{W}}\widehat{\boldsymbol{w}}^{(0)} + \varepsilon\widehat{\mathcal{W}}\widehat{\boldsymbol{w}}^{(1)} + \varepsilon^2\widehat{\mathcal{W}}\widehat{\boldsymbol{w}}^{(2)}.$$

When we insert the three equations (5.2.5), (5.2.6) and (5.2.7) we get

$$\widehat{\mathcal{W}}\widehat{\boldsymbol{w}} = -\varepsilon\boldsymbol{A}\widehat{\boldsymbol{w}}^{(0)} + \varepsilon^2(-\boldsymbol{A}\widehat{\boldsymbol{w}}^{(1)} - \boldsymbol{B}\widehat{\boldsymbol{w}}^{(0)}).$$

We already have expressions for $\boldsymbol{w}^{(0)}$ and $\boldsymbol{w}^{(1)}$ in (5.2.9) and (5.2.10). When we insert these we get after some calculation

$$\begin{aligned}\widehat{\mathcal{W}}\widehat{\boldsymbol{w}} &= \varepsilon A(\tau)e^{-i\omega(\tau-\tau_1)}\widehat{R}(\tau_1,\omega)\begin{bmatrix}0\\1\end{bmatrix}\\ &+\varepsilon^2\left(-A(\tau)\widehat{R}(\tau_1,\omega)e^{i\omega(\tau+\tau_1)}\Psi(\tau)\begin{bmatrix}1\\0\end{bmatrix}-\widehat{B}(\tau,\omega)e^{-i\omega(\tau-\tau_1)}\widehat{R}(\tau_1,\omega)\begin{bmatrix}1\\1\end{bmatrix}\right)\end{aligned}$$

Since we are interested now in the transmitting wave, we are only interested in the right-going part of this system. This corresponds to the top component of the vector equation above. Notice how the first ε-term disappears since it has now right-going component.

$$\begin{aligned}(\partial_\tau+i\omega)\widehat{R}(\tau,\omega) &= \varepsilon^2\left(-A(\tau)\widehat{R}(\tau_1,\omega)e^{i\omega(\tau+\tau_1)}\Psi(\tau)-\widehat{B}(\tau,\omega)e^{-i\omega(\tau-\tau_1)}\widehat{R}(\tau_1,\omega)\right)\\ &= \varepsilon^2\left(-A(\tau)e^{i\omega(\tau+\tau_1)}\Psi(\tau)-\widehat{B}(\tau,\omega)e^{-i\omega(\tau-\tau_1)}\right)\times\widehat{R}(\tau_1,\omega)\end{aligned}$$

We can now investigate this equation at $\tau=\tau_1$:

$$(\partial_\tau+i\omega)\widehat{R}(\tau_1,\omega)=\varepsilon^2\left(-A(\tau_1)e^{2i\omega\tau_1}\Psi(\tau_1)-\widehat{B}(\tau_1,\omega)\right)\times\widehat{R}(\tau_1,\omega)$$

We see now that we have an equation in τ_1 only. Through a mathematical sleight of hand we can now consider this an equation in τ; it makes no difference whether it is called τ_1 or τ. We could have expanded around any τ in (5.2.2). So now we have

$$\partial_\tau\widehat{R}(\tau,\omega)=\left(-i\omega-\varepsilon^2A(\tau)e^{2i\omega\tau}\Psi(\tau)-\varepsilon^2\widehat{B}(\tau,\omega)\right)\times\widehat{R}(\tau,\omega),$$

which is just an homogeneous differential equation with a non-constant coefficient of the kind one is likely to meet even in high school. It is also a prettier looking version of Burridge et al. [1993, equation (55)] whose $P(z,.)$ is given by Burridge et al. [1993, equation (53)]. By theorem E.0.24

$$\widehat{R}(\tau,\omega)=e^{-i\omega\tau}e^{-\int_0^\tau A(s)\Psi(s)e^{2i\omega s}ds}e^{-\int_0^\tau\widehat{B}(s,\omega)ds}\widehat{R}(0,\omega).$$

If we define integrals of the exponents as

$$\widehat{a}(\tau,\omega)=\int_0^\tau A(s)\int_s^T A(t)e^{-2i\omega t}dte^{2i\omega s}ds,\quad\text{and}\quad\widehat{b}(\tau,\omega)=\int_0^\tau\widehat{B}(s,\omega)ds$$

we may rewrite our solution as

$$\widehat{R}(\tau,\omega)=e^{-i\omega\tau}\underbrace{e^{-\widehat{a}(\tau,\omega)}}_{\text{elastic}}\underbrace{e^{-\widehat{b}(\tau,\omega)}}_{\text{viscoelastic}}\widehat{R}(0,\omega),$$

and the material transfer function is clearly

$$\widehat{\mathfrak{T}}(T,\omega)=e^{-i\omega T}e^{-\widehat{a}(T,\omega)}e^{-\widehat{b}(T,\omega)}.$$

Note that here we have removed the ε^2 scale,since from now on we assume that the terms $\widehat{a}(\tau,\omega)$ and $\widehat{b}(\tau,\omega)$ are intrinsically small. Also, this is the solution in Burridge et al. [1993, equation (57) and (58)]. Furthermore, one may recognize $\widehat{a}(\tau,\omega)$ and

$\widehat{b}(\tau,\omega)$ in Burridge et al. [1993, equation (59) and (60)]. Recall that Burridge et al. [1993] also takes discontinuous jumps into consideration. If you remove those, Burridge et al. [1993, equation (59)] reduces exactly to the expression for $\widehat{a}(\tau,\omega)$ above.

Burridge et al. [1993] stops here. The article gives no further interpretation of what exactly $\widehat{a}(\tau,\omega)$ and $\widehat{b}(\tau,\omega)$ mean. They are content with a model which is possible to implement in a numerical study. Le and Burridge [1998] however offers some more concrete insight, but we will take it even further. We will apply our concrete 1-dimensional context and understand the substance behind both terms. The simplest one to understand is $\widehat{a}(\tau,\omega)$. This is also fully explained in Le and Burridge [1998]. We may rewrite it as

$$\begin{aligned}\widehat{a}(T,\omega) &= \int_0^T A(s)\left(\int_s^T A(t)e^{-2i\omega t}dt\right)e^{2i\omega s}ds \\ &= \int_0^T\int_s^T A(s)A(t)e^{-2i\omega(t-s)}dtds.\end{aligned}$$

And through the variable change $t = u + s$ we get

$$\widehat{a}(T,\omega) = \int_0^T\left(\int_0^{T-u} A(s)A(s+u)ds\right)e^{-2i\omega u}du. \tag{5.2.11}$$

This we recognize as the Fourier transform of something. Let the continuous sample autocorrelation function be

$$\phi_{A(\tau)}(z) := \frac{1}{T}\int_0^{\max(T-|z|,0)} A(\tau)A(\tau+|z|)d\tau.$$

If we again define $\phi^+_{A(\tau)}(z)$ for only positive lags

$$\phi^+_{A(\tau)}(z) = \begin{cases}\phi_{A(\tau)}(z) & \text{for } z > 0\\ 0 & \text{otherwise}\end{cases}$$

and its Fourier transform $S^+_{A(\tau)}(\omega) = \mathcal{F}\left\{\phi^+_{A(\tau)}(z);\omega\right\}$ which we recognize to be exactly the expression in (5.2.11). We get from (5.1.12)

$$b(T,t) = \tfrac{1}{2}\int_0^T \frac{\partial_t\kappa_{\text{vis}}(s,t)}{\kappa_\infty(s)}ds, \quad \text{and} \quad \widehat{b}(T,\omega) = \tfrac{1}{2}i\omega\int_0^T\frac{\widehat{\kappa}_{\text{vis}}(s,\omega)}{\kappa_\infty(s)}ds.$$

We may further develop $\widehat{b}(T,\omega)$ by remembering that $\widehat{\kappa}_{\text{vis}}(\tau,\omega) = \widehat{\kappa}(\tau,\omega) - \kappa_\infty(\tau)$ which gives

$$\widehat{b}(T,\omega) = \tfrac{1}{2}i\omega\int_0^T\frac{\widehat{\kappa}(s,\omega)}{\kappa_\infty(s)}ds - \tfrac{1}{2}Ti\omega. \tag{5.2.12}$$

Finally we can find an explicit expression for the attenuation

$$|\widehat{\mathfrak{T}}(T,\omega)| = \left(\widehat{\mathfrak{T}}(T,\omega)\widehat{\mathfrak{T}}^*(T,\omega)\right)^{1/2} = e^{-\frac{1}{2}\widehat{a}(T,\omega)-\frac{1}{2}\widehat{a}^*(T,\omega)}e^{-\frac{1}{2}\widehat{b}(T,\omega)-\frac{1}{2}\widehat{b}^*(T,\omega)}. \tag{5.2.13}$$

The elastic attenuation becomes

$$\begin{aligned}\tfrac{1}{2}(\widehat{a}(T,\omega)+\widehat{a}^*(T,\omega)) &= \tfrac{1}{2}TS_{A(\tau)}(2\omega)\\ &= |\tfrac{1}{2}\mathcal{F}\{\partial_\tau\log Z(\tau);2\omega\}|^2 \quad \text{by theorem } A.0.12\\ &= |\tfrac{1}{2}2\omega\mathcal{F}\{\log Z(\tau);2\omega\}|^2 \quad \text{by property } A.0.4\\ &= T\tfrac{1}{2}\omega^2 S_{\log Z(\tau)}(2\omega) \quad \text{by theorem } A.0.12\end{aligned} \tag{5.2.14}$$

This is very satisfying indeed as this is exactly the ODA dampening as explained in section 3.3. We saw there the discrete version of this, which gives a dampening proportional to the spectrum of the reflection coefficients. Then in section 3.4, we saw how this, through the argument of Banik et al. [1985], is equivalent to (5.2.14). The discrete reflection coefficient version is given in Le and Burridge [1998, equation (3) and (4)]. This corresponds exactly to the time-domain version of the exponent in (3.3.7). Next let us turn our attention to the absorptive term and hope that we can make sense of it. Here even Le and Burridge [1998] gives little interpretation, partly because they have a more general 3-dimensional set up. We, however, are able to get very specific. Clearly, by (5.2.12) we have

$$\begin{aligned}\tfrac{1}{2}(\widehat{b}(T,\omega)+\widehat{b}^*(T,\omega)) &= \mathfrak{Re}\ \widehat{b}(T,\omega)\\ &= -\tfrac{1}{2}\omega\ \mathfrak{Im}\left\langle\frac{\widehat{\kappa}(\tau,\omega)}{\kappa_\infty(\tau)}\right\rangle T \end{aligned}\tag{5.2.15}$$

where $\langle\cdot\rangle$ is the spatial average

$$\left\langle\frac{\widehat{\kappa}(\tau,\omega)}{\kappa_\infty(\tau)}\right\rangle = \frac{1}{T}\int_0^T \frac{\widehat{\kappa}(s,\omega)}{\kappa_\infty(s)}ds$$

Finally, using the homogenized speed

$$\frac{1}{\bar{c}} = \langle c(z)^{-1}\rangle = \sqrt{\rho}\,\langle\sqrt{\kappa_\infty}\rangle$$

and the fact that $T = L/\bar{c}$ we can come to a close and summarize what we have learned. From (5.2.13) we get

$$|\widehat{\mathfrak{T}}(L,\omega)| = e^{-\mathcal{A}_{\mathrm{A}}(\omega)L}e^{-\mathcal{A}_{\mathrm{B}}(\omega)L},\tag{5.2.16}$$

where we have the purely elastic ODA attenuation

$$\mathcal{A}_{\mathrm{A}}(\omega) = \tfrac{1}{2\bar{c}}\omega^2 S_{\log Z(\tau)}(2\omega)$$

and the absorptive attenuation

$$\mathcal{A}_{\mathrm{B}}(\omega) = -\tfrac{1}{2}\omega\sqrt{\rho}\,\langle\sqrt{\kappa_\infty}\rangle\ \mathfrak{Im}\left\langle\frac{\widehat{\kappa}(z,\omega)}{\kappa_\infty(z)}\right\rangle.\tag{5.2.17}$$

The last term looks very much like the absorption of a viscoelastic systems given by (2.4.7). This becomes even more specific once we look at this in the fractional Zener case.

To summarize, if we assume that spatial structure in the instantaneous elastic properties of the medium is small (ε), and that absorption is even smaller (ε^2), we have found that the two effects are *additive* in the exponential domain. Furthermore, in the final sum, both effects contribute on the same scale (ε^2).

5.3 Extending Burridge et al.'s model to fractional viscoelasticity

Finally we extend our model to the fractional viscoelastic case. From (4.1.8) we know that

$$\kappa_\infty = \kappa_0\left(\frac{\tau_\sigma}{\tau_\epsilon}\right)^\beta.$$

When we apply this to the fraction inside the $\mathfrak{Im}$ operator of (5.2.17) we get

$$\frac{\kappa(z,\omega)}{\kappa_\infty(z)} = \left(\frac{\tau_\epsilon}{\tau_\sigma}\right)^\beta \frac{1+(i\omega\tau_\sigma)^\beta}{1+(i\omega\tau_\epsilon)^\beta} = \left(\frac{\tau_\epsilon}{\tau_\sigma}\right)^\beta \breve{\kappa}(\omega), \tag{5.3.1}$$

which no longer depends on z, so we can drop the $\langle\cdot\rangle$ in $\mathcal{A}_{\mathrm{B}}(\omega)$. Recall from section 4.2 that $\breve{\kappa}(\omega)$ is the unscaled generalized compressibility without the κ_0 constant. The absorptive term (5.2.17) becomes

$$\mathcal{A}_{\mathrm{B}}(\omega) = -\tfrac{1}{2}\left(\frac{\tau_\epsilon}{\tau_\sigma}\right)^{\beta/2} \omega\sqrt{\rho}\langle\sqrt{\kappa_0}\rangle\, \mathfrak{Im}\, \breve{\kappa}(\omega), \tag{5.3.2}$$

or fully written out

$$\mathcal{A}_{\mathrm{B}}(\omega) = \frac{\omega}{2\bar{c}_0}\left\{\left(\frac{\tau_\epsilon}{\tau_\sigma}\right)^{\beta/2} - \left(\frac{\tau_\sigma}{\tau_\epsilon}\right)^{\beta/2}\right\} \frac{\sin(\frac{\pi}{2}\beta)}{(\omega\tau_\epsilon)^{-\beta} + 2\cos(\frac{\pi}{2}\beta) + (\omega\tau_\epsilon)^\beta}.$$

But the basic assumption of the Burridge et al. model is that viscoelasticity is very small. In section 4.2 we saw this to be true if $\frac{\tau_\epsilon}{\tau_\sigma} \approx 1$. In this case we can ignore the $(\frac{\tau_\epsilon}{\tau_\sigma})^{\beta/2}$ term of (5.3.2). The resulting expression, we have already seen in the discussion surrounding (4.2.7), that it is very close to

$$\mathcal{A}_{\mathrm{B}}(\omega) \approx -\tfrac{1}{2}\omega\sqrt{\rho}\, \mathfrak{Im}\, \sqrt{\langle\kappa_0\rangle\breve{\kappa}(\omega)},$$

which is just the familiar absorptive attenuation of an homogeneous viscoelastic body with the spatial average of the compressibility modulus! In fact we could write it as

$$\mathcal{A}_{\mathrm{B}}(\omega) \approx \langle\mathcal{A}_{\mathrm{vis}}(z,\omega)\rangle.$$

Recall from section 4.2 that the fractional Zener model has the asymptotic behavior

$$\begin{aligned} \mathcal{A}_{\mathrm{B}}(\omega) &\sim_{\omega\to 0} A_{\mathrm{low}}\omega^{1+\beta} \\ \mathcal{A}_{\mathrm{B}}(\omega) &\sim_{\omega\to\infty} A_{\mathrm{high}}\omega^{1-\beta}. \end{aligned}$$

And recall from figure 4.2 that there is only a short transition between these regimes at the point $\omega = 1/\tau_\epsilon$. This we may express as

$$\mathcal{A}_{\mathrm{B}}(\omega) \approx A_{\mathrm{low}}\omega^{1+\beta}\mathbf{1}_{(-\infty,1/\tau_\epsilon]}(\omega) + A_{\mathrm{high}}\omega^{1-\beta}\mathbf{1}_{(1/\tau_\epsilon,\infty)}(\omega)$$

where $\mathbf{1}(\omega)$ is the indicator function. If in addition, as in the chapter on scattering, $S_{\log Z(\tau)} = 1/\omega^\alpha$, we get the total attenuation

$$\mathcal{A}_{\mathrm{A}}(\omega) + \mathcal{A}_{\mathrm{B}}(\omega) \approx A_1\omega^{2-\alpha} + A_2\omega^{1+\beta}\mathbf{1}_{(-\infty,1/\tau_\epsilon]}(\omega) + A_3\omega^{1-\beta}\mathbf{1}_{(1/\tau_\epsilon,\infty)}(\omega).$$

But when we add two power-laws, one will dominate, except for only a short transition between the regions of dominance. From this we may gather that the total attenuation still follows a power-law within separate ranges. However, in terms of the exponents of the resulting power-laws, we will not observe any new behavior. Because within a given frequency range of dominance, only *one* of the exponents in above power-laws dictates the behavior. In short, the resulting attenuation, depending on the constants A_1 and A_2 and A_3, has separate ranges following power-laws. But the exponent γ of each such region is either $2-\alpha$, $1-\beta$ or $1+\beta$.

Chapter 6

Spatial structure in relaxation and retardation times

So far we have seen that scattering occurs when we have spatial variation in acoustic impedance. In the chapter on scattering this was set in motion by a spatial variation in κ_0. Then, in the combination model due to Burridge et al., we isolated the instantaneous response $J_{\text{in}} = \kappa_\infty$ and gave spatial structure to that. Here we follow the natural next step and give spatial structure to the remaining viscoelastic state variables; the relaxation and retardation times τ_σ and τ_ϵ. We will look at a stratified medium with different $\tau_{\sigma,j}$ and $\tau_{\epsilon,j}$ in each layer $j \in (1, ..., N)$. Furthermore, the layers are of equal width Δz.

6.1 Generalized concepts and the exact solution to stratified viscoelastic medium

We seek again to solve the wave equation in the frequency domain. Each layer is an homogeneous viscoelastic body governed by wave equation 2.3.1:

$$\partial_z \widehat{\boldsymbol{v}}(\omega) = -i\omega M(\omega)\widehat{\boldsymbol{v}}(\omega), \quad \text{where} \quad M(\omega) = \begin{bmatrix} 0 & \rho \\ \widehat{\kappa}(\omega) & 0 \end{bmatrix}.$$

Again we may diagonalize $M(\omega)$ as

$$M(\omega) = E(\omega)\Lambda(\omega)E^{-1}(\omega),$$
$$\text{with } \Lambda(\omega) = \begin{bmatrix} \sqrt{\rho}\sqrt{\kappa(\omega)} & 0 \\ 0 & -\sqrt{\rho}\sqrt{\kappa(\omega)} \end{bmatrix}, E(z) = \tfrac{1}{\sqrt{2}} \begin{bmatrix} Z(\omega)^{1/2} & -Z(\omega)^{1/2} \\ Z(\omega)^{-1/2} & Z(\omega)^{-1/2} \end{bmatrix}.$$

This time, however, $Z(\omega)$ is what we may call the generalized acoustic impedance

$$Z(\omega) = \sqrt{\frac{\rho}{\kappa(\omega)}}.$$

We may then define the generalized left- and right-going waves

$$\widehat{\boldsymbol{w}}(z, \omega) := E(\omega)^{-1}\widehat{\boldsymbol{v}}(z, \omega),$$

and we can write our wave equation on diagonalized form

$$\partial_z \widehat{\boldsymbol{w}}(z,\omega) = -ik\bar{\Lambda}\widehat{\boldsymbol{w}}(z,\omega),$$

where $k(\omega) = \omega\sqrt{\rho}\sqrt{\kappa(\omega)}$ is the wave number and $\bar{\Lambda}$ is as in (5.1.13). This is trivially solvable by theorem E.0.22. In the apostrophe notation of figure 3.2 we find the propagation matrix across one layer to be

$$\widehat{\boldsymbol{w}}'_j(\omega) = \widehat{P}_j(\omega)\widehat{\boldsymbol{w}}_j(\omega) \tag{6.1.1}$$

where

$$\widehat{P}_j(\omega) = e^{ik_j\bar{\Lambda}\Delta z} = \begin{bmatrix} e^{-ik_j\Delta z} & 0 \\ 0 & e^{+ik_j\bar{\Lambda}\Delta z} \end{bmatrix}.$$

Finally, at the intersection we must ensure continuity of the pressure and velocity field which by the same algebra as in section 3.1, yields the generalized reflection and transmission coefficients

$$\mathcal{R}_j(\omega) = \frac{Z_j(\omega) - Z_{j+1}(\omega)}{Z_j(\omega) + Z_{j+1}(\omega)}, \quad \text{and} \quad \mathcal{T}_j(\omega) = \frac{2\sqrt{Z_j(\omega)Z_{j+1}(\omega)}}{Z_j(\omega) + Z_{j+1}(\omega)}.$$

Again, we get generalized reflection and scattering if we have a variation in generalized acoustic impedance. And by the same argumentation as in section 3.2 we get that the effect of one layer is

$$\widehat{\boldsymbol{w}}_{j+1}(\omega) = \widehat{J}_j\widehat{\boldsymbol{w}}_j(\omega),$$

where $\widehat{J}_j(\omega)$ combines propagation across the layer and then hitting an interface

$$\widehat{J}_j(\omega) = \mathcal{I}_j(\omega)\widehat{P}_j(\omega) = \frac{1}{\mathcal{T}_j(\omega)}\begin{bmatrix} 1 & \mathcal{R}_j(\omega) \\ \mathcal{R}_j(\omega) & 1 \end{bmatrix}\begin{bmatrix} e^{-ik_j\Delta z} & 0 \\ 0 & e^{ik_j\Delta z} \end{bmatrix}. \tag{6.1.2}$$

The difference from the Goupillaud case as described in section 3.2 is that now we have a generalized interface matrix which depends on frequency, and the propagation matrix $\widehat{P}_j(\omega)$ is different for each layer. Ultimately, we seek to describe the combined action of all the layers

$$K_N(\omega) = J_N(\omega)J_{N-1}(\omega)\cdots J_1(\omega).$$

This allows us to describes the relationship between the waves on each side of the slab:

$$\widehat{\boldsymbol{w}}_{N+1}(\omega) = \widehat{K}_N(\omega)\widehat{\boldsymbol{w}}_1(\omega). \tag{6.1.3}$$

We can not in general describe this solution. But with some assumptions we may gain some headway. This is our next mission.

6.2 Proposed model: Nearly elastic Zener model with spatially inhomogeneous relaxation and retardation times

In this proposed model we assume the classic Zener model and that we have an inhomogeneous structure such that every layer has different relaxation and retardation times. The compressibility modulus κ_0 is assumed to stay constant. There is no

autocorrelation structure between the layers, meaning that the retardation times in each layer is independent of all the others. Each retardation time is sampled independently from a certain distribution which is specified later. Finally, we assume that we have a nearly elastic situation which we quantify as

$$\frac{\tau_\sigma}{\tau_\epsilon} = 1 - \varepsilon. \tag{6.2.1}$$

If we look at the unscaled generalized compressibility $\breve{\kappa}(\omega) = \kappa(\omega)/\kappa_0$ we find that for each layer we have

$$\breve{\kappa}(\omega) = \frac{1 + i(1-\varepsilon)\tau_\epsilon\omega}{1 + i\tau_\epsilon\omega} = 1 + \varepsilon\mathscr{Q}(\omega,\tau), \quad \text{where} \quad \mathscr{Q}(\omega,\tau) := -\frac{i\tau_\epsilon\omega}{1+i\tau_\epsilon\omega}.$$

It is clear here that when $\varepsilon = 0$ the generalized compressibility reduces to $\kappa(\omega) = \kappa_0$ which is the purely elastic Hooke's law. Furthermore, what is very convenient for our theory is that the deviation $\mathscr{Q}(\omega,\tau)$ from the elastic situation obeys

$$|\mathscr{Q}(\omega,\tau)|^2 = \frac{\tau_\epsilon^2\omega^2}{1+\tau_\epsilon^2\omega^2} \leq 1.$$

So it is limited no matter the magnitude of frequency and τ_ϵ. We will further look at how all the other generalized variables ($Z(\omega)$, $\mathcal{R}(\omega)$, $\mathcal{T}(\omega)$ etc) deviate from the elastic situation for small ε. To meet this end we introduce the following lemma.

Lemma 6.2.1. *Given a complex function f(z) analytic around $z = 1$ and a complex linear function $\breve{\kappa}(\varepsilon) = 1 + \varepsilon\mathscr{Q}(\omega,\tau)$, the following holds true:*

$$\partial_\varepsilon^n f(\breve{\kappa}(\varepsilon))|_{\varepsilon=0} = f^{(n)}(1)\mathscr{Q}(\omega,\tau)^n$$

Likewise, given a complex function g(x,y) analytic around $(x,y) = (1,1)$ and two complex linear function $\breve{\kappa}_x(\varepsilon) = 1+\varepsilon\mathscr{Q}_x(\omega,\tau)$ and $\breve{\kappa}_y(\varepsilon) = 1+\varepsilon\mathscr{Q}_y(\omega,\tau)$, the following holds true:

$$\partial_\varepsilon^n f(\breve{\kappa}_x(\varepsilon),\breve{\kappa}_y(\varepsilon))|_{\varepsilon=0} = \sum_{k=0}^{n}\binom{n}{k}\partial_x^k\partial_y^{n-k}f(x,y)\big|_{(x,y)=(1,1)}\mathscr{Q}_x(\omega,\tau)^k\mathscr{Q}_y(\omega,\tau)^{n-k}$$

Proof. This is a straight forward application of the product rule and chain rule. □

This is quite satisfying. The lemma says that if you have a function of $\kappa(\omega)$, say the generalized acoustic impedance $Z(\omega)$, all the terms in the Taylor expansion with respect to ε are bounded, no matter the magnitude of ω or τ_ϵ. Therefore, we may safely ignore the higher order terms $O(\varepsilon^2)$ as we know they can not blow up for extreme values of ω and τ_ϵ. Let us begin with the generalized reflection coefficients:

$$\mathcal{R}_j(\omega) = \frac{Z_j(\omega) - Z_{j+1}(\omega)}{Z_j(\omega) + Z_{j+1}(\omega)} = \frac{\breve{\kappa}_{j+1}(\omega)^{1/2} - \breve{\kappa}_j(\omega)^{1/2}}{\breve{\kappa}_{j+1}(\omega)^{1/2} + \breve{\kappa}_j(\omega)^{1/2}}.$$

We may take the derivative with respect to ε and find

$$\partial_\varepsilon\mathcal{R}_j(\omega) = \frac{1}{4}\left(\frac{i\omega\tau_{\epsilon,j}}{1+i\omega\tau_{\epsilon,j}} - \frac{i\omega\tau_{\epsilon,j+1}}{1+i\omega\tau_{\epsilon,j+1}}\right) := \mathscr{R}_j(\omega)$$

which means that

$$\mathcal{R}_j(\omega) = \varepsilon\mathscr{R}_j(\omega) + O(\varepsilon^2).$$

As promised by lemma 6.2.1 the first derivative is bounded

$$|\mathscr{R}_j(\omega)| \leq \tfrac{1}{4}.$$

In danger of rehashing the same point too many times, we know from lemma 6.2.1 that all the other terms hiding behind $O(\varepsilon^2)$ will not blow up for extreme values of ω and τ_ϵ. This point will not be stated again. The transmission coefficients may be approximated in the same way. Remember that $\mathcal{T}_j(\omega) = \sqrt{1-\mathcal{R}_j(\omega)^2}$. From this we find that

$$\partial_\varepsilon \frac{1}{\mathcal{T}_j(\omega)}\bigg|_{\varepsilon=0} = -\frac{1}{\mathcal{T}_j(\omega)^2}\frac{1}{2}\frac{1}{\mathcal{T}_j(\omega)}(-2\mathcal{R}_j(\omega))\partial_\varepsilon \mathcal{R}_j(\omega)\bigg|_{\varepsilon=0} = 0,$$

so clearly

$$\frac{1}{\mathcal{T}_j(\omega)} = 1 + O(\varepsilon^2).$$

In light of the ε expansions of the reflection and transmission coefficients, we approximate the layer propagation matrix $J_j(\omega)$ from (6.1.2).

$$\begin{aligned}\widehat{J}_j(\omega) &= \left\{ \frac{1}{\mathcal{T}_j} I + \frac{\mathcal{R}_1}{\mathcal{T}_j} \begin{bmatrix} 0 & 1 \\ 1 & 0 \end{bmatrix} \right\} \widehat{P}_j(\omega) \\ &= \widehat{P}_j(\omega) + \varepsilon \mathscr{R}_j \begin{bmatrix} 0 & 1 \\ 1 & 0 \end{bmatrix} \widehat{P}_j(\omega) + O(\varepsilon^2).\end{aligned}$$

Let us define the product

$$\mathcal{P}_m^n(\omega) = \prod_{j=m}^{n} \widehat{P}_j(\omega),$$

which is diagonal. Finally we can approximate the cumulative action

$$\begin{aligned}K_N(\omega) &= J_N(\omega)J_{N-1}(\omega)\cdots J_1(\omega)\boldsymbol{w}_1(\omega) \\ &= \mathcal{P}_1^N(\omega) + \varepsilon \sum_{n=0}^{N-1} \mathscr{R}_{n+1}\mathcal{P}_1^n \begin{bmatrix} 0 & 1 \\ 1 & 0 \end{bmatrix} \mathcal{P}_{n+1}^N + O(\varepsilon^2) \\ &= \begin{bmatrix} e^{-i\langle k_j(\omega)\rangle L} & 0 \\ 0 & e^{+i\langle k_j(\omega)\rangle L} \end{bmatrix} + \varepsilon \begin{bmatrix} 0 & f_N(\omega) \\ g_N(\omega) & 0 \end{bmatrix} + O(\varepsilon^2) \qquad (6.2.2)\end{aligned}$$

where we have used $N\Delta z = L$, and the fact that the product of a diagonal, anti-diagonal and diagonal matrix is anti-diagonal. Hiding behind the ε^2 terms are, amongst other, terms of the form

$$\varepsilon^2 \mathscr{R}_j(\omega)\mathscr{R}_k(\omega)\mathcal{P}_1^{j-1}(\omega) \begin{bmatrix} 0 & 1 \\ 1 & 0 \end{bmatrix} \mathcal{P}_j^{k-1}(\omega) \begin{bmatrix} 0 & 1 \\ 1 & 0 \end{bmatrix} \mathcal{P}_k^N(\omega)$$

Herein lies the beginnings of a study of the autocorrelation of the $\mathscr{R}$'s. We will not go down this path here. We simply ignore them since they are of ε^2 order, though this is slightly simple minded since there are many of them; $N\varepsilon^2$ might be big enough to warrant further study. Intuitively though, since the $\mathscr{R}$'s are independent, the total sum of all the terms of the above kind will on average probably disappear.

To complete we may write out the elements of (6.1.3)

$$\begin{bmatrix} \widehat{R}_{N+1} \\ \widehat{L}_{N+1} \end{bmatrix} = \begin{bmatrix} \widehat{K}_N^{(1,1)} & \widehat{K}_N^{(1,2)} \\ \widehat{K}_N^{(2,1)} & \widehat{K}_N^{(2,2)} \end{bmatrix} \begin{bmatrix} \widehat{R}_1 \\ \widehat{L}_1 \end{bmatrix}. \qquad (6.2.3)$$

As it stands, this statement relates the waves on the left hand side of the slab to the waves on the right hand side of the slab. We now wish to apply the switch around property D.0.17 to twist this into an "outgoing waves as a function of incoming waves" statement. This can be applied immediately because we know that $\det \mathcal{I}_j(\omega) = 1$ and $\det \widehat{P}_j(\omega) = 1$ and hence $\det K_N(\omega) = 1$:

$$\begin{bmatrix} \widehat{R}_{N+1} \\ \widehat{L}_1 \end{bmatrix} = \frac{1}{\widehat{K}_N^{(2,2)}(\omega)} \begin{bmatrix} 1 & \widehat{K}_N^{(2,1)}(\omega) \\ -\widehat{K}_N^{(1,2)}(\omega) & 1 \end{bmatrix} \begin{bmatrix} \widehat{R}_1 \\ \widehat{L}_{N+1} \end{bmatrix}.$$

Using the initial condition $\widehat{L}_{N+1} = 0$ (we are not sending a left going wave through the medium at the same time) we get the material transfer function and reflection function

$$\widehat{\mathfrak{T}}(\omega) = \frac{1}{\widehat{K}_N^{(2,2)}(\omega)} \quad \text{and} \quad \widehat{\mathfrak{R}}(\omega) = -\frac{\widehat{K}_N^{(1,2)}(\omega)}{\widehat{K}_N^{(2,2)}(\omega)}. \tag{6.2.4}$$

We are lucky as the transfer function does not require us to understand the $f(\omega)$ and $g(\omega)$ functions of (6.2.2). Ignoring the ε^2 terms from our approximation (6.2.2) gives us the approximate transfer function

$$\widehat{\mathfrak{T}}(\omega) \approx e^{i\langle k_j \rangle L}$$

which is just the classic propagation with the average of the wave numbers! This gives us the attenuation

$$\mathcal{A}(\omega) = \langle \mathcal{A}_{\text{vis}}(\omega) \rangle = -\omega\sqrt{\rho}\, \mathfrak{Im}\, \langle \kappa_j(\omega) \rangle.$$

This is exactly the same result as we found in section 5.3. We can make even further advances by noting that we are studying the case where τ_ϵ and τ_σ are almost the same. We have already shown in (4.2.7) that for small ε we can write this as

$$\begin{aligned} \mathcal{A}(\omega) &= \frac{1}{2c_0} \left\langle \left\{ 1 - \frac{\tau_\sigma}{\tau_\epsilon} \right\} \frac{\omega}{(\omega\tau_\epsilon)^{-1} + \omega\tau_\epsilon} \right\rangle \qquad \text{Zener exponent } \beta = 1 \\ &= \frac{\varepsilon}{2c_0} \langle \Phi(\tau_\epsilon; \omega) \rangle \qquad \text{by (6.2.1)} \end{aligned} \tag{6.2.5}$$

where

$$\Phi(\tau_\epsilon; \omega) = \frac{\omega}{(\omega\tau_\epsilon)^{-1} + \omega\tau_\epsilon}.$$

Let us further assume that the $\tau_{\epsilon,j}$ for each layer follows the Weibull distribution.

$$\tau_{\epsilon,j} \sim X, \quad \text{with pdf} \quad g(x; \nu, \lambda) = \begin{cases} \frac{\nu}{\lambda} \left(\frac{x}{\lambda}\right)^{\nu-1} e^{-(x/\lambda)^\nu} & x \geq 0, \\ 0 & x < 0, \end{cases}$$

Why do we choose the Weibull distribution? It is important to note that many other distributions could be chosen. There is nothing magic about the Weibull. Inspired by van der Ziel's ideal from section 3.4.1 we seek to use a distribution close to τ^{-1}. However, this is not really a distribution since it cannot be normalized to integrate to 1. Therefore, one possible choice of distribution is the Weibull distribution with scale parameter ν, as for small values if ν, the Weibull resembles the the τ^{-1} distribution and gives us the results we need.

By the law of large numbers, the average $\langle \Phi(\tau_{\epsilon,j};\omega)\rangle$ converges in probability to the expected value

$$\langle \Phi(\tau_{\epsilon,j};\omega)\rangle = \frac{1}{N}\sum_{j=1}^{N}\Phi(\tau_{\epsilon,j};\omega) \to \mathbb{E}\left[\Phi(X;\omega)\right].$$

This expected value is simply the integral

$$\mathbb{E}\left[\Phi(X;\omega)\right] = \int_0^\infty \frac{\omega}{(\omega x)^{-1}+\omega x} g(x;\nu,\lambda)dx = \int_0^\infty \frac{x'}{1+x'^2} g\left(\tfrac{x'}{\omega};\nu,\lambda\right)dx.$$

Inserting the probability distribution $g(x;\nu,\lambda)$ and putting the expectation into (6.2.5) gives us the attenuation

$$\mathcal{A}(\omega) = \frac{\varepsilon}{2c_0}\nu\lambda^{-\nu}C(\nu,\omega)\omega^{1-\nu}, \quad \text{with} \quad C(\nu,\omega) := \int_0^\infty \frac{x^\nu}{1+x^2}e^{-\left(\frac{x}{\omega\lambda}\right)^\nu}dx. \quad (6.2.6)$$

In the classic Zener model, we recall from figure 4.2 that we have relaxation type losses with ω^2 for small frequencies and ω^0 for high frequencies. So what does a spatial average of such processes behave like? Let us theoretically investigate the asymptotic behavior. We could define $\omega' = \lambda\omega$, so in the following, without loss of generality, we assume $\lambda = 1$.

Recall the functions $\psi(x) = e^{-x}$ and $f(x) = (1+x)^{-1}$ from section 4.1. Then define

$$\psi'(x) := \psi(x^\nu) = e^{-x^\nu}.$$

We may then solve the integral (6.2.6) by taking its Mellin transform. Recall the Mellin transform of $\psi(x)$ and $f(x)$ from (4.1.2) and (4.1.4). By applying property F.0.26 we get

$$\begin{aligned}
\mathcal{M}\left\{\int_0^\infty \frac{x^\nu}{1+x^2}e^{-\left(\frac{x}{\omega}\right)^\nu};u\right\}dx &= \mathcal{M}\left\{\left[\frac{x^\nu}{1+x^2}\vee\psi'\right]\left(\tfrac{1}{\omega}\right);u\right\} \\
&= \mathcal{M}\left\{x^\nu f(x^2);1-u\right\}\mathcal{M}\left\{\psi(x^\nu);u\right\} \\
&= \tfrac{1}{2}\mathcal{M}\left\{f(x);\tfrac{1-u+\nu}{2}\right\}\tfrac{1}{\nu}\mathcal{M}\left\{\psi(x);\tfrac{u}{\nu}\right\} \\
&= \tfrac{1}{2\nu}\Gamma(\tfrac{1}{2}+\tfrac{\nu}{2}-\tfrac{1}{2}u)\Gamma(\tfrac{1}{2}-\tfrac{\nu}{2}+\tfrac{1}{2}u)\Gamma(\tfrac{u}{\nu}).
\end{aligned}$$

Finally we find the attenuation by taking the inverse Mellin-transform of the above, and we get

$$\begin{aligned}
\mathcal{A}(\omega) &= \frac{\varepsilon}{2c_0}\nu\omega^{1-\nu}\int_0^\infty \frac{x^\nu}{1+x^2}e^{-\left(\frac{x}{\omega}\right)^\nu}dx \\
&= \frac{\varepsilon}{4c_0}\omega^{1-\nu}H_{12}^{21}\left[\frac{1}{\omega}\middle|\begin{matrix}(\frac{1}{2}(1-\nu),\frac{1}{2}) \\ (\frac{1}{2}(1-\nu),\frac{1}{2}),(0,\frac{1}{\nu})\end{matrix}\right] && \text{by (F.0.4)} \\
&= \frac{\varepsilon}{4c_0}\omega^{1-\nu}H_{21}^{12}\left[\omega\middle|\begin{matrix}(\frac{1}{2}(1+\nu),\frac{1}{2}),(1-\frac{1}{\nu},\frac{1}{\nu}) \\ (\frac{1}{2}(1+\nu),\frac{1}{2})\end{matrix}\right] && \text{by prop. F.0.29} \\
&= \frac{\varepsilon}{4c_0}H_{21}^{12}\left[\omega\middle|\begin{matrix}(1,\frac{1}{2}),(0,\frac{1}{\nu}) \\ (1,\frac{1}{2})\end{matrix}\right] && \text{by prop. F.0.27}
\end{aligned}$$

which by Mathai et al. [2010, Theorem 1.2] obeys the asymptotic behaviors

$$\mathcal{A}(\omega) \underset{\omega\to 0}{\sim} \omega^2, \quad \text{and} \quad \mathcal{A}(\omega) \underset{\omega\to\infty}{\sim} \omega^0.$$

We still have a relaxation type process, so what have we gained? There is indeed a middle band which converges quickly to $\omega^{1-\nu}$. Indeed, as ν becomes very small we would expect the "constant" $C(\nu,\omega)$ to be close to

$$C(0,\omega) = \int_0^\infty \frac{1}{1+x^2} e^{-1} dx = \frac{\pi}{2e}, \tag{6.2.7}$$

so the total attenuation, for small ν, becomes

$$\mathcal{A}(\omega) \approx \frac{\pi\varepsilon}{4c_0 e} \nu \lambda^{-\nu} \omega^{1-\nu}. \tag{6.2.8}$$

In fact, even though $C(\omega,\nu)$ depends on ω we will numerically substantiate calling it a constant. In a middle range of the frequency space, for small ν, it quickly becomes nearly constant over several decades.

Let us stop for a moment and ruminate on the physical interpretation of this model. We have already mentioned the fact that one may construct the fractional Zener model by adding up a certain weighted sum of relaxation losses [Näsholm and Holm, 2011]. One may think of this as an homogeneous medium with many different molecules mixed into the same space; each molecule with a different relaxation time. Then the resulting complex medium yields attenuation which follows a fractional Zener model with an arbitrary exponent β. In contrast, here we have an inhomogeneous material such that each layer is purely *one* relaxation process with its own relaxation time. Then the spatial average creates attenuation with arbitrary exponent $1-\nu$.

6.3 Brief numerical experiment

We will now look at how our theoretical approximation holds up against the exact solution to a wave traveling through a stratified medium as described in section 6.1. Implicitly in the theory described in the two previous chapters, we already have the technical know how to find the exact transfer function of a stratified medium in the frequency domain. We may give the following handy pseudo code summary of the algorithm.

Algorithm 6.3.1 (Computation of exact propagation in a stratified medium)**.**

given generalized compressibility function $\kappa(\omega;\kappa_0,\tau_\epsilon,\tau_\sigma)$
  material variables $\{\rho_j\}_{j=1}^N$, $\{\tau_{\epsilon,j}\}_{j=1}^N$, $\{\tau_{\sigma,j}\}_{j=1}^N$ and $\{\kappa_{0,j}\}_{j=1}^N$
  discretization of frequency space $\{\omega_k\}_{k=1}^M$
  layer size Δz
For each $\omega \in \{\omega_k\}_{k=1}^M$
  Compute $\{k_j(\omega_k)\}_{j=1}^N, \{Z_j(\omega_k)\}_{j=1}^N, \{\mathcal{R}_j(\omega_k)\}_{j=1}^N$ and $\{\mathcal{T}_j(\omega_k)\}_{j=1}^N$
  Set $\widehat{K}_0 := I$
  Recursively compute for all N layers:

$$\widehat{K}_j := \frac{1}{\mathcal{T}_j(\omega_k)} \begin{bmatrix} 1 & \mathcal{R}_j(\omega_k) \\ \mathcal{R}_j(\omega_k) & 1 \end{bmatrix} \begin{bmatrix} e^{-ik_j\Delta z} & 0 \\ 0 & e^{ik_j\Delta z} \end{bmatrix} \widehat{K}_{j-1}$$

  $|\mathfrak{T}(\omega)| := |(\widehat{K}_N^{(2,2)})^{-1}|$
  $|\mathfrak{R}(\omega)| := |\widehat{K}_N^{(1,2)}(\widehat{K}_N^{(2,2)})^{-1}|$

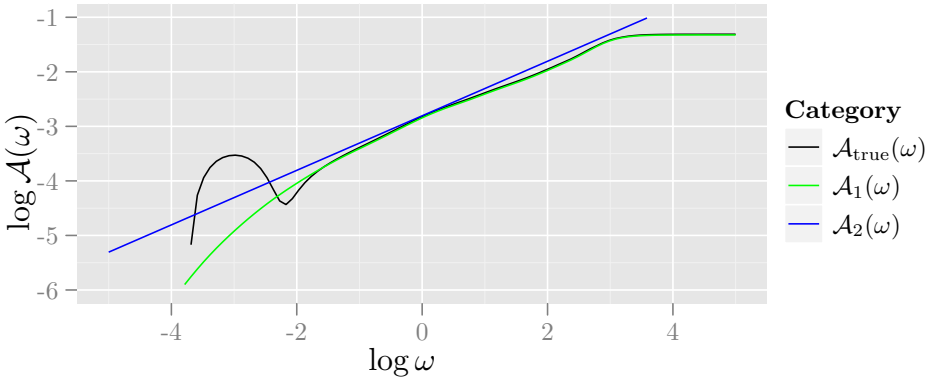

Figure 6.1: Attenuation with $\varepsilon = 0.1$, $\nu = 0.5$, $\lambda = 1000$ and $N = 1000$

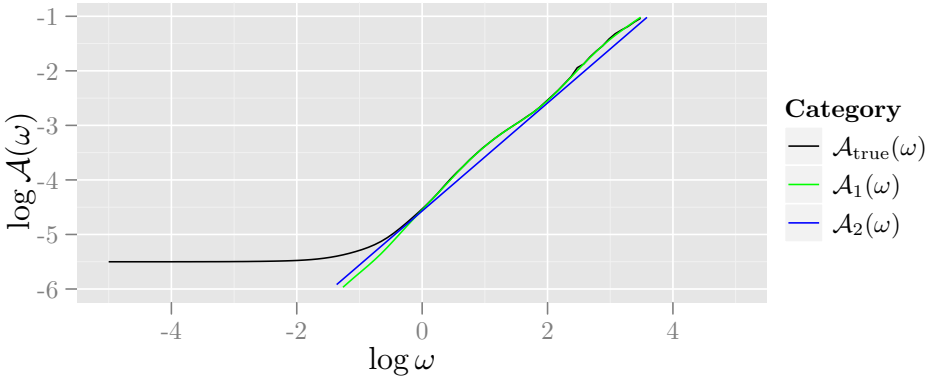

Figure 6.2: Attenuation with $\varepsilon = 0.01$, $\nu = 0.01$, $\lambda = 1000$ and $N = 1000$

This numerical recipe is naive at best. Especially for large frequencies it becomes unstable since the exponential of large numbers quickly become caught in the `Inf` bracket. The algorithm should be further developed to perform its calculations in the exponential domain where numbers are much smaller.

We create N layers by drawing N retardation times τ_ϵ from the Weibull distribution with parameters λ and ν. In R this is simply done with the `rweibull()` function. Then by (6.2.1) calculate $\tau_{\sigma,j} = (1-\varepsilon)\tau_{\epsilon,j}$. Furthermore, we have assumed the following unitary physical constants

$$\kappa_0 = 1\text{Pa}^{-1}, \qquad \rho = 1\text{kg/m}, \quad \text{and} \quad L = 1\text{m}.$$

In figure 6.1 and figure 6.2, we compare the true solution $\mathcal{A}_{\text{true}}(\omega)$ computed with algorithm 6.3.1 to the following entities. The first is by (6.2.5)

$$\mathcal{A}_1(\omega) = \frac{\varepsilon}{2c_0}\left\langle \frac{\omega}{(\omega\tau_{\epsilon,j})^{-1} + \omega\tau_{\epsilon,j}} \right\rangle = \frac{\varepsilon}{2c_0}\frac{1}{N}\sum_{j=1}^{N} \frac{\omega}{(\omega\tau_{\epsilon,j})^{-1} + \omega\tau_{\epsilon,j}}.$$

Note that this is a stochastic entity which varies from every particular realization of a medium. Then we found that as N grows it converges towards the deterministic (6.2.6):

$$\mathcal{A}_2(\omega) = \frac{\varepsilon}{2c_0}\nu\lambda^{-\nu}C(\nu,\omega)\omega^{1-\nu}.$$

In figure 6.1 we computed the constant $C(\nu = 0.5, 1)$ numerically, and in figure 6.2 $\nu = 0.01$ is small enough that the theoretical $C(0,\omega) = \frac{\pi}{2e}$ works well.

We see that in both figures $\mathcal{A}_1(\omega)$ follows the real solution exactly over the entire middle range. Furthermore, we see that the theoretical $\mathcal{A}_2(\omega) \propto \omega^{1-\nu}$ seems a very good prediction indeed.

All in all, the predictions $\mathcal{A}_1(\omega)$ and $\mathcal{A}_2(\omega)$ seem very stable in ε and ν. Though when ε increases the number of artifacts as seen in the bottom of figure 6.1 increases. Whether this is due to numerical instability in algorithm 6.3.1, or it is due to the fact that we deviate from model assumption of a small ε, is not well understood. Experimentation have shown that values for ε as large as 0.4 give meaningful results.

Chapter 7

Future work

7.1 Improvements of proposed model

The proposed model in chapter 6 raises many interesting questions and paths of further exploration. For instance, further understanding of the flat tail for low frequencies of figure 6.2 is needed. Physically speaking, since each layer has attenuation following ω^2 for low frequencies, we would expect the resulting spatial average to possess the same quality. Would the tail of 6.2 eventually fall if we only computed for frequencies small enough? If so, perhaps the flat tail represents an extreme sample of a relaxation time for one particular layer? We see then that it would be interesting to study the stochastic properties of the resulting system. What is the variance of the attenuation $\mathrm{Var}\left[\mathcal{A}(\omega)\right]$? Can we be more sophisticated in describing the frequency dependent convergence of the deterministic integral $C(\omega, \nu)$ from (6.2.6) to the real constant (6.2.7)?

We should also look at a physical interpretation of the reflection coefficients $\mathscr{R}$. How do they act in the time domain? Answering this could lead us to understand the wave coda. Also, how would a spatial autocorrelation structure of the $\mathscr{R}_j$ coefficients alter the result? Here there are many interesting and unanswered questions.

We could probably get the same type of convergence towards a power-law spectrum with many different distributions. There is nothing special about the Weibull distribution. It would be interesting to attempt to characterize the necessary and sufficient conditions on our distributions to obtain a power-law spectrum.

Lastly, we should also improve the algorithm 6.3.1 – at least understand in what ways it is likely to err.

7.2 Viscoelastic version of the Goupillaud medium

Let us attempt to create a viscoelastic version of the Goupillaud medium model. For this we assume again that the spatial variation is located in the compressibility modulus κ_0. Thus we will have a sequence of $\kappa_{0,j}$'s, one for each layer $j \in (1, \ldots, N)$. As explained in section 6.1 we get a generalized acoustic impedance for each layer

$$Z_j(\omega) = \sqrt{\frac{\rho}{\kappa_j(\omega)}},$$

as well as generalized left- and right-going waves. However, in this context something different happens to the generalized reflection coefficients – as opposed to chapter 6. Note that we can split the generalized compressibility into its spatially varying component and its spatially invariant component in the familiar unscaled $\breve{\kappa}$ notation:

$$\kappa_j(\omega) = \kappa_{0,j}\breve{\kappa}(\omega).$$

Note again the here j represents the spatial variation. From this it is be natural to define Z_0 and c_0 as

$$Z_{0,j} = \sqrt{\frac{\rho}{\kappa_{0,j}}} \quad \text{and} \quad c_{0,j} = \sqrt{\frac{1}{\rho\kappa_{0,j}}}.$$

Here these entities are based on the equilibrium or zero frequency behavior of the linear viscoelastic system and stands in contrast to the impedance and speed of sound as examined in chapter 5 which were based upon the instantaneous or infinite frequency behavior. From this point of view the generalized reflection coefficients become

$$\mathcal{R}_j = \frac{Z_j(\omega) - Z_{j+1}(\omega)}{Z_j(\omega) + Z_{j+1}(\omega)} = \frac{Z_{0,j} - Z_{0,j+1}}{Z_{0,j} + Z_{0,j+1}}.$$

The frequency dependent $\breve{\kappa}(\omega)$ cancels out and we are left with the familiar real reflection coefficients.

The essence of the Goupillaud medium is that propagation across each layer leads to the same change on the wave. We may say that we have a viscoelastic Goupillaud medium if the following relation

$$\tfrac{1}{2}\tau_0 = \tfrac{\Delta z_j}{c_j}$$

is constant for all layers. Then the propagation across each layer is identical.

$$\widehat{P}(\omega) = e^{-ik_j\Delta z_j\bar{\Lambda}} = e^{-i\omega\sqrt{\breve{\kappa}(\omega)}\frac{\Delta z_j}{c_{0,j}}\bar{\Lambda}} = e^{-i\omega\sqrt{\breve{\kappa}(\omega)}\frac{1}{2}\tau_0\bar{\Lambda}}.$$

Trivially, we see that for $\breve{\kappa}(\omega) = 1$ we recover the elastic propagation of chapter 3. More importantly though, in the language of chapter 3, more specifically (3.2.3), we get propagation with the propagator

$$\xi = e^{-i\omega\sqrt{\breve{\kappa}(\omega)}\tau_0}.$$

We may then define the unscaled attenuation and dispersion as

$$\breve{\mathcal{A}}(\omega) = -\omega\,\mathfrak{Im}\,\sqrt{\breve{\kappa}(\omega)} \quad \text{and} \quad \breve{\mathcal{D}}(\omega) = \omega\,\mathfrak{Re}\,\sqrt{\breve{\kappa}(\omega)}$$

which gives us the propagator

$$\xi = e^{-i\breve{\mathcal{D}}(\omega)\tau_0 - \breve{\mathcal{A}}(\omega)\tau_0}.$$

Looking back at (3.3.8) gives the attenuation

$$|\mathfrak{T}(\xi)|^2 = |\xi|^{-N} e^{-N[\phi_{\mathcal{R}}[0] + S^+_{\mathcal{R}}(\xi)^* + S^+_{\mathcal{R}}(\xi)]}.$$

Here $|\xi|^N$ represents the wavefront. The interesting part is the second term which contains the wave elements which have bounced back and forth inside the slab. We

may then interpret the exponent above as

$$\begin{aligned}\mathcal{A}_{\text{tail}}(\omega) &:= \phi_{\mathcal{R}}[0] + S^{+}_{\mathcal{R}}(\xi)^{*} + S^{+}_{\mathcal{R}}(\xi) \\ &= \sum_{n=0}^{\infty} \phi_{\mathcal{R}}[n] \left(e^{in\breve{\mathcal{D}}(\omega)\tau_0 - n\breve{\mathcal{A}}(\omega)\tau_0} + e^{-in\breve{\mathcal{D}}(\omega)\tau_0 - n\breve{\mathcal{A}}(\omega)\tau_0} \right) \\ &= \sum_{n=-\infty}^{\infty} \phi_{\mathcal{R}}[n] e^{-|n|\breve{\mathcal{A}}(\omega)\tau_0} e^{-in\breve{\mathcal{D}}(\omega)\tau_0}.\end{aligned}$$

To study this we should define the operator

$$\begin{aligned}\mathcal{Q}\left\{f(x);\phi,\theta\right\} &:= \mathcal{F}\left\{ f(x)e^{-\phi|x|};\theta \right\} \\ &= \mathcal{F}\left\{f(x);\theta\right\} *_{\theta} \mathcal{F}\left\{ e^{-\phi|x|};\theta \right\} \\ &= \mathcal{F}\left\{f(x);\theta\right\} *_{\theta} \left\{ \frac{2\phi}{\phi^2+\theta^2} \right\}.\end{aligned}$$

In this formalism we can express the attenuation of the tail as

$$\begin{aligned}\mathcal{A}_{\text{tail}}(\omega) &= \mathcal{Q}\left\{ \phi_{\mathcal{R}}[n]; \breve{\mathcal{A}}(\omega)\tau_0, \breve{\mathcal{D}}(\omega)\tau_0 \right\} \\ &= S_{\mathcal{R}}(\theta) *_{\theta} \left\{ \frac{2\breve{\mathcal{A}}(\omega)}{\breve{\mathcal{A}}(\omega)^2+\theta^2} \right\} \Bigg|_{\theta=\breve{\mathcal{D}}(\omega)\tau_0}.\end{aligned}$$

But by the argument in section 3.4 due to Banik et al. [1985] we may write this as

$$\mathcal{A}_{\text{tail}}(\omega) = \frac{1}{2\tau_0}\theta^2 S_{\log Z_0(\tau)}(2\theta) *_{\theta} \left\{ \frac{2\breve{\mathcal{A}}(\omega)}{\breve{\mathcal{A}}(\omega)^2+\theta^2} \right\} \Bigg|_{\theta=\breve{\mathcal{D}}(\omega)\tau_0}. \tag{7.2.1}$$

Looking at this formula many opportunities for power-law behavior present themselves. Often we will typically have close to no dispersion [Holm and Näsholm, 2011], which means that $\breve{\mathcal{D}}(\omega) = \omega$. Then the classic spectrum of the $\log Z_0(\tau)$ emerges, which we have already seen in section 3.4, can be made to follow a power-law. What if $\breve{\mathcal{A}}(\omega)$ follows a power-law (which it clearly would in the fractional Zener case)? And what about frequency regions with heavy dispersion? And most importantly, how does the convolution affect the answer? We can obviously not describe the solution for very general situations, but for specific circumstances, can we make sense of 7.2.1? For instance, if one of the terms in the convolution behaves closely to $\delta(\omega)$ we could ignore the convolution all together and focus our attention on the other term.

7.3 Numerical analysis of the Burridge et al. combination model

As expressed in the introductory section 1.4, my original intent was to perform numerical analysis of the Burridge et al. combination model in the extended fractal regime. However, the proposed model of section 6 was deemed more interesting. In appendix H one may find a description of the following topics pertaining to the Burridge et al. model:

- Simulation of fractal random processes
- Solution to the wave equation in the Le and Burridge [1998] context
- Calculation of the Burridge et al. approximations in the time domain

Most of these algorithms I also implemented and may be found in appendix I. Everything is prepared for a detailed numerical analysis of the interaction between scattering and viscoelastic absorption in 1-dimensional space.

For some of the time domain calculations mentioned in appendix H one needs to evaluate the Mittag-Leffler function. However, this function is not available in R. The numerical evaluation of the Mittag-Leffler function is discussed in appendix H.5 and implemented in appendix I. A future task would be to make the necessary finishing touches, debug, and then get it accepted to the official R online library at `http://www.r-project.org/`.

7.4 Combining fractional viscoelasticity with long-range dependence

Can we extend the combination model of chapter 5 to work for spatial structures with long-range dependence? In accordance with Garnier and Sølna [2010, equation (4)] we could implement spatial structure in the compressibility modulus as

$$\kappa_0(z) = \begin{cases} \bar{\kappa}_0 \left\{ 1 + \varepsilon \nu \left(\frac{s}{\varepsilon^2} \right) \right\} & \text{for } z \in [0, L] \\ \bar{\kappa}_0 & \text{otherwise.} \end{cases}$$

The theory of Garnier and Sølna [2010] states that, in an elastic material, taking the limit of the resulting wave propagation as $\varepsilon \to 0$ gives deterministic spreading akin to the ODA theory of section 3.3, and a random arrival time [Garnier and Sølna, 2010, section III.A]. Qualitatively speaking, as $\varepsilon \to 0$ we see that the $\frac{z}{\varepsilon^2}$ argument of our process $\nu(z)$ pulls the "whole" process into our material slab which stretches from $z = 0$ to $z = L$. In this way, the wave experiences all the scales at once, and the wave inherits only the deterministic statistical properties of the autcorrelation function of $\nu(z)$.

Though the theory of Garnier and Sølna [2010] is only valid for elastic media, is it possible to extend it so we could make the fractional viscoelastic combination model of chapter 5 work with long-range dependent spatial structure?

7.5 Causality of the Burridge et al. combination model

Physical speaking, since the ODA theory is causal and the fractional Zener model is causal, we would expect the combination model of chapter 5 to be causal as well. However, it remains to be proven that the attenuation (5.3.2), or (4.2.6), has a dispersion counterpart which makes the dispersion relation implicit in (5.2.12) causal. Since we know by section (4.2) that we have a finite sound speed c_∞ at the infinite frequency limit, we may use the relations (2.4.10) to put the finishing touches on our combination model.

Chapter 8

Conclusion

Motivated by measurements in a variety of applications, ranging from medical ultrasound to seismology, we have sought to explain power-law attenuation on the form

$$|\text{Signal out}| = \exp\{-A\omega^\gamma L\} \times |\text{Signal in}|$$

with an exponent γ in the range of $(0, 2)$. We have found two models which successfully do precisely this.

The scattering ODA theory from chapter 3 may for materials with fractal spatial structure yield power-law attenuation with $\gamma \in (0, 2)$. In section 3.4 we saw many possible mathematical processes that may describe such a spatial fractal structure. The Ornstein-Uhlenbeck process seems physical in the sense that is is stationary. Though there are some studies looking directly at the autocorrelation structure of the sedimentary layers [Walden and Hosken, 1985; Dolan et al., 1998], there is more to a process than simply its autocorrelation function. Most notably. another characteristic which may be physically investigated is the assumption of Gaussian distribution. Another question raised regarding the ODA scattering regime is that it is one-dimensional in nature. The theory may be extended to 3 dimensions [Burridge et al., 1993] by stacking many thin sheets on top of each other, though the spatial variation is still only present in one dimension. Such an extension makes sense in seismology where the ground is often organized in near-horizontal layers. However, in medical ultrasound, a stratified description of the liver makes less sense.

The fractional viscoelastic Zener model as explained in chapter 4 may also yield power-law attenuation with $\gamma \in (0, 2)$. However, there is some doubt about the physical interpretation of the fractional derivative in its constitutive equation. As presented in 4.4 the recent work Näsholm and Holm [2011] may provide this physical grounding by seeing the fractional Zener model as a weighted sum of classic Zener models. Presumably each addition of a classic Zener model corresponds to a molecule and the sum as a whole becomes a mixed medium with arbitrary fractional Zener exponent $0 < \beta < 1$.

Both of these models, scattering in fractal media and the fractional Zener model are known to satisfy the Kramers-Kronig relation and are therefore causal.

In chapter 5 we combined the two models. By adding small spatial structure in acoustic impedance (ε) and even smaller viscoelasticity (ε^2), we found that the effects would simply add up on an equal scale (ε^2). Furthermore, this implies that we will in principle observe no new behavior, only that the two regimes will compete and dominate on different frequency bands. However, in medical ultrasound where

viscoelastic absorption is believed to be stronger than scattering, the assumption of chapter 5 are restrictive. If we assume viscoelasticity to be the dominant effect, how will this change the outcome? Could the viscoelastic version of the Goupillaud medium introduced in section 7.2 be a possible venue of exploration? Also, as alluded to in section 7.4, how will spatial processes of long-range dependence change the interaction between scattering and viscoelasticity?

Also important in medical applications is the power-law with exponent near $\gamma = 1$ though this has proven elusive. The spatial processes introduced in 3.4 can come close, but may not model the $\gamma = 1$ case exactly. In the fractional Zener model, as seen in section 4.2, as $\gamma \to 1$ ($\beta \to 0$) we approach an attenuation $A\omega^1 \propto \beta^2 c_0^{-1}(\ln \frac{\tau_\epsilon}{\tau_\sigma})\omega^1$. As β becomes small it seems that such observations would only be feasible for $\tau_\epsilon \gg \tau_\sigma$ or $c_0 \ll 1$ m/s, but such circumstances seem unlikely in medical ultrasound. Then we found in the proposed stratified model presented in chapter 6 that if τ_ϵ and τ_σ are independently drawn from a τ^{-1}-like distribution; the Weibull distribution with small ν, the attenuation is close to something proportional to $\nu\omega^1$. Hence it collapses more slowly to 0 than the fractional Zener model. This can be metaphorically illustrated, akin to the ARMA approximation due to van der Ziel of section 3.4.1, by the fact that the speed of convergence towards the ω^1 line is unequally distributed; a small part of frequency space converges very quickly.

As a final judgment we remark that, in measured data, one cannot easily observe the difference between our models; indeed they will all produce attenuation of exactly the same kind. As a practical consequence one must be extremely cautious in the choice of model for a particular circumstance. Even if only *one* effect is believed to be present, as we learned in chapter 5, they may both be there, but one may dominate and mask the other. Simply observing power-law attenuation is not enough to conclude which model is appropriate. Further experiments – for instance measurements of energy absorption or studying the wave coda – are necessary to decide on a model. Even measuring dispersion may be misleading. As we learned in section 4.2 the fractional Zener model for $\tau_\sigma/\tau_\epsilon \approx 1$ gives almost constant speed throughout the spectrum.

All in all, if our theories have merit, what we have achieved is significant. We have seen in chapter 7 a host of interesting opportunities for further study which this thesis inspires. And as a final conclusion let us celebrate the knowledge we have gained. Many important imaging technologies predicate on the theories as explained between these covers. These imaging applications range from ultrasound [Holm and Näsholm, 2011], elastography [Sinkus et al., 2007] and photoacoustic imaging and tomography [Treeby and Cox, 2009], to seismic imaging. Without the explicit knowledge of acoustic propagation through complex media, such as biological tissues and sedimentary layers of the earth's upper crust, these technologies – and the vital information derived therefrom – could not exist.

Appendix A

Digital signal processing

The following Fourier analysis may be found in Gasquet and Witomski [1998], and the corresponding theory pertaining to the Laplace transform may be found in Golubitsky and Dellnitz [1999].

Definition A.0.1. The Fourier transform of a discrete series $x[n]$ is given by

$$\mathcal{F}\{x[n];\omega\} = \sum_{n=-\infty}^{\infty} x[n]e^{-i\omega n},$$

and the Fourier transform of a function $f(t)$ is given by

$$\mathcal{F}\{f(t);\omega\} = \int_{-\infty}^{\infty} f(t)e^{-i\omega t}dt$$

Definition A.0.2. The Laplace transform of a function $f(t)$ is given by

$$\mathcal{L}\{f(t);s\} = \int_{-\infty}^{\infty} f(t)e^{-ts}dt$$

Definition A.0.3. The z-transform of a discrete series $x[n]$ is given by

$$\mathcal{Z}\{x[n];z\} = \sum_{n=-\infty}^{\infty} x[n]z^{-n}$$

Property A.0.4. The Laplace and Fourier transforms of the derivative of the function $f(x)$ is given by

$$\begin{aligned}\mathcal{F}\{D_t f(x);\omega\} &= i\omega\widehat{F}(\omega)\\ \mathcal{L}\{f'(x);s\} &= s\widehat{F}(s) - f(0^+),\end{aligned}$$

where $f(0^+) = \lim_{x\to 0} f(x)$.

These immediately generalize to

Property A.0.5. The Laplace and Fourier transforms of the n-th derivative of the function $f(x)$ is given by

$$\mathcal{F}\left\{D_t^n f(x);\omega\right\} = (i\omega)^n \widehat{F}(\omega)$$
$$\mathcal{L}\left\{f^{(n)}(x);s\right\} = s^n \widehat{F}(s) \sum_{k=0}^{n-1} s^k f^{(n-k-1)}(0^+),$$

where $f^{(k)}(0^+) = \lim_{x\to 0} f^{(k)}(x)$.

The following theorems connect the first and final values of the time-domain to limits in the frequency domain.

Theorem A.0.6 (Final and initial value theorem)**.** *The final and initial value theorems respectively state that*

$$\lim_{x\to\infty} f(x) = \lim_{s\to 0^+} s\widehat{F}(s)$$
$$\lim_{x\to 0^+} f(x) = \lim_{s\to\infty} s\widehat{F}(s)$$

The equivalent result for the z-transform follows

Theorem A.0.7 (Final and initial value theorem)**.** *The final and initial value theorems respectively state that*

$$\lim_{n\to\infty} x[n] = \lim_{z\to 0^+} X(z)$$
$$x[0] = \lim_{z\to\infty} X(z)$$

Property A.0.8. The derivative of a convolution of two functions obey the following property.

$$\partial_t \left(f(t) * g(t)\right) = \left(\partial_t f(t)\right) * g(t) = f(t) * \left(\partial_t g(t)\right), \tag{A.0.1}$$

Property A.0.9. The Fourier transform obeys the following properties

$$\mathcal{F}\left\{f(\tfrac{x}{|a|});\omega\right\} = |a|\mathcal{F}\left\{f(x);|a|\omega\right\} \tag{A.0.2}$$
$$\mathcal{F}\left\{f(x-a);\omega\right\} = e^{-ia\omega}\mathcal{F}\left\{f(x);\omega\right\} \tag{A.0.3}$$
$$\mathcal{F}\left\{f(-x);\omega\right\} = \mathcal{F}\left\{f(x);\omega\right\}^* \tag{A.0.4}$$

The next property may be found in Claerbout [1976, chapter 2.3]. It states that if we have a minimum phase filter and add something small, you will still have a minimum phase filter. The reader is warned that in this old book [Claerbout, 1976], z of the z-transform takes the place of z^{-1} in the modern formalism. Everything known to the modern signal processor is turned on its head, for instance, minimum phase filters have their poles and zeros outside the unit circle.

Property A.0.10. Let $F(z)$ be minimum phase. If $G(z)$ is an arbitrary response function whose spectrum is less than the spectrum of $F(z)$, i.e $F(z)F(1/z) > G(z)G(1/z)$ for all z, then $F(z) + G(z)$ is also minimum phase.

Finally we introduce two theorems which were made for the theory of this thesis.

Theorem A.0.11. *Given a series $x[n]$ which is zero for n outside $\{1, \ldots, N\}$, and a sample autocovariance function*

$$\phi_x[k] := \frac{1}{N} \sum_{n=0}^{\max(N-|k|)} x[n]x[n+|k|]$$

we have the following result

$$\mathcal{F}\{\phi_x[k]; \omega\} = \frac{1}{N} |\mathcal{F}\{x[n]; \omega\}|^2,$$

or more generally

$$\mathcal{F}\{\phi_x[k]; a\omega\} = a\frac{1}{N} |\mathcal{F}\{x[n]; a\omega\}|^2$$

for $a > 0$.

Proof.

$$\begin{aligned}
\mathcal{F}\{\phi_x[k]; a\omega\} &= \tfrac{1}{a}\mathcal{F}\{\phi_x[k/a]; \omega\} && \text{by (A.0.2)} \\
&= \tfrac{1}{a}\mathcal{F}\left\{\tfrac{1}{N} x[n/a] * x[-n/a]; \omega\right\} \\
&= \tfrac{1}{a}\tfrac{1}{N}\mathcal{F}\{x[n/a]; \omega\}\,\mathcal{F}\{x[n/a]; \omega\}^* && \text{by (A.0.4)} \\
&= a\tfrac{1}{N}|\mathcal{F}\{x[n]; a\omega\}|^2 && \text{by (A.0.2)}
\end{aligned}$$

□

The above theorem is a **Wiener-Khinchin** type theorem, which states that the Fourier transform of the autocorrelation function is the same as the power spectral density. Roughly speaking, by taking the ensemble expectation of the expressions above one would get the Wiener-Khinchin theorem.

Theorem A.0.12. *Given a continuous function $f(x)$ which is zero for x outside $(0, T)$, and a sample autocovariance function*

$$\phi_f(z) := \frac{1}{T} \int_0^{\max(T-|z|)} f(u)f(u+z)du$$

we have the following result

$$\mathcal{F}\{\phi_f(z); \omega\} = \frac{1}{T} |\mathcal{F}\{f(x); \omega\}|^2,$$

or more generally

$$\mathcal{F}\{\phi_f(z); a\omega\} = a\frac{1}{T} |\mathcal{F}\{f(x); a\omega\}|^2$$

for $a > 0$.

Proof. Exactly as in theorem A.0.11 □

Appendix B

Fractional calculus

The following may be found in Mathai et al. [2010, chapter 3].

Definition B.0.13. The left-sided Riemann-Liouville fractional derivative of order $\alpha \in \mathbb{R}$ and $\alpha \geq 0$ is defined by

$$({}_a^{RL}D_x^\alpha f)(x) = \frac{1}{\Gamma(n-\alpha)} \frac{d^n}{dx^n} \int_a^x \frac{f(t)}{(x-t)^{\alpha-n+1}} dt, \qquad n = \lfloor \alpha \rfloor + 1,$$

where $\lfloor \alpha \rfloor$ is the integral part of α.

Definition B.0.14. The left-sided Caputo fractional derivative of order $\alpha \in \mathbb{R}$ and $\alpha \geq 0$ is defined by

$$({}_a^{C}D_x^\alpha f)(x) = \frac{1}{\Gamma(n-\alpha)} \int_a^x \frac{f^{(n)}(t)}{(x-t)^{\alpha-n+1}} dt, \qquad n = \lfloor \alpha \rfloor + 1,$$

where $\lfloor \alpha \rfloor$ is the integral part of α.

Notation 1. For short, we denote by $D_{RL}^\alpha = {}_0^{RL}D_x^\alpha$ the Riemann-Liouville fractional derivative and $D_C^\alpha = {}_0^{C}D_x^\alpha$ the Caputo fractional derivative, both of fractional order α and with lower integration limit $a = 0$.

Property B.0.15. The Laplace transform of the Caputo derivative of a function $f(x)$ is given by

$$\mathcal{L}\left\{(D_C^\alpha f)(x); s\right\} = s^\alpha \widehat{F}(s) - \sum_{k=0}^{\lceil \alpha \rceil - 1} s^{\alpha-k-1} f^{(k)}(0^+),$$

where $\lceil \alpha \rceil$ is the integer rounded up from α, $f^{(k)}(0^+) = \lim_{x \to 0} f^{(k)}(x)$ and $\widehat{F}(s)$ is the Laplace transform of $f(x)$.

Appendix C

Chart of physical variables

Bulk modulus	K
Compressibility modulus	κ_0
Displacement	u
Impedance	$Z = \rho c = \sqrt{\frac{\rho}{\kappa_0}} = \sqrt{\rho K}$
Pressure	p
Speed of sound	$c = \sqrt{\frac{K}{\rho}} = \sqrt{\frac{1}{\kappa_0 \rho}}$
Strain	ϵ
Stress	$\sigma = -p$
Velocity	$v = \partial_t u$
Young's module	$E_0 = \frac{1}{\kappa_0}$
Creep compliance	$J(t)$
Relaxation modulus	$G(t)$
Retardation time	τ_ϵ
Relaxation time	τ_σ

Appendix D

Useful linear algebra

Let $\{\lambda_i\}_{i=1}^n$ be the eigenvalues of a the $n \times n$ matrix M. Remember these useful identities.

$$\det M = \prod_{i=1}^{n} \lambda_i \tag{D.0.1}$$

$$\text{tr } M = \sum_{i=1}^{n} \lambda_i \tag{D.0.2}$$

Following this we have a simple result that we will use as a tool so often that it will be presented as its own result.

Property D.0.16. The matrix $M = \begin{bmatrix} 0 & a \\ b & 0 \end{bmatrix}$ has eigenvalues $\lambda = \pm\sqrt{ab}$ and is diagonalized as follows:

$$M = E \begin{bmatrix} \sqrt{ab} & 0 \\ 0 & -\sqrt{ab} \end{bmatrix} E^{-1}, \text{ where } E = \frac{1}{\sqrt{2}} \begin{bmatrix} Z^{1/2} & -Z^{1/2} \\ Z^{-1/2} & Z^{-1/2} \end{bmatrix},$$

and $Z = \sqrt{\frac{a}{b}}$.

The eigenvalues follow immediately by applying (D.0.1) and (D.0.2):

$$\det M = -ab = \lambda_1 \lambda_2 \quad \text{and} \quad \text{tr } M = \lambda_1 + \lambda_2 = 0.$$

The rest is left for the reader.

Property D.0.17. Given a matrix $M = \begin{bmatrix} a & b \\ c & d \end{bmatrix}$ and two vectors satisfying the equation

$$\begin{bmatrix} x_1 \\ y_1 \end{bmatrix} = M \begin{bmatrix} x_0 \\ y_0 \end{bmatrix}.$$

Then we can switch the bottom two elements of the vectors and get a new equation on the form

$$\begin{bmatrix} x_1 \\ y_0 \end{bmatrix} = \frac{1}{d} \begin{bmatrix} |M| & b \\ -c & 1 \end{bmatrix} \begin{bmatrix} x_0 \\ y_1 \end{bmatrix}$$

Definition D.0.18. The matrix exponential of a square matrix M is

$$e^M = \sum_{k=0}^{\infty} \frac{1}{k!} M^k.$$

Property D.0.19. Let M be a square matrix with factorization $M = E\Lambda E^{-1}$. Then the matrix exponential has the following properties:

- $e^0 = I$
- $(e^M)^{-1} = e^{-M}$
- $e^{E\Lambda E^{-1}} = Ee^{\Lambda}E^{-1}$
- $e^{M_1+M_2} = e^{M_1}e^{M_2}$ only when $M_1M_2 = M_2M_1$.

If Λ is diagonal with elements $\Lambda = \text{diag}(\lambda_1, \ldots, \lambda_n)$, then

- $e^{\Lambda} = \text{diag}(e^{\lambda_1}, \ldots, e^{\lambda_n})$.

Appendix E

Systems of linear differential equations

These results may be found in any introductory text book on systems of ordinary differential equations. See for instance Golubitsky and Dellnitz [1999].

Theorem E.0.20. *A general linear system of differential equations*

$$\partial_z X(z) + Q(z)X(z) = G(z),$$

where $X(z)$ and $G(z)$ are n-dimensional vectors, and $Q(z)$ is an $n \times n$ matrix, will have n linearly independent solutions $\{X_i(z)\}_{i=0}^{n}$. The general solution will be linear combinations of these.

Definition E.0.21. The fundamental matrix $Y(z)$ is the matrix whose columns are the solutions to the differential equation:

$$Y(z) = (\, X_1(z) \,|\, \ldots \,|\, X_n(z) \,).$$

The fundamental matrix $Y(z)$ will also satisfy the original differential equation.

Theorem E.0.22. *Given an homogeneous linear system of differential equations with constant coefficient matrix Q*

$$\partial_z X(z) + QX(z) = 0,$$

the fundamental matrix is

$$Y(z) = e^{-zQ},$$

and the general solutions is thus

$$X(z) = e^{-zQ}C$$

where C is a constant vector. With the appropriate initial conditions C can be uniquely determined, and we have a unique solution.

Theorem E.0.23. *Given an inhomogeneous linear system of differential equations with constant coefficient matrix Q*

$$\partial_z X(z) + QX(z) = G(z),$$

and Y is the fundamental matrix of the corresponding homogeneous system $\partial_z X(z) + QX(z) = 0$, we define

$$D = \int_0^z Y^{-1}(s)G(s)ds.$$

The general solutions is then given by

$$X(z) = Y(z)(D(z) + C) = Y(z)\left(\int_0^z Y^{-1}(s)G(s)ds + C\right),$$

where C again is a constant vector. With appropriate initial conditions C can be uniquely determined and we have a unique solution.

Theorem E.0.24. *Given an homogeneous linear equation with non-constant coefficient $g(z)$*

$$\partial_z f(z) + g(z)f(z) = 0,$$

the general solution is given by

$$f(z) = e^{-\int_0^z g(s)ds}C$$

where C is a real constant. With appropriate initial conditions C can be uniquely determined and we have a unique solution.

Appendix F

The Gamma function, Mellin transform, the H-function and the Mittag-Leffler function

The Gamma function is given by

$$\Gamma(z) = \int_0^\infty t^{z-1} e^{-t} dt.$$

One useful identity involving the Γ function is

$$\Gamma(1-z)\Gamma(z) = \frac{\pi}{\sin \pi z}. \tag{F.0.1}$$

The gamma function has no zeros, but it has infinitely many poles at $z = 0, -1, -2, \ldots$ [Mathai et al., 2010]. The residue at each pole is

$$\mathfrak{Res}\left\{\Gamma(z); -n\right\} = \frac{(-1)^n}{n!}, \qquad \text{for} n = 0, 1, 2, \ldots \tag{F.0.2}$$

Furthermore, the following asymptotic relation holds [Lim and Muniandy, 2003, equation (15)].

$$\Gamma(x + i|y|) = \sqrt{2\pi}|y|^{x-1/2} e^{-\frac{\pi}{2}|y|} \left[1 + O(\tfrac{1}{y})\right]. \tag{F.0.3}$$

The Mellin transform is given by Mathai et al. [2010, chapter 2]

$$\mathcal{M}\left\{f(x); s\right\} = F(s) = \int_0^\infty f(x) x^{s-1} \mathrm{dx},$$

and its inverse is

$$\mathcal{M}^{-1}\left\{F(s)\right\}(x) = f(x) = \frac{1}{2\pi i} \int_{c-i\infty}^{c+i\infty} F(s) x^{-s} \mathrm{ds}.$$

Following is a useful result which may greatly facilitate when computing the Mellin transform. It is simply an application of the Cauchy Residue theorem to a specific situation.

Theorem F.0.25. *Let f(z) be analytic in $\mathbb{C}$ except for a finite number of poles, none of which lie on the positive real axis. Suppose $a > 0$ and a is not an integer. Suppose that (i) there exist constants $M, R > 0$ and $b > a$ such that $|f(z)| \leq M/|z|^b$ for $|z| > R$ and (ii) and constants $S, W > 0$ and $0 < d < a$ such that for $0 < |z| \leq S$, $|f(z)| \leq W/|z|^d$. Then $\int_0^\infty z^{a-1} f(z)dz$ is absolutely integrable and*

$$\int_0^\infty z^{a-1} f(z)dz = -\frac{\pi e^{-\pi a i}}{\sin a\pi} \sum \mathfrak{Res} \left\{ z^{a-1} f(z); \text{at the poles of } f(z) \right\}$$

See the proof in Gajjar [2010].

Let us define a multiplicative convolution as

$$(f \vee g)(x) = \int_0^\infty f(t)g(xt)dt$$

then the Mellin transform obeys the following property.

Property F.0.26. The following holds true:

- $\mathcal{M}\{af(x) + bg(x); s\} = a\mathcal{M}\{f(x); s\} + b\mathcal{M}\{g(x); s\}$
- $\mathcal{M}\{f \vee g; s\} = \mathcal{M}\{f; 1-s\}\mathcal{M}\{g; s\}$
- $\mathcal{M}\{f(ax); s\} = a^{-s}\mathcal{M}\{f(x); s\}$
- $\mathcal{M}\{x^a f(x); s\} = \mathcal{M}\{f(x); s+a\}$
- $\mathcal{M}\left\{f(x^\beta); s\right\} = \frac{1}{\beta}\mathcal{M}\left\{f(x); \frac{s}{\beta}\right\}$
- $\mathcal{M}\left\{x^\lambda f[(ax)^\beta]; s\right\} = \frac{1}{\beta}a^{-(s+\lambda)}\mathcal{M}\left\{f(x); \frac{s+\lambda}{\beta}\right\}$

Note especially the second item which is analogous to the property of the Fourier transform which takes convolution in one domain to multiplication in the other. Also note that the last item on this list is just a conglomeration of the previous three.

The Fox-H function $H_{pq}^{mn}(x)$ is given by

$$H_{pq}^{mn}(x) = H_{pq}^{mn}\left[x \middle| \begin{matrix} (a_1, A_1), (a_2, A_2), ..., (a_p, A_p) \\ (b_1, B_1), (b_2, B_2), ..., (b_q, B_q) \end{matrix}\right] = \frac{1}{2\pi i}\int_L \Theta(s)x^{-s}ds, \quad \text{(F.0.4)}$$

where the integral is a Mellin-Barnes type integral with

$$\Theta(s) = \frac{\prod_1^m \Gamma(b_j + B_j s)\prod_1^n \Gamma(1 - a_j - A_j s)}{\prod_{m+1}^q \Gamma(1 - b_j - B_j s)\prod_{n+1}^q \Gamma(a_j + A_j s)}, \quad \text{(F.0.5)}$$

with $m, n, p, q \in \mathbb{N}_0$, $0 \leq n \leq p$, $1 \leq m \leq q$, with $a_j, b_j \in \mathbb{C}$ and $A_j, b_j \in \mathbb{R}^+$. Also L is a suitable contour separating the poles of $\Gamma(b_j + B_j s)$ from the poles of $\Gamma(1 - a_j - A_j s)$. See Mathai et al. [2010, chapter 1] for details.

The Fox-H function can be manipulated in countless ways [Mathai et al., 2010, chapter 1]. Here are some useful properties.

Property F.0.27. The following holds true:

$$H_{pq}^{mn}\left[x \middle| \begin{matrix} (a_p, A_p) \\ (b_q, B_q) \end{matrix}\right] = z^\sigma H_{pq}^{mn}\left[x \middle| \begin{matrix} (a_p - \sigma A_p, A_p) \\ (b_q - \sigma B_q, B_q) \end{matrix}\right]$$

where $\sigma \in \mathbb{C}$.

Property F.0.28. The following holds true:

$$H_{pq}^{mn}\left[x\left|\begin{array}{c}(a_p,A_p)\\(b_q,B_q)\end{array}\right.\right]=kH_{pq}^{mn}\left[x^k\left|\begin{array}{c}(a_p,kA_p)\\(b_q,kB_q)\end{array}\right.\right]$$

where $k>0$.

Property F.0.29. The following holds true:

$$H_{pq}^{mn}\left[x\left|\begin{array}{c}(a_p,A_p)\\(b_q,B_q)\end{array}\right.\right]=H_{qp}^{nm}\left[\frac{1}{x}\left|\begin{array}{c}(1-b_q,B_q)\\(1-a_p,A_p)\end{array}\right.\right]$$

The Fox-H function has many Gamma based functions as special cases. For the applications presented in this thesis the Mittag-Leffler is the most relevant. The following may be found in the Mittag-Leffler review paper Haubold et al. [2011]. The two parameter Mittag-Leffler function is given by

$$E_{\alpha,\beta}(z)=\sum_{n=0}^{\infty}\frac{z^n}{\Gamma(\alpha n+\beta)}, \tag{F.0.6}$$

which only converges when $\mathfrak{Re}\,(\alpha)>0$. The one parameter Mittag-Leffler is

$$E_{\alpha}(z)=E_{\alpha,1}(z)=\sum_{n=0}^{\infty}\frac{z^n}{\Gamma(\alpha n+1)}.$$

Property F.0.30. The following holds true:

$$z^{\beta}E_{\beta,\beta+1}(-z^{\beta})=1-E_{\beta}(-z^{\beta})$$

Property F.0.31. The following holds true:

$$\partial_z\left[z^bE_{a,b+1}(-z^a)\right]=z^{b-1}E_{a,b}(-z^a)$$

We have the following link between the Mittag-Leffler and the Fox-H function

$$H_{12}^{11}\left[z\left|\begin{array}{c}(0,1)\\(0,1)(a,b)\end{array}\right.\right]=E_{b,1-a}(-z) \tag{F.0.7}$$

Finally, the Mittag-Leffler function satisfies the following integral [Mainardi and Spada, 2011, equation (3.7)]

$$E_{\beta}(-t^{\beta})=\int_0^{\infty}e^{-\frac{1}{x}t}f(x;\beta)dx,\quad\text{where}\quad f(x;\beta)=\frac{1}{x\pi}\frac{\sin(\beta\pi)}{x^{\beta}+2\cos(\beta\pi)+x^{-\beta}},$$

for $0<\beta\leq 1$.

Appendix G

Code

G.1 Simulate true propagation in layered media: propagate.r

```
source("misc.r")

# Compute reflection and transmission coefficients from impedance
interface.coeffs ← function(Z) {
  Z0 ← Z[-length(Z)]
  Z1 ← Z[-1]
  refl ← (Z0 - Z1)/(Z0 + Z1)
  trans ← 2*sqrt(Z0*Z1)/(Z0 + Z1)
  return(data.frame(refl=c(refl,0), trans=c(trans,1)))
}

# Interface matrix from R and T
Imatrix ← function(R,T) { array( 1/T*c(1,R,R,1), dim=c(2,2) ) }

# Solve the differential equation with the propagation matrix method of
    chapter 6
propagate ← function ( N, dz, medium, omegas, comp )
{
  M ← length(omegas)
  T ← rep(0,M)
  R ← rep(0,M)

  for (j in 1:M) {

    comps ← comp(omegas[j], medium$beta, medium$comp0, medium$tau_del,
        medium$tau_eps)
    comps[ is.nan(comps) ] = 1
    wn ← omegas[j] * sqrt(medium$rho) * sqrt(comps)
    Z ← sqrt ( medium$rho / comps )
    coeffs ← interface.coeffs(Z)
    K ← diag(c(1,1))

    for (k in 1:N) {
      Imat ← Imatrix ( coeffs[k,]$refl, coeffs[k,]$trans )
      Pmat ← diag ( exp( c(-1,1) * 1i * wn[k] * dz ) )
      K ← Imat %*% Pmat %*% K
    }

    T[j] ← abs( 1 / K[2,2] )
```

```
    R[j] ← abs( - K[2,1] / K[2,2] )

  }
  return( list( omega=omegas, trans=T, refl=R ) )
}

# General propagation information
propagation.data ← function ( L, rho, Jin ) {
  p ← list()
  p$N ← length(Jin)
  p$nPrUnit ← N/L
  p$dz ← 1/p$nPrUnit
  p$Z ← sqrt(rho/Jin)
  p$c ← p$Z/rho
  p$Jin ← Jin
  p$rho ← rho
  p$coeffs ← interface.coeffs(p$Z)
  p$homc ← 1 / mean( 1 / p$c)
  p$homtau ← p$dz / p$homc
  p$T ← L * 1 / p$homc
  return(p)
}
```

G.2 The fractional Zener model: fraczener.r

```
# FRACTIONAL ZENER

# Compressibility frequecny domain
fracZener.comp ← function(omega,beta,Jeq,tau_del,tau_eps) {Jeq * (1.0 +
    (1i*tau_del*omega)^beta)/(1.0 + (1i*tau_eps*omega)^beta) }

# Attenuation frequecny domain
fracZener.att ← function(omega,beta,Jeq,tau_del,tau_eps) {
    -omega*Im(sqrt(fracZener.comp(omega,beta,Jeq,tau_del,tau_eps))) }

# Normalized attenuation frequecny domain
fracZener.scaledatt ← function(omega,beta,tau_del,tau_eps) {
    fracZener.att(omega,beta,1,tau_del,tau_eps)/fracZener.att(1.0/tau_eps,beta,1,tau_del,tau_eps)
    }

# Dispersion in frequency domain
fracZener.disp ← function(omega,beta,Jeq,tau_del,tau_eps) {
    omega*Re(sqrt(fracZener.comp(omega,beta,Jeq,tau_del,tau_eps))) }
```

G.3 Numerical analysis of proposed model: relaxdist.r

```
source("propagate.r")
source("fraczener.r")

# load(medium, file="scenario1.dat")
# nu ← 0.5
# lambda ← 1000
# eps ← 0.1

# Size and number of layers
N ← 1000
L ← 1
dz ← L/N

# Discretization of frequency space
```

```
M ← 100
omegas ← 10^seq(from=-5,to=5,length=M)

# Medium constants
medium ← list()
medium$rho ← 1
medium$comp0 ← 1
medium$beta ← 1
c0 ← 1 / sqrt( medium$rho * medium$comp0 )

# Parameters
eps ← 0.5
nu ← 0.1
lambda ← 1000

# Draw retardation times from weibull distribution
medium$tau_eps ← rweibull(N, shape=nu, scale=lambda)
medium$tau_del ← medium$tau_eps * ( 1 - eps )

# Exact solution of propagation through stratified medium
out ← propagate ( N, dz, medium, omegas, fracZener.comp )
plot( omegas, 1 - out$trans, log="xy", type="l" )

# Sample approximation (A1)
attapprox ← c()
for (om in omegas) attapprox ← c(attapprox, eps / (2*c0) * mean( om / (
    (om*medium$tau_eps)^(-1) + (om*medium$tau_eps) ) ) )
lines(omegas, attapprox,  col="red")

# Deterministic approximation (A2)
C ← pi / (2 * exp(1) )
#f ← function(x,nu) { x^nu / ( 1 + x^2 ) * exp( -(x/lambda)^nu ) }
#C ← integrate(f,0,Inf,nu)$value
attapprox2 ←  (eps*nu)/(2*c0)*L*lambda^(-nu)*C*omegas^(1-nu)
lines( omegas, attapprox2, col="green" )

# ggplot2
library(ggplot2)
library(tikzDevice)
options(tikzLatex = "TEXINPUTS=..//:$TEXINPUTS pdflatex")
options(tikzLatexPackages = c("\\usepackage{master}\n") )
tikz('ownmodel2.figure.tex', height=2.2, width=5.2, standAlone=FALSE)
data ← data.frame(omega=omegas,
    Category=rep("$\\attC_{\\textrm{true}}(\\omega)$",M),
    attenuation=(1-out$trans) )
data ← rbind( data, data.frame(omega=omegas,
    Category=rep("$\\attC_1(\\omega)$",M), attenuation=attapprox ) )
data ← rbind( data, data.frame(omega=omegas,
    Category=rep("$\\attC_2(\\omega)$",M), attenuation=attapprox2 ) )

p ← ggplot(data)
p ← p + geom_line ( aes(x=log10(omega), y=log10(attenuation),
    group=Category, colour=Category))
p ← p + labs(x = "$\\Omega = \\log{\\omega}$",
    y="$\\log{\\totatt(\\omega)}$") + ylim(-6,-1)
p ← p + scale_colour_manual(values = c("black","green","blue")) +
    scale_linetype_manual(values = c(3,1,1))
p
dev.off()
system("cp ownmodel2.figure.tex ~/master/figs")


```

```
69 #out ← propagate ( N, dz, medium, c(10^10), fracZener.comp )
70
71 #nus ← seq(from=0,to=10,length=100)
72 #I ← c()
73 #for (nu in nus) I ← c(I, integrate( f, 0, Inf, nu )$value)
74 #plot(nus,I,type="l")
75 #lines(nus,pi/(2*exp(1))/(1 + (nus^2)/5),type="l",col="red")
76
77
78 #save(medium, file="scenario1.dat")
```

Appendix H

Numerical analysis of the Burridge et al. combination model

After having found theoretical approximations of the purely scattering case (chapter 3) and the combination case (chapter 5), we seek to verify the quality of these approximations by comparing them to the real wave propagation. It is our goal then to create an algorithm for solving the exact wave propagation. Note that the attenuation due to viscoelasticity described in chapter 4 is the real solution. We will, in our analysis, simulate exclusively in the frequency domain. Though before we can solve the wave equation we need to produce the spatial structure. This is also described in what follows. All code is implemented in the free programming language R and can be found in appendix G.

H.1 The model parameters and basic assumptions

The first step is to initialize the underlying physical variables; density ρ and retardation time τ_ϵ. We will also employ two scale parameters σ and θ which control the magnitude of respectively the apparent scattering attenuation and the intrinsic viscoelastic absorption. A sensible choice of the relaxation time τ_σ would be

$$\tau_\sigma = \left\{1 - \frac{2\theta}{\tau_\epsilon^\beta \sin(\frac{\pi}{2}\beta)}\right\}^{1/\beta} \tau_\epsilon, \quad \text{or} \quad \tau_\sigma = \left\{1 - \frac{2\tau_\epsilon^\beta \theta}{\sin(\frac{\pi}{2}\beta)}\right\}^{1/\beta} \tau_\epsilon.$$

The first gives by (4.2.3) an attenuation of $\theta\omega^{1+\beta}$ for low-frequencies, and the second gives for small θ an approximate attenuation of $\theta\omega^{1-\beta}$ for high frequencies.

The next step is to create our spatial structure. We will in our numerical analysis assume no spatial variation in τ_σ and τ_ϵ. Although we have developed theory in chapter 5 which may deal with this, we will not entertain that complication here. Note that this would be a sharp departure from the articles Burridge et al. [1993] and Le and Burridge [1998] as they only deal with spatial structure in the instantaneous response J_{in}. Let us assume the spatial structure takes the shape of a thinly layered stratified medium. Of course, one could approximate continuous spatial variation by

a discretized stratified medium, but if we assume the medium is stratified to begin with, we get the satisfaction of affirming that our algorithm yields the exact solution. Let us say we have $j \in (1, \ldots, N)$ different layers. As explained in section 3.4 we will define the instantaneous response as Burridge et al. [1993, equation (91)]

$$J_{\text{in},j} = J_{\text{in}} e^{-\sigma \nu_j},$$

where ν_j is a discrete process we will learn to simulate shortly. From this we may calculate the physical variables

$$J_{\text{eq},j} = J_{\text{in},j} \left(\frac{\tau_\epsilon}{\tau_\sigma} \right)^\beta, c_j = \sqrt{\frac{1}{\rho J_{\text{in},j}}}, Z_j = \sqrt{\frac{\rho}{J_{\text{in},j}}}, \mathcal{R}_j = \frac{Z_j - Z_{j+1}}{Z_j + Z_{j+1}}, \mathcal{T}_j = \frac{2\sqrt{Z_j Z_{j+1}}}{z_j + Z_{j+1}}$$

as defined in section 5.1 and in section 3.1. The astute reader will notice that we have one less reflection coefficient than the number of layers. We solve this by setting $\mathcal{R}_N = 1$ and $\mathcal{T}_N = 0$, i.e. that the outside world on the other side of the slab is identical to the last layer.

H.2 Simulation of random process

When we study Gaussian processes with a given autocovariance function we have complete knowledge of the joint distribution of any finite collection of points. In other words, if we wish to simulate a discrete set of N points from our process, it reduces to sampling from an N dimensional multivariate normal distribution whose covariance matrix is known. So given a Gaussian process with autocovariance function $\phi(z)$ and a set of points through space $z_1, z_2, \ldots, z_N$ – usually regularly spaced, though not necessarily – the following algorithm will produce a sample path.

Algorithm H.2.1 (Simulation of Gaussian process)**.**

given a grid $\{z_n\}_{n=1}^N$ of length N
      autocovariance function $\phi(z)$
Populate the autocovariance matrix Γ
    $\Gamma_{(i,j)} := \phi(z_i - z_j)$, $1 \leq i, j \leq N$.
Obtain the Cholesky decomposition C
    $C^T C = \Gamma$
Sample N i.i.d. standard normal values
    $\boldsymbol{u} \sim \mathcal{N}_N(0, I)$
Compute final process $\{\nu_n\}_{n=1}^N$
    $\boldsymbol{\nu} := C\boldsymbol{u}$

Note that the Cholesky decomposition is available in many high-level numerical programming languages, which is indeed the case with R, and the function is `chol()`. Using standard multivariate normal theory it is trivial to show that the last step of the algorithm produces a sample from the correct multivariate normal distribution:

$$C\boldsymbol{u} \sim C\mathcal{N}(0, I) \sim \mathcal{N}(0, C^T I C) \sim \mathcal{N}(0, \Gamma)$$

This method of simulation is the method proposed in Garnier and Sølna [2010]. We simulate from the fractional Ornstein-Uhlenbeck given by the autocovariance function (3.4.13). The integral in (3.4.13) is solved numerically through the standard R function `integrate()`.

In addition we will simulate a process which has the correct spectrum, but has none of the other important statistical structures of Gaussianity and stationarity. For its wonderful simplicity we will choose the method proposed in Gingl et al. [1989]. This is simply a rescaled random walk;

Algorithm H.2.2 (Scaled Brownian motion)**.**

```
given length of process N
      step distribution f(x)
      scale argument α
Sample steps from f(x) i.i.d:   x_k ~ f(x)
Generate preliminary walk y'_{k+1} := y'_k + x_k
Compute the final rescaled process
    g_α(x) := sign(x)|x|^α
    y_k := g_α(y'_k), 1 ≤ k ≤ N
```

Note that x_k can be from any distribution. Note that this is not proven to give a power-law spectrum, but experimentally verified by Gingl. et al. They report that they tried several such rescaling functions $g(x)$, but found the above to be most effective. In my own experience, using uniform distributions for the x_k's works very well. This is method is obviously very quick and easy, both in implementation, memory use and CPU load. Indeed, one can write it in two lines of MATLAB code!

```
g ← function(x,alpha) { g ← sign(x)*abs(x)^alpha };
y ← g(cumsum(rnorm(1000)),0.2);
```

H.3 Solution to governing differential equation

The following numerical procedure was devised by the author based on the general knowledge of stratified medium of section 3. Ultimately the exact solution to our problem is the solution to the differential equation (5.1.7):

$$\partial_z \widehat{\boldsymbol{w}}(z,\omega) = -i\omega\Lambda(z)\widehat{\boldsymbol{w}}(z,\omega) - \boldsymbol{A}_{\mathrm{Bur}}(z)\widehat{\boldsymbol{w}}(z,\omega) - \widehat{\boldsymbol{B}}_{\mathrm{Bur}}(z,\omega)\widehat{\boldsymbol{w}}(z,\omega). \tag{H.3.1}$$

Notice from (5.1.8) that within each layer $\boldsymbol{A}_{\mathrm{Bur}}(z) = 0$, since there is no $Z(z)$ variation across the layer. By (H.3.1) the propagation within each layer is described by

$$\partial_z \widehat{\boldsymbol{w}}_j(z,\omega) = \widehat{Q}_j(\omega)\widehat{\boldsymbol{w}}_j(z,\omega)$$

where

$$\widehat{Q}_j(\omega) = i\omega\left(-\frac{1}{c_j}\begin{bmatrix} 1 & 0 \\ 0 & -1 \end{bmatrix} + \frac{1}{2}\kappa_{\mathrm{vis},j}(\omega)Z_j\begin{bmatrix} -1 & 1 \\ -1 & 1 \end{bmatrix}\right). \tag{H.3.2}$$

This is immediately solvable by Theorem E.0.22:

$$\widehat{\boldsymbol{w}}_j(z,\omega) = e^{\widehat{Q}_j(\omega)z}\widehat{\boldsymbol{w}}_j(0,\omega)$$

In the apostrophe notation of Figure 3.2 we have

$$\widehat{\boldsymbol{w}}'_j(\omega) = e^{\widehat{Q}_j(\omega)\Delta z}\widehat{\boldsymbol{w}}_j(\omega). \tag{H.3.3}$$

At each interface we have the reflection/transmission relation given by (3.1.1)

$$\widehat{w}_{j+1}(\omega) = J_j \widehat{w}'_j(\omega), \quad \text{where} \quad J_j = \frac{1}{\mathcal{T}_j}\begin{bmatrix} 1 & \mathcal{R}_j \\ \mathcal{R}_j & 1 \end{bmatrix} \tag{H.3.4}$$

Combining (H.3.3) and (H.3.4) we get

$$\widehat{\boldsymbol{w}}_{j+1}(\omega) = J_j e^{\widehat{Q}_j(\omega)\Delta z}\widehat{\boldsymbol{w}}_j(\omega)$$

This allows us to write the wave in layer $j+1$ in terms of the wave in the first layer

$$\widehat{\boldsymbol{w}}_{j+1}(\omega) = \widehat{K}_j(\omega)\widehat{\boldsymbol{w}}_1(\omega) \tag{H.3.5}$$

where the propagation matrix K_j contains the cumulative propagation effects from all layers from 1 to j:

$$\widehat{K}_j(\omega) = J_j e^{\widehat{Q}_j(\omega)\Delta z} \cdots J_1 e^{\widehat{Q}_1(\omega)\Delta z}.$$

When j has reached N we get from (H.3.5) the equation describing the relationship between the waves on each side of the slab:

$$\widehat{\boldsymbol{w}}_{N+1}(\omega) = \widehat{K}_N(\omega)\widehat{\boldsymbol{w}}_1(\omega)$$

or

$$\begin{bmatrix} \widehat{R}_{N+1} \\ \widehat{L}_{N+1} \end{bmatrix} = \begin{bmatrix} \widehat{K}_N^{(1,1)} & \widehat{K}_N^{(1,2)} \\ \widehat{K}_N^{(2,1)} & \widehat{K}_N^{(2,2)} \end{bmatrix} \begin{bmatrix} \widehat{R}_1 \\ \widehat{L}_1 \end{bmatrix}. \tag{H.3.6}$$

As it stands, this statement relates the waves on the left hand side of the slab to the waves on the right hand side of the slab. We now wish to apply the switch around property D.0.17 to twist this into an "outgoing waves as a function of incoming waves" statement. For that we need to compute the determinant of the propagation matrix $\widehat{K}_{N+1}(\omega)$. Remember from (3.1.2) that $\det J_j = 1$. From the standard matrix exponential identity $\det e^A = e^{\operatorname{tr} A}$ and the fact that $\operatorname{tr} \widehat{Q}_j = 0$ we get

$$\begin{aligned} \det \widehat{K}_j &= \det\left(J_j e^{\widehat{Q}_j(\omega)\Delta z} \cdots J_1 e^{\widehat{Q}_1(\omega)\Delta z}\right) \\ &= \prod_1^j \det\left(J_j\right) \det\left(e^{\widehat{Q}_j(\omega)\Delta z}\right) \\ &= \prod_1^j e^{\Delta z \operatorname{tr} Q_j} = 1 \end{aligned}$$

Finally, this allows us to switch around (H.3.6) by property D.0.17 and get

$$\begin{bmatrix} \widehat{R}_{N+1} \\ \widehat{L}_1 \end{bmatrix} = \frac{1}{\widehat{K}_N^{(2,2)}(\omega)} \begin{bmatrix} 1 & \widehat{K}_N^{(2,1)}(\omega) \\ -\widehat{K}_N^{(1,2)}(\omega) & 1 \end{bmatrix} \begin{bmatrix} \widehat{R}_1 \\ \widehat{L}_{N+1} \end{bmatrix}$$

Using the initial condition $\widehat{L}_{N+1} = 0$ (we are not sending a left going wave through the medium at the same time) we get the outgoing waves

$$\widehat{R}_{N+1}(\omega) = \frac{1}{\widehat{K}_N^{(2,2)}(\omega)}\widehat{R}_1(\omega), \quad \text{and} \quad \widehat{L}_1(\omega) = -\frac{\widehat{K}_N^{(1,2)}(\omega)}{\widehat{K}_N^{(2,2)}(\omega)}\widehat{R}_1(\omega) \tag{H.3.7}$$

These give respectively the material transfer function $\mathfrak{T}(\omega)$ and the reflection function $\mathfrak{R}(\omega)$. Finally we have a handy pseudo-code summary of the algorithm.

Algorithm H.3.1 (Computation of exact propagation in a stratified medium)**.**

```
given material variables ρ, τ_ε, τ_σ and {J_in,j}_{j=1}^N
      accompanying {c_j}_{j=1}^N, {Z_j}_{j=1}^N, {R_j}_{j=1}^N and {T_j}_{j=1}^N
      discretization of frequency space {ω_k}_{k=1}^M
      layer size Δz
For each ω ∈ {ω_k}_{k=1}^M
    Compute Q̂_j(ω) as defined (H.3.2)
    Recursively compute for all N layers:
        K̂_{j+1} := J_j e^{Q̂_j(ω)Δz} K̂_j with K̂_0 := I
    T(ω) := (K̂_N^(2,2))^{-1}
    R(ω) := −K̂_N^(2,1) (K̂_N^(2,2))^{-1}
```

H.4 The matrix exponential

The solution to linear systems of differential equations can be written in terms of a matrix exponential (see appendix E). It is therefore no surprise that much effort has been made to develop robust methods for numerical evaluation of the matrix exponential. The naive approach would be to sum up the series representation (D.0.18) up to a certain finite term. This however, is generally accepted to be nothing less than a terrible choice. The interested reader may consult the review paper Moler and Loan [2003] for an extensive introduction to the subject. Note that many high-level languages (in particular MATLAB) has a built in matrix exponential function, though R surprisingly does not. There are some available packages, but alas of dubious quality. We, however, are lucky not to be required to implement a function operating under all generalities as we are subject to some very specific circumstances. As seen in (H.3.3) and (H.3.2) we need only to perform the exponential of 2-by-2 matrices whose trace is zero. Predicated on this knowledge we are able to custom tailor a simple and elegant procedure.

It is known (see for instance theorem 2.2 of Bernstein and So [1993]) that for a 2-by-2 matrix $M \in \mathbb{C}^{2\times 2}$ one can write the matrix exponential as

$$e^M = \frac{\lambda_1 e^{\lambda_2} - \lambda_2 e^{\lambda_1}}{\lambda_1 - \lambda_2} I_2 + \frac{e^{\lambda_1} - e^{\lambda_2}}{\lambda_1 - \lambda_2} M, \tag{H.4.1}$$

where I_2 is the 2-by-2 identity matrix and λ_1 and λ_2 are eigenvalues of M. When $\operatorname{tr} M = 0$ we have by (D.0.2) $\lambda_1 = -\lambda_2$. Then (H.4.1) reduces to

$$e^M = \cosh(\lambda)\, I_2 + \frac{\sinh(\lambda)}{\lambda}\, M, \tag{H.4.2}$$

where λ can be either of the two eigenvalues. Furthermore, we know from basic linear algebra that the eigenvalues are solutions of the characteristic polynomial

$$\lambda^2 - (\operatorname{tr} M)\,\lambda + \det M = 0.$$

But again, $\operatorname{tr} M = 0$ so

$$\lambda = \pm\sqrt{-\det M}.$$

A special case occurs when $\det M = 0$. Then $\lambda = 0$ and (H.4.2) can not be evaluated. Taking the limit of $\lambda \to 0$ in (H.4.2) we get

$$e^M = I_2 + M.$$

For those familiar with the details of linear algebra, we could argue the last step in a more algebraically satisfying way. Since M only has 0 eigenvalues we know that M is nilpotent. Since the degree of M must be equal or less to its dimension, $M^2 = 0$. We can then use the series representation of the matrix exponential from Definition D.0.18 which will, by the nilpotent property, truncate after only the two first terms. We arrive again at $e^M = I_2 + M$. To sum it all up we have the following algorithm.

Algorithm H.4.1 (Matrix exponential of a 2-by-2 matrix whose trace is zero)**.**

given matrix $M \in \mathbb{C}^{2\times 2}$ **with** tr $M = 0$
if $\det M = 0$ **then**
    $e^M = I_2 + M$
else
    $\lambda = \sqrt{-\det M}$
    $e^M = \cosh(\lambda) I_2 + \frac{\sinh(\lambda)}{\lambda} M$
end if

H.5 Computation of the Burridge et al. approximations in the time domain

The following is a sketch of how to compute the Burridge et al. approximation (5.2.16) in the fractional setting in the time domain. This is described well in Burridge et al. [1993, section IV.A] and Le and Burridge [1998]. We need make no changes to the how the scattering term is dealt with in Le and Burridge [1998, section I.A]. But looking closer at the absorptive term as explained in Le and Burridge [1998, section I.C] it is clear that in the fractional viscoelastic case the exponentials will be exchanged with Mittag-Leffler functions. Unfortunately, the Mittag-Leffler function does not exist in R, so after studying mainly Gorenflo et al. [2002], but also the more rigorous Hilfer and Seybold [2006], the following numerical recipe was implemented. The code may be found in appendix I. We are dealing with Mittag-Leffler functions $E_{\alpha,\beta}(t)$ where

$$0 < \alpha \leq 1, 0 < \beta \leq 1, \text{ and } t \in \mathbb{R}.$$

Based on these restrictions we are able to simplify the algorithm in Gorenflo et al. [2002] somewhat and obtain the recipe seen in algorithm H.5.1. Note that the precision ρ means we have the following guarantee:

$$|E^{numerical}_{\alpha,\beta}(t) - E^{true}_{\alpha,\beta}(t)| < |\rho|$$

The computation of the derivative of the Mittag-Leffler may be seen in algorithm H.5.2. With minor extra work we could complete these to algorithms to work for all input arguments, error test them, and get them accepted into the online R library.

Algorithm H.5.1 (Computation of Mittag-Leffler $E_{\alpha,\beta}(t)$)**.**

given parameters $\alpha, \beta \in \mathbb{R}$, $0 < \alpha \leq 1$
  argument $t \in \mathbb{R}$
  precision $\rho \in \mathbb{R}$, $\rho \neq 0$
if $t = 0$ **then**
  $E_{\alpha,\beta}(t) = \frac{1}{\Gamma(\beta)}$
else if $|t| < r_0 = 0.9$ **then**
  $N = \lceil \max\left\{ \frac{2-\beta}{\alpha}, \frac{\ln|\rho|(1-|t|)}{\ln|t|} \right\} \rceil + 1$
  $E_{\alpha,\beta}(t) = \sum_{n=0}^{N} \frac{t^n}{\Gamma(\alpha n+\beta)}$
else if $|t| < r_1 = (-2\log[\rho\pi\sin(\alpha\pi)])^{\alpha}$
  $\omega(x,y) = x^{1/\alpha}\sin(y/\alpha) + y(1+(1-\beta)/\alpha)$
  $A(x,y) = \frac{1}{\alpha} x^{(1-\beta)/\alpha} \exp\left[x^{1/\alpha}\cos(y/\alpha) \right]$
  $B(r;t,\lambda) = \frac{1}{\pi} A(r,\lambda) \frac{r\sin[\omega(r,\lambda)-\lambda] - t\sin[\omega(r,\lambda)]}{r^2 - 2rt\cos\lambda + t^2}$
  $C(\phi;t,\lambda) = \frac{\lambda}{2\pi} A(\lambda,\phi)\, \mathfrak{Re}\, \frac{\exp i\omega(\lambda,\phi)}{\lambda\exp(i\lambda) - t}$
  if $t > 0$ **then**
    $R = \max\left\{ 1, 2|t|, (|\beta|+1)^{\alpha}, \left(-\log\frac{\pi\rho}{6}\right)^{\alpha}, \left(-2\log\frac{\pi\rho}{6(|\beta|+2)(2|\beta|)^{|\beta|}}\right)^{\alpha} \right\}$
    $\beta \leq 1 : E_{\alpha,\beta}(t) = A(t,0) + \int_0^R B(r;t,\pi\alpha)dr$
    $\beta > 1 : E_{\alpha,\beta}(t) = A(t,0) + \int_{1/2}^R B(r;t,\pi\alpha)dr + \int_{-\pi\alpha}^{\pi\alpha} C(\phi;t,1/2)d\phi$
  else
    $R = \max\left\{ 2^{\alpha}, 2|t|, 2(|\beta|+1)^{\alpha}, \left(-2\log\frac{\pi 2^{\beta}\rho}{12}\right)^{\alpha}, \left(-4\log\frac{\pi 2^{\beta}\rho}{12(|\beta|+2)(4|\beta|)^{|\beta|}}\right)^{\alpha} \right\}$
    $\beta \leq 1 : E_{\alpha,\beta}(t) = \int_0^R B(r;t,2\pi\alpha/3)dr$
    $\beta > 1 : E_{\alpha,\beta}(t) = \int_{1/2}^R B(r;t,2\pi\alpha/3)dr + \int_{-2\pi\alpha/3}^{2\pi\alpha/3} C(\phi;t,1/2)d\phi$
  end if
else
  $N = \lceil \frac{1}{\alpha}|t|^{1/\alpha} \rceil + 1$
  $t > 0 : E_{\alpha,\beta}(t) = \frac{1}{\alpha} t^{(1-\beta)/\alpha} \exp(t^{1/\alpha}) - \sum_{k=1}^{N} \frac{z^{-k}}{\Gamma(\beta-\alpha k)}$
  $t < 0 : E_{\alpha,\beta}(t) = -\sum_{k=1}^{N} \frac{z^{-k}}{\Gamma(\beta-\alpha k)}$
end if

Algorithm H.5.2 (Computation of the derivative of Mittag-Leffler $E'_{\alpha,\beta}(t)$)**.**

given parameters $\alpha, \beta \in \mathbb{R}$, $0 < \alpha \leq 1$
      argument $t \in \mathbb{R}$
      precision $\rho \in \mathbb{R}$, $\rho \neq 0$
if $t = 0$ **then**
    $E'_{\alpha,\beta}(t) = \frac{1}{\Gamma(\alpha+\beta)}$
else if $|t| < r_0 = 0.9$ **then**
    $\omega = \alpha + \beta - \frac{3}{2}$
    $D = \alpha^2 - 4\alpha\beta + 6\alpha + 1$
    $N = \lceil \max\left\{ \frac{3-\alpha-\beta}{\alpha}, \frac{1-2\omega\alpha+\sqrt{D}}{2\alpha^2}, \frac{\ln|\rho|(1-|t|)}{\ln|t|} \right\} \rceil + 1$
    $E'_{\alpha,\beta}(t) = \sum_{n=0}^{N} \frac{(n+1)t^n}{\Gamma(\alpha+\beta+\alpha n)}$
else
    $E'_{\alpha,\beta}(t) = \frac{E_{\alpha,\beta-1}(t) - (\beta-1)E_{\alpha,\beta}(t)}{\alpha t}$
end if

Appendix I

Code relating to Burridge et al.'s combination model

I.1 Simulate random processes: sample.r

```
# Auto covariance function for fractional Brownian motion
acf.fBM ← function(z0, z1, H) {
  0.5 * ( abs(z0)^(2*H) + abs(z1)^(2*H) - abs(z0-z1)^(2*H) )
}

# Auto covariance function for fractional Ornstein-Uhlenbeck
acf.fOU ← function(z0, z1, H, lc, sigmasq) {
  lag ← z1 - z0
  expr.int1 ← function ( x, z, H, lc ) { exp(-abs(x)/lc)*abs(x+z)^(2*H) }
  A ← sigmasq / (H*gamma(2*H)*lc^(2*H))
  A * ( 0.25/lc * integrate( expr.int1, -Inf, Inf, lag, H, lc )$value -
      0.5*abs(lag)^(2*H) )
}


# Simulate a Gaussian random process from its explicit definition of auto
    covariance function
rGaussianProcess ← function( z, acf, stationary, ... ) {
   n ← length(z)
   Gamma ← array(0, dim=c(n,n))

   # For stationary processes there is a shortcut since
       acf(z5,z2)=acf(z10,z13); same lag
   if (stationary==TRUE) {
     phi ← z*0
     for (i in 1:n) phi[i] ← acf(z[i],z[1],...)
     Gamma ← toeplitz(phi)
   } else {
     for (i in 1:n) for (j in i:n) Gamma[i,j] ← Gamma[j,i] ←
         acf(z[i],z[j],...)
   }

   # Sample from multivariate normal distribution by way of the cholesky
       decomposition
   C ← chol(Gamma)
   U ← array( rnorm(n), dim=c(n,1) )
   return( t(C) %*% U )

```

```
}


# Simluate rescaled Brownian motion
rScaledBrownianMotion ← function(N, noisegenerator, alpha) {
  g ← function(x, alpha) { sign(x)*abs(x)^alpha }
  g(cumsum(noisegenerator(N)),alpha)
}
```

I.2 Simulate propagation: propburr.r

```
# Propagate wave in frequency domain in accordance with algorithm H.3.1
propagate.burridge ← function (p, omegas, compvis )
{
  M ← length(omegas)
  M1 ← array( c(1,0,0,-1), dim=c(2,2) )
  M2 ← array( c(-1,-1,1,1), dim=c(2,2) )
  T ← rep(0,M)
  R ← rep(0,M)

  for (j in 1:M) {
    K ← diag(c(1,1))
    for (k in 1:p$N) {
      J ← Jmatrix ( p$coeffs[k,]$refl, p$coeffs[k,]$trans )
      Q ← 1i*omegas[j]*( - 1/p$c[k] * M1 + 0.5 *
          compvis(omegas[j],p$Jin[k]) * p$Z[k] * M2 )
      K ← J %*% expm(Q*p$dz) %*% K
    }
    T[j] ← abs( 1 / K[2,2] )
    R[j] ← abs( - K[2,1] / K[2,2] )
  }
  return( list( omega=omegas, trans=T, refl=R ) )
}
```

I.3 Collateral algorithms: misc.r

```
# Mittag-Leffler for 0 < a < 1, b anything, and precision p
mittaglefflerr ← function( t, a, b ) {
  if ( !( (a > 0) & (a <= 1) ) ) return(NA)
  p = 1e-30
  if ( t == 0 ) {
    return( 1/gamma(b) )
  } else if ( abs(t) < 1 ) {
    N = ceiling ( max( c( (2-b)/a, log(p*(1-abs(t)))/log(abs(t)) ) ) ) + 1
    S = sum ( t^(0:N) / gamma ( a*(0:N) + b ), na.rm=TRUE )
    return(S)
  } else if (abs(t) < (-2*log(p*pi*sin(pi*(1-a))))^a ) {
    om ← function(x,y) { x^(1/a)*sin(y/a)+y*(1+(1-b)/a) }
    A ← function(x,y) { 1/a*x^((1-b)/a)*exp(x^(1/a)*cos(y/a)) }
    B ← function(r,t,l) {
        1/pi*A(r,l)*(r*sin(om(r,l)-l)-t*sin(om(r,l)))/(r^2-2*r*t*cos(l)+t^2)
        }
    C ← function(phi,t,l) { l/(2*pi)*A(l,phi)*Re (
        exp(1i*om(l,phi))/(l*exp(1i*l)-t) ) }
    if (t > 0) {
      R ← max( c( 1, 2*abs(t), (abs(b)+1)^a, (-log(pi*p/6))^a,
          (-2*log(pi*p/(6*(abs(b)+2)*(2*abs(b))^abs(b))))^a ) )
      if (b <= 1) {
        return( A(t,0) + integrate( B, 0, R, t, pi*a )$value )
      } else {
```

```
21        return( A(t,0) + integrate( B, 1/2, R, t, pi*a )$value + integrate(
              C, -a*pi, a*pi, t, 1/2 )$value )
22      }
23    } else {
24      R ← max( c( 2^a, 2*abs(t), 2*(abs(b)+1)^a, (-2*log(pi*2^b*p/12))^a,
            (-4*log(pi*2^b*p/(12*(abs(b)+2)*(4*abs(b))^abs(b))))^a ) )
25      if (beta <= 1) {
26        return( integrate( B, 0, R, t, 2*pi*a/3 )$value )
27      } else {
28        return( integrate( B, 1/2, R, t, 2*pi*a/3 )$value + integrate( C,
              -2*a*pi/3, 2*a*pi/3, t, 1/2 )$value )
29      }
30    }
31  } else {
32    N = min ( c (50, ceiling( 1/a * abs(t)^(1/a) ) + 1 ) )
33    S = sum( t^(-(1:N)) / gamma ( b - (1:N)*a ), na.rm = T )
34    if ( t < 0 ) return ( -S ) else return( 1/a * t^((1-b)/a) *
          exp(t^(1/a)) - S )
35  }
36 }
37
38 # Mittag-Leffler first derivative
39 mittaglefflerderiv ← function(t,a,b) {
40   if ( !( (a > 0) && (a <= 1) ) ) return( NA )
41   p ← 1e-10
42   if (t == 0) {
43     return(1/Gamma(a+b))
44   } else if (abs(t) < 0.5) {
45     om ← a + b - 3/2
46     D ← a^2 - 4*a*b + 6*a + 1
47     N ← ceiling ( max( c ( (3-a-b)/a , (1 - 2*om*a + sqrt(D))/(2*a^2),
           log(p*(1-abs(t)))/log(abs(t)) ) ) ) + 1
48     return ( sum ( (1:(N+1)) * t^N / Gamma(b + a + a*(0:N)) ) )
49   } else {
50     return ( (mittaglefflerr(t,a,b-1) - (b-1)*mittaglefflerr(t,a,b))/(a*t) )
51   }
52 }
53
54 # Exponential of matrix whose trace is zero
55 expm ← function(M) {
56   if ( length(dim(M)) != 2 ) return(NA)
57   if ( !( (dim(M)[1] == 2) && (dim(M)[2] == 2) ) ) return(NA)
58   detM ← M[1,1] * M[2,2] - M[1,2]*M[2,1]
59   if (detM == 0) {
60     return ( diag(2) + M )
61   } else {
62     lambda ← sqrt(-detM)
63     return( cosh(lambda)*diag(2) + sinh(lambda)/lambda*M )
64   }
65 }
```

Bibliography

Bagley, R. (2007). On the equivalence of the Riemann-Liouville and the Caputo fractional order derivatives in modeling of linear viscoelastic materials. *Fractional Calclulus and Applied Analysis*, 10(2):123–126.

Banik, N. C., l. Lerche, and Shuey, R. T. (1985). Stratigraphic filtering, Part I: Derivation of the O'Doherty-Anstey formula. *Geophysics*, 50(12):2768–2774.

Beran, J. (1994). *Statistics for long-memory processes*. Chapman & Hall.

Bernstein, D. S. and So, W. (1993). Some explicit formulas for the matrix exponential. *IEEE Transactions on Automatic Control*, 38(8):1228–1232.

Burridge, R., de Hoop, M. V., Hsu, K., Le, L., and Norris, A. (1993). Waves in stratified viscoelastic media with microstructure. *The Journal of the Acoustical Society of America*, 94(5):2884–2894.

Campbell, J. A. and Waag, R. C. (1984). Measurements of calf liver ultrasonic differential and total scattering cross sections. *J. Acoust. Soc. Am*, 75(2):603–611.

Claerbout, J. F. (1976). *FUNDAMENTALS OF GEOPHYSICAL DATA PROCESSING: With Applications to Petroleum Prospecting*. McGraw-Hill Book Company.

Derksen, H. E. and Verveen, A. A. (1966). Fluctuations of resting neural membrane potential. *Science*, 151:1388–1389.

Dolan, S. S., Bean, C. J., and Riollet, B. (1998). The broad-band fractal nature of heterogeneity in the upper crust from petrophysical logs. *Geophys. J. Int.*, 132:489–507.

Fouque, J.-P., Garnier, J., Papanicolaou, G., and Sølna, K. (2007). *Wave Propegation and Time Reversal in Randomly Layered Media*. Springer.

Freeman, W. J., Holmes, M. D., Burke, B. C., and Vanhatalo, S. (2003). Spatial spectra of scalp EEG and EMG from awake humans. *Clinical Neurophysiology*, 114(6):1053—1068.

Gajjar, J. S. B. (2010). Mathematical methods – magic022. `http://maths.dept.shef.ac.uk/magic/course_files/145/completenotes.pdf`.

Garnier, J. and Sølna, K. (2010). Effective fractional acoustic wave equation in one-dimensional random multiscale media. *J. Acoust. Soc. Am.*, 127:62–72.

Gasquet, C. and Witomski, P. (1998). *Fourier Analysis and Applications*. Springer.

Gingl, Z., Kiss, L., and Vajtai, R. (1989). l/f^k noise generated by scaled brownian motion. *Solid State Communications*, 71(9):765–767.

Golubitsky, M. and Dellnitz, M. (1999). *Linear Algebra and Differential Equations Using MATLAB*. Brooks Cole.

Gorenflo, R., Loutchko, J., and Luchko, Y. (2002). Computation of the Mittag-Leffler function $E_{\alpha,\beta}(z)$ and its derivative. *Fractional Caluclulus and Applied Analysis*, 5(4):491–518.

Haubold, H. J., Mathai, A. M., and Saxena, R. K. (2011). Mittag-leffler functions and their applications. *Journal of Applied Mathematics*.

Hilfer, R. and Seybold, H. (2006). Computation of the generalized Mittag-Leffler function and its inverse in the complex plane. *Integral Transforms and Special Functions*, 17(9).

Holm, S. and Näsholm, S. P. (2011). A causal and fractional all-frequency wave equation for lossy media. *The Journal of the Acoustical Society of America*, 130(4):2195–2202.

Holm, S. and Sinkus, R. (2010). A unifying fractional wave equation for compressional and shear waves. *J. Acoust. Soc. Am.*, 127:542–548.

Kadaba, M. P., Bhagat, P. K., and Wu, V. C. (1980). Attenuation and backscattering of ultrasound in freshly excised animal tissue. *IEEE Transactions on Biomedical Engineering*, BME-27(2).

Kinsler, L. E., Frey, A. R., Coppens, A. B., and Sanders, J. V. (1999). *Fundamentals of Acoustics*. Wiley.

Le, L. H. and Burridge, R. (1998). Waves in elastic and anelastic stratified microstructure: A numerical comparison. *The Journal of the Acoustical Society of America*, 103(1):99–105.

Lim, S. C. and Muniandy, S. V. (2003). Generalized ornstein–uhlenbeck processes and associated self-similar processes. *J. Phys. A: Math. Gen.*, 36:3961–3982.

Mainardi, F. and Spada, G. (2011). Creep, relaxation and viscosity properties for basic fractional models in rheology. *Eur. Phys. J. Special Topics*, 193:133–160.

Mathai, A., Saxena, R. K., and Haubold, H. J. (2010). *The H-Function: Theory and Application*. Springer.

Moler, C. and Loan, C. V. (2003). Nineteen dubious ways to compute the exponential of a matrix , twenty-five years later. *SIAM review*, 45(1):3–49.

Nachman, A. I., III, J. F. S., and Waag, R. C. (1990). An equation for acoustic propagation in inhomogenous media with relaxation losses. *J. Acoust. Soc. Am*, 88:1584–1595.

Näsholm, S. P. and Holm, S. (2011). Linking multiple relaxation, power-law attenuation, and fractional wave equations. *The Journal of the Acoustical Society of America*, 130(5):3038–3045.

O'Doherty, R. and Anstey, N. A. (1971). Reflection on amplitudes*. *Geophysical Prospecting*, 19(3):430–458.

Plaszczynski, S. (2007). Generating long streams of $1/f^k$ noise. *Fluctuation and Noise Letters*, 7:R1–R13.

Podlubny, I. (1998). *Fractional differential equations: an introduction to fractional derivatives, fractional differential equations, to methods of their solution and some of their applications*. Academic Press.

Resnick, J. R. (1990). Stratigraphic filtering. *PAGEOPH*, 132(1/2):49–65.

Schiessel, H., Metzler, R., Blumen, A., and Nonnenmacher, T. F. (1995). Generalized viscoelastic models: their fractional equations with solutions. *J. Phys. A: Math. Gen.*, 28:6567–6584.

Schoenberger, M. and Levin, F. K. (1974). Apparent attenuation due to intrabed multiples. *Geophysics*, 39(3):278–291.

Sinkus, R., Holm, S., Guzina, B., Näsholm, S. P., Garteiser, Doblas, Beers, V., and Vilgrain (2011). Revealing the origin of attenuation in tissue: Pure absorption or multiple scattering? presented at Int. Soc. Magn. Res. in Med, Montreal.

Sinkus, R., Siegmann, K., Xydeas, T., Tanter, M., Claussen, C., and Fink, M. (2007). Mr elastography of breast lesions: Understanding the solid/liquid duality can improve the specificity of contrast-enhanced mr mammography. *Magnetic Resonance in Medicine*, 58:1135–1144.

Szabo, T. L. and Wu, J. (2000). A model for longitudinal and shear wave propagation in viscoelastic media. *The Journal of the Acoustical Society of America*, 107(5):2437–2446.

Treeby, B. E. and Cox, B. T. (2009). Fast, tissue-realistic models of photoacoustic wave propagation for homogeneous attenuating media. *Proc. of SPIE*, 7177 717716–1.

Walden, A. T. and Hosken, J. W. J. (1985). An investigation of the spectral properties of primary reflection coefficients. *Geophysical Prospecting*, 33:400–435.

Weaver, R. L. and Pao, Y.-H. (1981). Dispersion relations for linear wave propagation in homogeneous and inhomogeneous media. *J. Math. Phys.*, 22.

Wornell, G. W. (1996). *Signal processing with fractals*. Prentice-Hall Inc.